DOT/FAA/TC-17/27

Federal Aviation Administration
William J. Hughes Technical Center
Aviation Research Division
Atlantic City International Airport
New Jersey 08405

Thermal Imaging for Aircraft Rescue and Fire Fighting Applications

May 2017

Final Report

U.S. Department of Transportation
Federal Aviation Administration

NOTICE

Technical Report Documentation Page

1. Report No.	2. Government Accession No.	3. Recipient's Catalog No.
DOT/FAA/TC-17/27		

4. Title and Subtitle	5. Report Date
THERMAL IMAGING FOR AIRCRAFT RESCUE AND FIRE FIGHTING APPLICATIONS	May 2017

7. Author(s)	8. Performing Organization Report No.
Matthew Short, Jonathan Torres; and *Jack Kreckie	

9. Performing Organization Name and Address	10. Work Unit No. (TRAIS)
SRA International 1201 New Road, Suite 242 Linwood, NJ 08221 *ARFF Professional Services, LLC 432 Valerie Way, Unit 202 Naples, FL 34104	
	11. Contract or Grant No. DTFACT-15-D-00007

12. Sponsoring Agency Name and Address	13. Type of Report and Period Covered
U.S. Department of Transportation Federal Aviation Administration Airport Safety and Operations Division (AAS-300) 800 Independence Avenue SW Washington, DC 20591	Final Report
	14. Sponsoring Agency Code AAS-300

15. Supplementary Notes

The FAA Airport Technology Research and Development Branch COR was Keith Bagot.

16. Abstract

Thermal cameras are useful for a variety of aircraft rescue and fire fighting (ARFF) applications because of their ability to observe people and objects under otherwise low-visibility conditions. The purpose of this research is to examine the capabilities of thermal cameras for ARFF operations by conducting both full- and small-scale tests.

Testing in this research program included viewing hot spots from the fuselage exterior of both a passenger and cargo configurations, evaluating the effects various aircraft fuselage skin materials have on the camera's ability to see radiant heat, as well as testing the performance of various cameras in a Driver's Enhanced Vision System (DEVS) application.

Results from full-scale testing showed that all the thermal cameras tested were capable of identifying hot spots on the aircraft exterior. These hot spots were shown to directly correlate with damage to the aircraft insulation. All thermal cameras tested during small-scale testing presented a varying amount of error in the measurement of spot temperature on all aircraft skin materials. During the DEVS evaluations, the cameras with higher resolutions and high contrast filters outperformed the other cameras.

17. Key Words	18. Distribution Statement
Thermal imaging camera, Forward-looking infrared, Aircraft rescue and fire fighting, Driver's Enhanced Vision System, Passenger aircraft, Freighter aircraft	This document is available to the U.S. public through the National Technical Information Service (NTIS), Springfield, Virginia 22161. This document is also available from the Federal Aviation Administration William J. Hughes Technical Center at actlibrary.tc.faa.gov.

19. Security Classif. (of this report)	20. Security Classif. (of this page)	21. No. of Pages	22. Price
Unclassified	Unclassified	120	

TABLE OF CONTENTS

LIST OF FIGURES

LIST OF TABLES

LIST OF ACRONYMS

3-D	Three-dimensional
AC	Advisory Circular
ACY	Atlantic City International Airport
ARFF	Aircraft rescue and fire fighting
ATRD	Airport Technology Research and Development
CFRP	Carbon fiber-reinforced plastic
DDE	Digital detail enhancement
DEVS	Driver's Enhanced Vision System
DFW FTRC	Dallas/Fort Worth International Airport Fire Training Research Center
DVR	Digital video recorder
FAA	Federal Aviation Administration
FLIR	Forward-looking infrared
GLARE	Glass Laminate Aluminum-Reinforced Epoxy
HRET	High-Reach Extendable Turret
IR	Infrared
kW	Kilowatt
PID	Proportional-integral-derivative
SSR	Solid-state relay
TIC	Thermal imaging camera
ULD	Unit load device
VAC	Volts of alternating current
WJHTC	William J. Hughes Technical Center

EXECUTIVE SUMMARY

Thermal cameras are used for a variety of aircraft rescue and fire fighting (ARFF) applications because of their ability to detect people and objects under otherwise low-visibility conditions. Thermal cameras use special optics and imaging sensors to create a digital image of the infrared range of the electromagnetic spectrum. They assist ARFF personnel with navigating through low-visibility conditions, locating victims, finding heat sources, and measuring temperatures. The purpose of this research is to examine the capabilities of thermal cameras for ARFF operations by conducting both full- and small-scale tests.

Testing included viewing hot spots from the fuselage exterior of both a passenger and cargo aircraft configurations, evaluating the effects various aircraft skin materials have on the camera's ability to see radiant heat, and testing the performance of different cameras used with a Driver's Enhanced Vision System (DEVS) application.

Full-scale testing used a quartz heater assembly, which was developed to heat the aircraft interior without fuel combustion. The assembly was used in two test scenarios: one within the interior of the Federal Aviation Administration (FAA) Lockheed (L) 1011 test article and the other located at the FAA ARFF test area. The L-1011 test article was converted from a passenger to a cargo configuration to allow the comparison of these wide-body aircraft configurations in regard to exterior thermal signature. Aircraft wet down was also conducted to gauge the effectiveness of this strategy. The exterior of the L-1011 test article was observed from the FAA Striker ARFF research vehicle's array of cameras, allowing the comparison of five thermal cameras simultaneously.

The small-scale panel testing at the FAA ARFF test area was conducted to quantify the accuracy of spot temperatures on varying aircraft fuselage skin materials using thermal cameras. The aircraft materials were also compared for their heat transfer ability, and the cameras were tested at varying distances and angles to the test panels.

In addition, the thermal cameras were tested for their DEVS capability. Each camera was tested for its comparative ability for this ARFF function in different road and weather conditions, in identifying hot brakes, in the presence of a pool fire, and in identifying aircraft from far distances.

Results from full-scale testing showed that all the thermal cameras tested were capable of identifying hot spots on the aircraft exterior caused by the quartz heater assembly. Windows, frame members around aircraft windows, and the crown area were consistently presented as a hot spot for both passenger and cargo configuration testing. These hot spots were shown to directly correlate with damage to the aircraft insulation. Autoignition of the cargo configuration's cargo liner occurred on two occasions, whereas it did not occur during passenger configuration testing. The aircraft wet-down strategy was shown to effectively reduce ancillary hot spots, allowing the correct identification of the test area.

All cameras tested presented a varying amount of error in the measurement of spot temperature on all panel types and at all angles during panel testing. It was determined that default camera

settings were not capable of accurately measuring temperature on aircraft materials. Panel testing showed Glass Laminate Aluminum Reinforced Epoxy (GLARE) panels to exhibit fewer hot spots compared to aluminum and carbon fiber panels. Carbon fiber was shown to transmit the least amount of heat compared to aluminum and GLARE panels.

Four different thermal cameras were evaluated and compared to a thermal camera that is used currently for a DEVS. For the functionality expected in an ARFF operation, the cameras with optics and sensor technology with the highest resolution and high contrast performance filter outperformed the other cameras.

1. INTRODUCTION.

Thermal cameras are useful for a variety of aircraft rescue and fire fighting (ARFF) applications because of their ability to detect people and objects under otherwise low-visibility conditions. Thermal cameras use special optics and imaging sensors to create a digital image of the infrared (IR) range of the electromagnetic spectrum. They assist ARFF personnel with navigating through low-visibility conditions, locating victims, finding heat sources, and measuring temperatures.

Despite the benefits offered by thermal cameras, there are limitations that ARFF personnel must take into account when using them. Failure to account for these limitations can result in misinterpretation of thermal camera images. Furthermore, there is a need to determine the performance capabilities of thermal cameras when applied to ARFF incidents. For these reasons, the Federal Aviation Administration (FAA) Airport Technology Research and Development (ATRD) team investigated the current capabilities and limitations of thermal cameras for ARFF applications.

1.1 PURPOSE.

The purpose of this research was to examine the capabilities of thermal cameras for ARFF operations by conducting both actual aircraft and simulated aircraft tests. The primary purpose of the research was to identify the limitation of this technology for use during ARFF first response. The capability to operate ARFF vehicles guided by thermal cameras, identification of aircraft hot spots, and the ability to determine temperature on a variety of aircraft materials were examined.

1.2 BACKGROUND.

A thermal camera converts IR (sometimes referred to as infrared light or infrared radiation) into a false color (including grayscale) visual image. The image is representative of the temperature of the objects in the image. In a white-hot grayscale IR image, dark gray represents colder temperatures, and light gray represents hotter temperatures. One noteworthy feature of thermal cameras is that smoke does not affect their operations the same way that color cameras are affected because smoke particles absorb IR and visible light. Smoke particles strongly absorb visible light, but only partially absorb IR radiation [1]. This allows the IR radiation to pass through smoke and be captured by thermal cameras.

The strength of IR emissions from an object depends on the emissivity of the object. Emissivity is “the ratio of the amount of radiation actually emitted from the surface to that emitted by a black body at the same temperature” [1]. Emissivity generally depends on the material, surface structure or finish, object geometry, observation angle, wavelength, and temperature. Solar radiation, wind, and moisture can affect the IR emissions that are captured by thermal cameras when used outdoors.

Thermal cameras used by ARFF personnel generally fall into one of two categories: commercial forward-looking infrared (FLIR) cameras and thermal imaging cameras (TIC). Both types of cameras rely on the same technology; however, they differ in the way that the camera is

operated. FLIR cameras can be configured to be sensitive to specific IR ranges, such as the shortwave IR range and the longwave IR range. With FLIR cameras, an operator can change the camera's emissivity values, temperature scale, and the color scale of the image. TICs are cameras specifically designed for firefighting operations and are only sensitive to longwave IR. They are ruggedized and waterproof for use in extreme conditions and are easier to operate than FLIR cameras. TIC IR settings cannot be modified by the user.

1.2.1 Thermal Camera Tactics.

Currently, classes focusing on thermal camera tactics are not available at fire training centers. Instead, TIC and FLIR camera tactics are discussed briefly during regular ARFF classes. The ATRD team attended a "Tactics and Strategies for Cargo Fires" class at Dallas/Fort Worth International Airport Fire Training Research Center (DFW FTRC) to learn how thermal camera tactics are demonstrated. DFW FTRC uses both TIC and FLIR technologies in training and emergency response.

The class includes lectures, as well as practical evolutions conducted on their Boeing (B) 727 F test article and the Airbus (A) 380 mockup. Students were shown how to use a TIC to evaluate the aircraft exterior for hot spots. They were taught that if there is a fire aboard a freighter aircraft, a hot spot on the skin may be visible using the TIC. Students evaluated each side of the fuselage exterior looking for indications of a fire inside, as shown in figures 1 and 2.

Figure 1. Instruction on Using a TIC

Figure 2. Students Evaluating Fuselage Using TICs

During the training, a hot spot simulator installed in the main cargo bay of the B-727 F test article was used to demonstrate thermal camera tactics, as shown in figure 3. When turned on, the simulator heated a small section on top of the test article's left wing, and students were instructed to locate it using the TIC.

Figure 3. Hot Spot Simulator

Another strategy that DFW FTRC demonstrated involved using a quick response truck to conduct a 360° scan around the aircraft, evaluating the thermal signature. The FLIR camera operator looks for hot spots and reports any anomalies to Incident Command. Once in position, all response vehicles will be able to monitor the FLIR images

1.2.2 Driver's Enhanced Vision System.

One of the main ARFF uses for FLIR cameras is in a Driver's Enhanced Vision System (DEVS). The DEVS is used by ARFF personnel to navigate to areas of interest under low-visibility conditions. The DEVS is made up of several subsystems: navigation, tracking, and night vision [2]. The navigation subsystem is used "to make the ARFF vehicle driver aware of the vehicle's location and to serve as an aid in locating the incident site" [2]. The purpose of the tracking

subsystem is “to transmit the vehicle position to the Emergency Command Center” [2]. The night vision subsystem is made up of a FLIR camera, which gives the ARFF vehicle driver the ability to identify objects such as a human body or an aircraft in nighttime, foggy, or smoky conditions. To be used as part of a DEVS, thermal cameras have to meet performance criteria specified in Advisory Circular (AC) 150/5210-19A [3]. Tables 1 and 2 show the minimum distances ARFF personnel should be able to detect a person and an aircraft in various weather conditions with the DEVS camera. A DEVS FLIR camera has the capability to aid a vehicle operator to identify intersections and edges of runways and taxiways in various weather conditions. These standards are used as a baseline for the evaluations.

Table 1. The DEVS Camera Requirements for Human Detection Distances [3]

Distance (ft)	Ambient Temperature *	Humidity (%)	Camera Dynamics	Weather
500	-20 to 115°F	0 to 100	Moving 55 mph	Clear
500	-20 to 115°F	0 to 100	Moving 50 mph	Light Fog
400	-20 to 115°F	0 to 100	Moving 40 mph	Heavy Fog
400	-20 to 115°F	0 to 100	Moving 40 mph	Smoke
300	-20 to 115°F	0 to 100	Moving 35 mph	Rain/Snow

*If winterization is necessary, the temperature performance range must be extended to at least -40°F (-40°C).

Table 2. The DEVS Camera Requirements for Aircraft Detection Distances [3]

Distance (ft)	Ambient Temperature *	Humidity (%)	Camera Dynamics	Weather
2500	-20 to 115°F	0 to 100	Moving 55 mph	Clear
1000	-20 to 115°F	0 to 100	Moving 50 mph	Light Fog
500	-20 to 115°F	0 to 100	Moving 40 mph	Heavy Fog
500	-20 to 115°F	0 to 100	Moving 40 mph	Smoke
500	-20 to 115°F	0 to 100	Moving 35 mph	Rain/Snow

*If winterization is necessary, the temperature performance range must be extended to at least -40° F (-40°C).

1.2.3 Past Research.

In 2011-2012, the FAA ATRD team conducted research regarding fires on freighter aircraft [4 and 5]. This research included tests for penetration of cargo liner material and full-scale freighter aircraft fire testing. The cargo liner testing was not intended to test the performance of the FLIR camera that was used; however, it did offer a chance to collect data from the FLIR camera and compare its performance with other temperature collecting devices [4]. Differences between data obtained from thermocouples and a FLIR camera from the tests indicated a clear

difference between the two data sources. The tests also showed that heat or hot spots may not be visible on a thermal camera on the outside of a fuselage. During the full-scale freighter aircraft tests, FLIR cameras and a TIC were arranged around the test aircraft to observe the interior fires [5]. Tests showed that many of the interior fires were not visible through any of the thermal cameras. Observations indicated the possibility that hot spots may not appear clearly until the interior of the fuselage has reached a dangerous condition (i.e., presence of a large fire and the fuselage is about to be breached).

1.3 OBJECTIVES.

The objectives for this report were to evaluate

- the performance of several TIC and FLIR cameras in detecting hot spot on a Lockheed (L) 1011 test article.
- the effectiveness of the wet-down strategy to increase the visibility of hot spots.
- the performance of thermal cameras on reading surface temperature of heated aircraft fuselage panels.
- new thermal cameras against Driver's Enhanced Vision Systems (DEVS) in identifying people, aircraft, and roads.

2. EXPERIMENTAL SETUP AND PROCEDURES.

The following sections will describe the different test articles, setups, and procedures used for the tests.

2.1 THE TICs AND FLIRs.

The cameras used for testing were: FLIR® Patrol IR (Patrol IR), FLIR® P660 (P660), FLIR® T420 (T420), ISG® ELITE XR (XR), FLIR® M625L (M625L), which are depicted and specified in table 3 and figure 4. The Patrol IR was used as a standard truck-mounted DEVS camera, while the M625L served as a truck-mounted camera with a higher resolution. The XR was the standard handheld TIC used by ARFF personnel, while the P660 and T420 cameras were used as handheld cameras with programmable thermal settings and different camera resolutions. All five listed cameras were used during L-1011 testing. The Patrol IR and M625L were excluded from panel testing due to their lack of portability, the permanence of mounting on the FAA 2005 Oshkosh® Striker 3000 (FAA Striker), and the lack of a spot temperature indicator. All cameras were reset to default settings if the camera functions permitted.

Table 3 compares the thermal camera specifications for a DEVS system with the other evaluated cameras. This table shows that all cameras tested met or exceeded most of the DEVS minimum specifications; the exception was the minimum operating temperature required for winterized operations.

Table 3. Camera Specifications

	DEVS Standard	Patrol IR	P660	T420	XR	M625L
IR detection range (µm*)	8 to 12	Not stated	Not stated	7.5 to 13	8 to 14	Not stated
Resolution	320 x 240	320 x 240	640 x 480	320 x 240	320 x 240	640 x 480
Field of view	27° x 18° ±4°	35° x 27°	24° x 24° with 45° x 45° option	25° x 19° with 45° x 45° option	59° x 59°	25° x 20°
Minimum operating temperature (°F)	-40	-4	-40	-4	Not stated	-13

*µm = micrometer

Figure 4. Infrared Cameras: (a) Patrol IR, (b) P660, (c) T420, (d) XR, and (e) M625L

2.2 TEST VEHICLE.

The FAA Striker was used as the test vehicle for full-scale tests. The test cameras were all mounted on top of the FAA Striker's cab roof, which allowed for the cameras to have similar frames of reference during the tests. All camera video data was saved to the truck's onboard digital video recorders (DVR). It should be noted that because two separate DVRs were used, timestamps varied from camera to camera in the still images shown. The camera array and screen array on the FAA Striker is shown in figure 5.

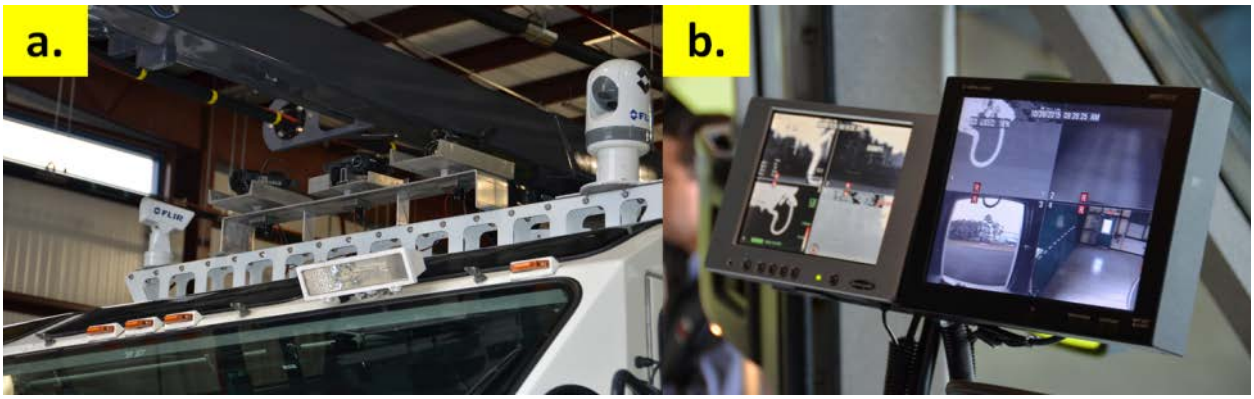

Figure 5. The FAA Striker (a) IR Camera and (b) Screen Array

2.3 QUARTZ HEATER ASSEMBLY.

A quartz heater assembly was used to simulate the heat output of a fire without the variability and damage caused by combustion. Electric heaters could accurately maintain a set-point temperature when compared to using other heat sources, such as hydrocarbon fires. The quartz heater assembly was designed to be used during full-scale and small-scale panel testing scenarios.

2.3.1 Mechanical Design.

The quartz heater assembly was comprised of four Omega® Engineering, Inc. model QH-121260-T electric radiant heaters, which were 12 by 12 inch (in.), 8640 W, and 60 W/in.^{2}. The heater operating temperatures were between ambient temperature and 1800°F. A stainless steel and aluminum housing was fabricated to contain the four heaters for ease of movement and adjustability in heater angle. The quartz heater assembly was designed to have an adjustable panel holder, which was used to simulate the skin of a unit load device (ULD) during L-1011 testing and to hold test panels during panel testing. This panel holder placed the panel at distances that were 1, 2, and 3 feet (ft) from the heater array; however, it could be completely removed. A photo of the quartz heater assembly is shown in figure 6.

Figure 6. Quartz Heater Assembly

2.3.2 Electrical Supply and Control Methods.

As a result of the large electrical demand of 34 kilowatt (kW), a power supply method was devised that split heater connections between an on-site generator and commercial electric power. Three electric radiant heaters were supplied from a Generac® model 7817750100 40 kW diesel generator, featuring a 480° volts of alternating current (VAC). This ensured an equal loading across all three phases of the generator, minimizing stress on the stator and increasing generator operational life. The fourth heater was supplied by 208-VAC commercial power supply at the testing site.

A single control system was not possible because of the combined electrical voltages and power supplies. The heater supplied by the lower voltage 208-VAC site power was expected to generate heat at a slower rate than the heaters supplied by the 480 VAC from the generator. To compensate, two identical but separate heater controls were used.

The control system used an Omron® Corporation model E5CC-QX3A5M-000 digital temperature controller and a Crydom® (Custom Sensors & Technologies, Inc.) model HD4850-10 solid-state relay (SSR) to control the electricity supplied to the heaters. SSRs were preferred over conventional contactors since they offer the ability to rapidly turn on and off the supplied power. This meant that a PID (proportional-integral-derivate) control method could be used to accurately maintain temperature of the heaters without prematurely wearing out the electrical switchgear. The objective of the control strategy was to operate all four heaters to achieve an average heater temperature equal to that of ±5% of a given temperature set point. The PID controllers were tuned to increase the accuracy of the controller. A wiring diagram of the heaters and control system is shown in figure 7.

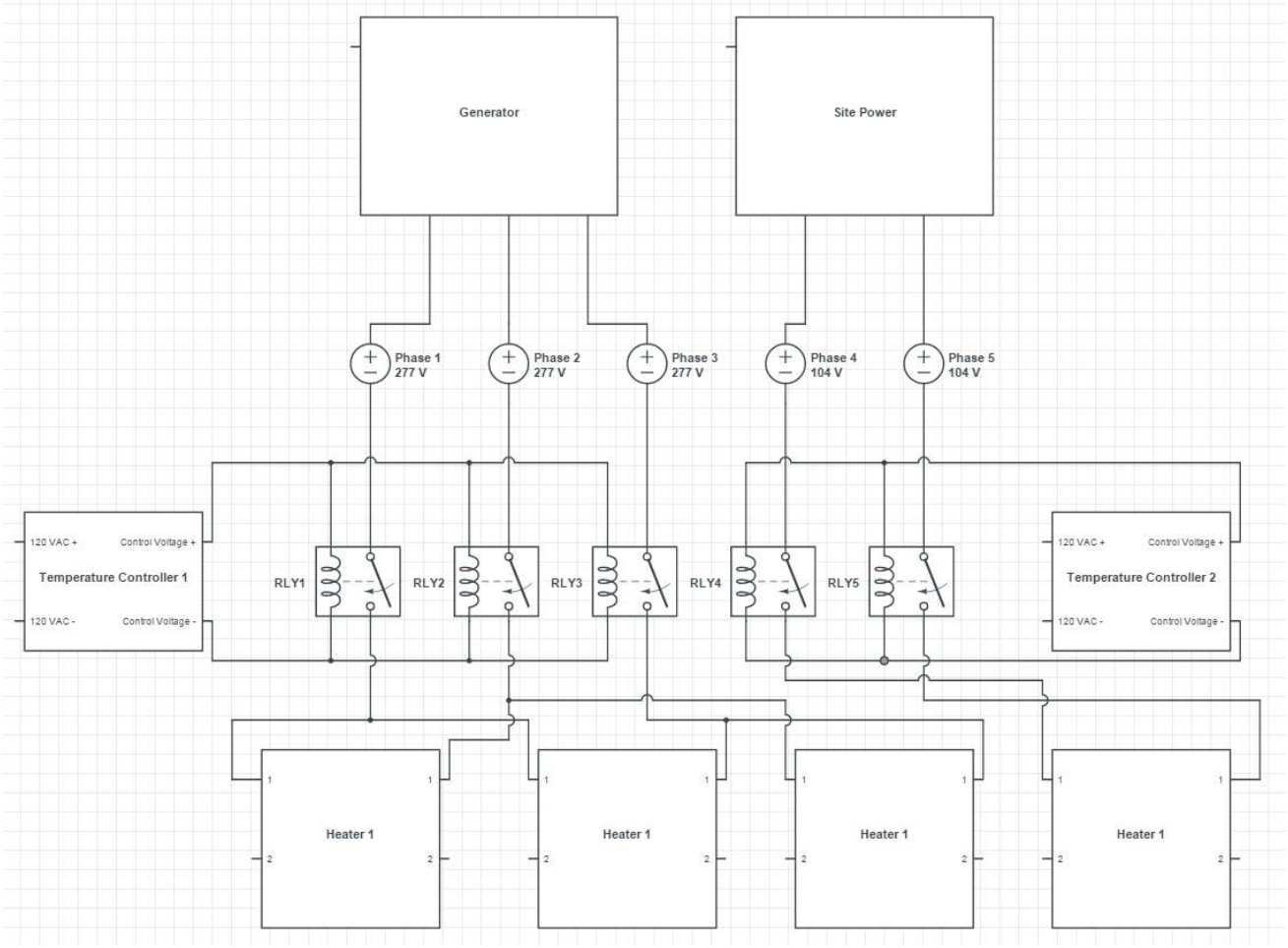

Figure 7. Quartz Heater Assembly Wiring Diagram

Four Omega thermocouples, model TJ69-CAIN-18U-9-CC-XCIB, were used to monitor the temperature of the heaters. Four thermocouples were used in the quartz heater assembly, two of which were used to operate the temperature controllers. All four were monitored for potential heater, control strategy, or electrical source failure.

2.4 FULL-SCALE TESTING.

Full-scale testing was conducted to evaluate the effectiveness of the TIC and FLIR cameras in detecting a hot spot on an aircraft's fuselage with a live fire inside the aircraft. In addition to this primary objective, the wet-down tactic of spraying the aircraft's fuselage with water from the FAA Striker was tested to gauge its ability to identify hot spots. The FAA L-1011 test article was used because it still had all of the interior liner intact in the passenger compartment. The L-1011 interior was segregated into three distinct test sections. Tests 1 through 3 were conducted on the L-1011 in a passenger configuration. Modifications to the plane interior or exterior were not made during passenger configuration testing. Tests 1 through 3 simulated a passenger-configured wide-body aircraft. Tests 4 through 7 used the cargo configuration to simulate a cargo-configured wide-body aircraft. After the test areas of the aircraft were damaged from tests 1 through 3, the L-1011 was modified by removing the damaged interior panels and

replacing the insulation. All damaged insulation was replaced with 3/8-in.-thick, 1.2-pounds per cubic ft Johns Manville™ Microlite® AA FG Insulation Premium NR water repellent fiberglass insulation. The walls were then covered in Conolite® cargo liner material, part number A60SG4W-48096. Windows were insulated and covered with painted aluminum window blanks, which were attached with rivets from the aircraft exterior.

2.4.1 The FAA Striker and Camera Positioning.

The FAA Striker was positioned at a standard stand-off distance used during ARFF response and was centered about the test section. The high-reach extendable turret (HRET) was then extended to the test area. The front of the FAA Striker was approximately 25 ft from the aircraft. During testing, the FAA Striker was repositioned to simulate a roll-up. This position would be similar to an ARFF response vehicle arriving on the scene for the first time. The front of the truck at its furthest distance was approximately 75 ft from the aircraft. Figure 8 shows an overhead image of the positioning of the FAA Striker.

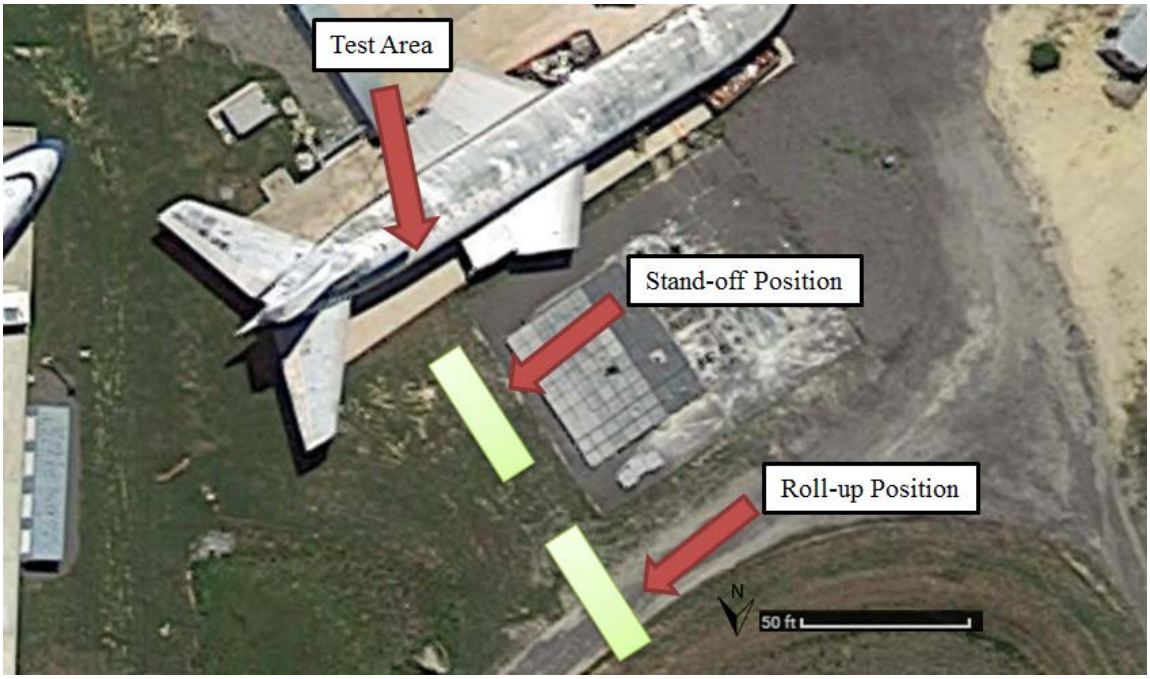

Figure 8. The FAA Striker Positioning Relative to an L-1011

2.4.2 The L-1011 Instrumentation.

Each test section was fitted with nine interior K-type thermocouples and three exterior bolt-on K-type thermocouples. Interior thermocouples were fastened with 1/2-in. outer diameter washers and 1/4- by 1/2-in. self-tapping screws. The thermocouple beads were pressed against the interior panels surface by applying a slight bend to the thermocouple wire. The washer or screw did not come in contact with the exposed thermocouple wire or thermocouple bead. Figures 9 through 11 show the locations of the interior and exterior thermocouples on sample test sections for both passenger and cargo configurations as well as the thermocouple numbering scheme.

Figure 9. The L-1011 Interior Thermocouple Locations Passenger Configuration

Figure 10. The L-1011 Interior Thermocouple Locations Cargo Configuration

Figure 11. The L-1011 Exterior Thermocouple Locations

2.4.3 Heater Placement and Configuration.

The quartz heater assembly was positioned at the center of each test area prior to test start. The heater was centered about interior thermocouples 4, 5, and 6. This placement corresponds to the center exterior thermocouple 2. Figure 12 shows the heater placement prior to a test start.

Figure 1. Quartz Heater Assembly Placement

2.4.4 Test Parameters.

A variety of testing scenarios were conducted. Heater parameters, interior configuration, test duration, exterior wet down, and simulation of cargo containerization (using an aluminum panel to simulate a ULD) were all variables investigated during testing. Table 4 shows the breakdown of all test scenarios.

Table 4. The L-1011 Test Parameters

Test Number	Heater Parameters	Interior Configuration	Test Duration	Exterior Wet Down
1	122°F increments for 5 minutes for 212°F to 572°F then 212°F increments for 10 minutes 572°F to 1472°F until test end	Passenger	1 hour 44 minutes 19 seconds	No
2	1112°F and hold until thermal signature, Maximum heater output until test end	Passenger	27 minutes 7 seconds	Yes
3	Maximum heater output and hold until thermal signature or test end	Passenger	16 minutes 55 seconds	Yes
4	Maximum heater output and hold until thermal signature or test end	Cargo	6 minutes 15 seconds	No
5	Maximum heater output and hold until thermal signature or test end	Cargo	15 minutes 39 seconds	Yes
6	Maximum heater output and hold until thermal signature or test end	Cargo with aluminum panel 1 ft from heater	16 minutes 40 seconds	No
7	Maximum heater output and hold until thermal signature or test end	Cargo with aluminum panel against heater	14 minutes 21 seconds	No

Prior to each test, the FAA Striker was positioned in place and cameras were powered on. The test began once the interior response team, control point, and FAA Striker team confirmed their readiness. The tests began when the heaters were turned on. The interior of the plane was allowed to heat until a test stop condition was met. Test stop conditions are met through one or more of the following:

- Five minutes of elapsed time after identification of a thermal signature by the FAA Striker operator through the thermal cameras
- Active fire aboard the aircraft

- Interior fire response team requests test stop

- A critical failure of testing equipment

The FAA Striker commenced exterior wet down during tests 2, 3, and 5. The vehicle operator used the HRET turret to apply water to the fuselage from the aft of the plane to the rear of the wing. It was assumed that the water application would balance any abnormal heat signatures from the sun on the fuselage, thus enhancing the heated area visibility. The water was flowed for a minimum of 15 seconds and directed at the fuselage crown. The FAA Striker operator commenced wet down when a thermal signature in the test area was recognized. Before and after photos for the wet-down strategy are shown in section 3.

Heater parameters were changed between tests 1 and 2 to more accurately simulate a fire on board the aircraft and to shorten test duration. Instead of incrementally changing the heaters' temperature, they were turned on to their maximum output. Test 7 was the exception wherein the heaters surpassed the thermocouple maximum operating temperature of 1800°F. The aluminum panel reflected the heat back into the quartz heaters. The temperature control was turned down to 1800°F to reduce the likelihood of heater assembly failure. A photo of the quartz heater assembly configuration to simulate a ULD is shown in figure 13.

Figure 13. Quartz Heater Assembly With Simulated ULD Panel

2.5 SMALL-SCALE TESTING.

Small-scale testing used the quartz heater assembly to heat panels that simulated an aircraft fuselage. A track was used to place cameras at consistent angles and distances from the heater. The objective of these tests was to determine the ability of the thermal camera to indicate temperature on test panels of varying materials at various angles and distances.

2.5.1 Test Panel Materials.

The materials selected for testing were based on common materials used as the fuselage skin in operational aircraft. To duplicate the cross section of an aircraft, a combination of panel and interior materials were used. From the interior or heater-facing side to the exterior or camera-facing side, the following materials were used: cargo liner, insulation (wrapped in metallic insulation moisture barrier), heater frame member, and exterior aluminum panel. Cargo liners, insulation, and exterior panels were changed after each test. Panels were not reused during testing.

Materials selected for exterior panel testing were as follows: unpainted aluminum, painted aluminum, Glass Laminate Aluminum-Reinforced Epoxy (GLARE) composite, and carbon fiber. The aluminum used was type 2024-T3 painted with gloss white multipurpose aerosol paint. The carbon fiber-reinforced plastic (CFRP) panels were a 16-ply carbon fiber with a symmetric layup scheme and a thickness of 1/8″. The plies were laid out in a quasi-isotropic shape at 45°, 0°, +45°, and 90° with respect to fiber direction, with the pattern repeated four times per panel. The GLARE panels were GLARE® 3 5/4 with a thickness of 1/8″. The GLARE 3 5/4 indicated that for every five layers of aluminum, there are four layers of glass fiber prepreg. All panels were cut into a 2- by 2-ft square. Table 5 shows the specifications on the materials used.

Table 5. Test Panel Materials Specifications

Test Panel	Material	Thickness (in.)
Aluminum	Aluminum 2024-T3	0.06
Carbon Fiber	CFRP	0.10
GLARE	GLARE® 3 5/4	0.10

2.5.2 Panel Instrumentation.

Test panels were instrumented with a total of ten K-type thermocouples. Five thermocouples were placed against the exterior panel, and five were placed against the interior panel. The thermocouples were at the centers of the heaters and in the center of the panel. The locations of the panel thermocouples with their number designations are shown in figures 14 and 15.

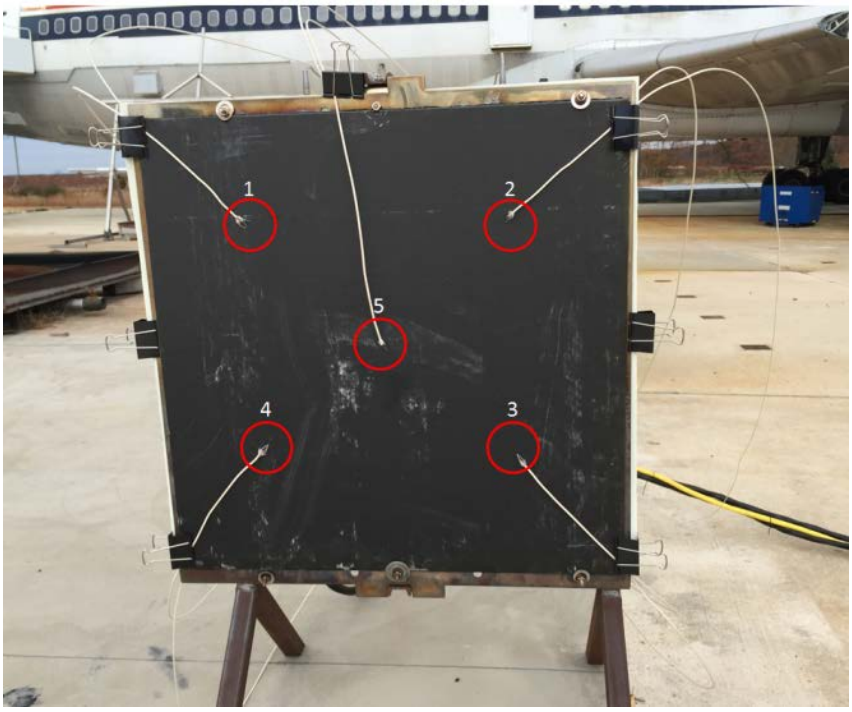

Figure 14. Camera Facing Panel Instrumentation

Figure 15. Heater Facing Panel Instrumentation

2.5.3 Camera Track Design.

The camera track was 25 ft long, allowing the camera dolly to roll from a position centered about the panel to a position 20 ft laterally to the side. The camera dolly was fabricated to be adjustable so that each camera height relative to the center of the heater assembly was consistent across all cameras. Figure 16 shows the camera track, dolly, and camera mount.

Figure 16. Camera Track System

2.5.4 Camera Track and Heater Positioning.

The heater assembly and camera track system were positioned to the specifications shown in figure 17. The heater was moved in the Y direction until the face of the heater was 10 ft from the camera lens. The test panel assembly was offset from the heater face by 1 ft for all tests. The distance between the camera lens and the heater panels was checked each time the camera was changed or the heater was moved. Camera height relative to the center of the heaters was also checked for each camera.

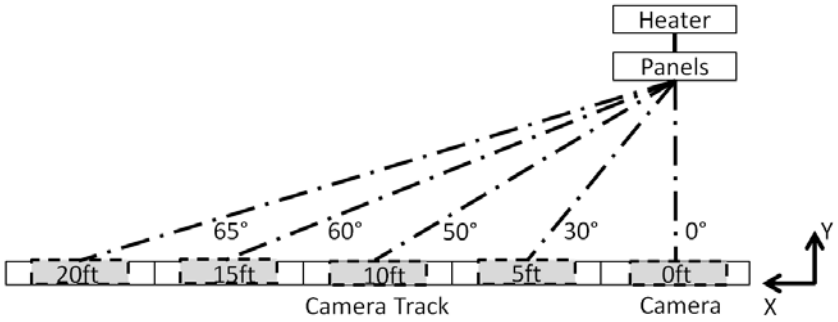

Figure 17. Camera Track and Heater Positioning

As the camera dolly was moved laterally, the angle of the camera relative to the heater had to be changed to keep the camera pointed at the same spot on the panel. To achieve consistent angles, a SUNWAYFOTO® DDP-64MX model indexing camera mount was used.

2.5.5 Test Parameters.

Identical test operations were conducted for the three cameras used. First, the camera was turned on and confirmed to be recording onto the DVR. Then, the heaters were turned on and set to a target temperature of 1112°F. The camera remained stationary until the heaters were within 5% of the target temperature. The camera was moved to the 5-ft, 10-ft, 15-ft, and 20-ft positions on the camera track. The indexing mount was positioned to the correct angle each time the camera dolly was moved. After 15 minutes of elapsed test time, the heaters were turned off and allowed to cool. The test was then concluded, and the cargo liner panel, insulation panel, and exterior panel were replaced prior to the next test. This process was repeated for each of the four exterior panel types for all three cameras. Table 6 shows the testing panel parameters.

Table 6. Panel Test Plan

Test Number	Camera	Exterior Panel
1	T420	Carbon fiber
2	T420	Aluminum—unpainted
3	T420	Aluminum—painted
4	P660	GLARE
5	P660	Carbon fiber
6	P660	Aluminum—unpainted
7	P660	Aluminum—painted
8	P660	GLARE
9	T420	GLARE
10	XR	GLARE
11	XR	Carbon fiber
12	XR	Aluminum—unpainted
13	XR	Aluminum—painted

2.6 THE DEVS TESTS.

DEVS tests consisted of looking at the performance of each of the cameras in different road and weather conditions, in identifying hot brakes, in the presence of a pool fire, and in identifying aircraft from far distances.

2.6.1 Road Test.

The DEVS thermal camera is advantageous to identify roads under low-visibility conditions. It is important mention that depending where an incident takes place, not all roads on which an ARFF vehicle driver has to drive are paved. Many of these paths are surfaced with gravel or dirt. To analyze how various road types are shown through different thermal cameras, the FAA Striker was driven through the path shown in figure 18 at the FAA William J. Hughes Technical Center (WJHTC). This path included roads surfaced with asphalt, dirt, and gravel.

Figure 18. Road Comparison Test Path

2.6.2 Wooded Area Test.

Many airports are located around wooded areas; and if an aircraft crashed in those wooded areas, the airport ARFF departments would respond to the incident. Thermal cameras could be beneficial in not only locating the aircraft, but in locating passengers that could be wandering in the area. For this evaluation, the FAA Striker was positioned in front of a wooded area at the WJHTC, and the cameras were panned left and right to evaluate the visibility they offered when looking at the wooded area.

2.6.3 Rain Test.

Thermal imaging technologies may offer an increased awareness of surroundings when low-visibility conditions are prevalent; one such condition is precipitation in the form of rain. To evaluate the performance of the thermal imaging array, the FAA Striker was driven on a road course in three varying precipitation levels. The first was a baseline without any precipitation, while the other two were low precipitation and heavy precipitation. The visibility levels for all cameras are provided in section 3.3.3.

2.6.4 Contrast Filter Test.

A thermal camera often expands to the temperature range so it can appropriately read the whole scene and not underreport colder areas or over report hotter areas. With a fire in view, the high temperature of the fire changes the temperature span and could sometimes improve or obscure visibility from the camera. Application of extinguishing agent also has the potential of altering the thermal camera's temperature range. To evaluate the response of the cameras in the presence of fire, the FAA ARFF truck was positioned at the end of the test pad and directed at a 6-ft-square fire pan and a three-dimensional (3-D) fire mockup. These two test setups were used with the TEKFLAME® training fuel, a JP-8 substitute.

2.6.5 Auto-Scaling Test.

Some thermal cameras contain an auto-scaling feature that changes the apparent temperature range within the viewable camera image. This feature may enhance or degrade the image quality depending on the conditions and the thermal camera use case. A fire test was developed to identify the auto-scaling impact on the cameras in the array that contain this feature.

Five gallons of TEKFLAME training fuel were dispensed into a 6-ft-square fire pan and ignited for the duration of 1 minute. The fire, ARFF personnel, and the surrounding area were monitored through the cameras. The image quality for each camera at each scaling setting is provided in section 3.3.5.

2.6.6 Daytime and Nighttime Long-Distance Detection Test.

According to the FAA AC 150/5210-19A, enhanced visions systems should be capable of the detecting aircraft at the distances identified in table 2, which shows detection distances up to 2500 ft [3]. To evaluate the capability of the FAA Striker's camera array to meet these standards, the vehicle was positioned at various locations around the airport operations area of Atlantic City International Airport (ACY). It should be noted that the FAA striker was stationary in its position. Using global positioning system coordinates and satellite imagery, aircraft distances were retroactively calculated. The camera array performance at various aircraft distances for both daytime and nighttime are provided in section 3.3.6.

2.6.7 Hot Brakes Test.

A common type of incident requiring ARFF response involves the brakes of an aircraft becoming overheated during landing. This hot brakes condition creates the potential for a brake or wheel

fire. Thermal images could provide ARFF personnel greater brakes condition details and indicate when the brakes have cooled down. To evaluate this, the ATRD team monitored braking tests that were being conducted by the FAA Aircraft Braking Friction Team with their B-727 F test article. These tests were conducted at the ACY Runway 4-22, where the test article would accelerate to 40 knots and immediately brake on a water-contaminated surface. After braking, the thermal signature of the brakes was recorded while the test article was taxiing back to its starting position.

3. RESULTS AND DISCUSSION.

Results and related discussion for each test scenario will be discussed in the following sections.

3.1 FULL-SCALE TESTING.

This section addresses the test results from the experiments which used the FAA L-1011 test article.

3.1.1 Characteristic Curves and Maximum Temperatures.

Consistent heater warming was observed across all tests where the heater was given the same input. The typical temperature curves for the heaters and interior thermocouples are illustrated in the figures that follow. Exemptions to these characteristic curves and the cause for their deviations are topics for further discussion.

The heater assembly reached within 5% of its maximum temperature of 1750°F within 10 minutes of the test start. The characteristic warming curve for the heater assembly is displayed in figure 19. It should be noted that panel 4 was powered by the lower 208-VAC site power, and therefore, operated at a lower maximum temperature of 1550°F.

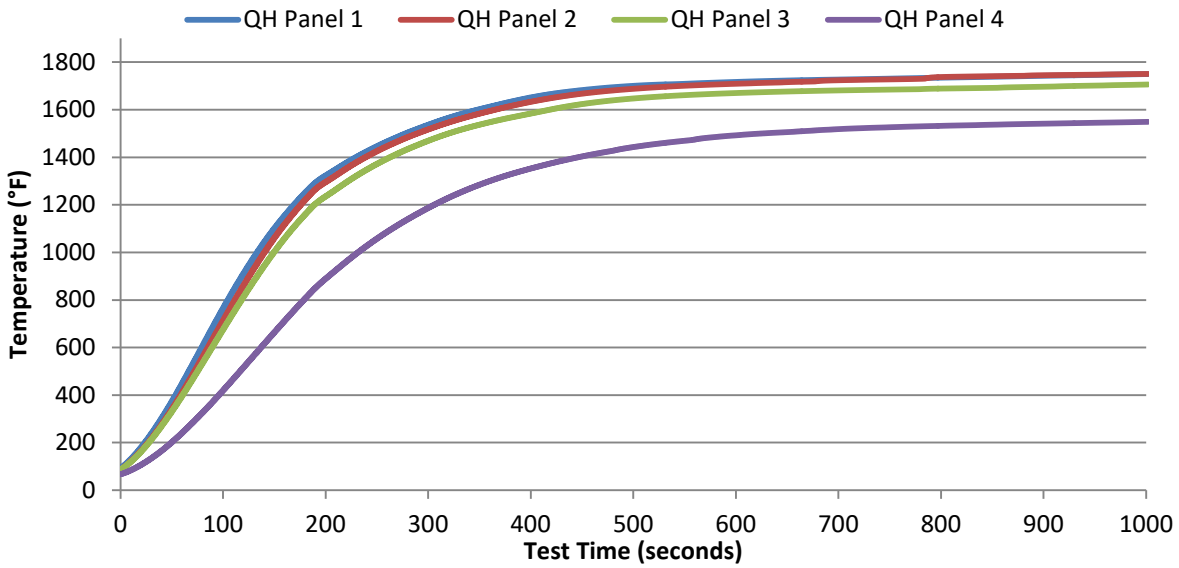

Figure 19. Quartz Heater Thermocouples: Test 6

Interior temperatures for all tests were shown to directly correlate to the quartz heater assembly's distance from the aircraft wall. Figure 20 shows the interior temperature for test 5, which is a cargo configuration test.

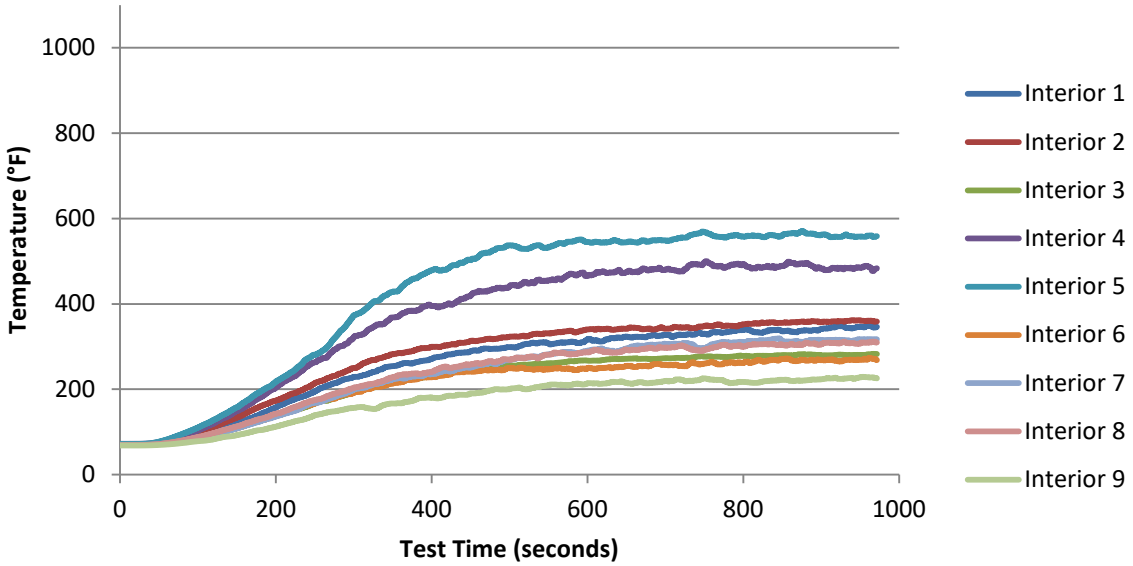

Figure 20. Interior Thermocouples: Test 5

Figure 21 depicts the maximum interior temperatures from test 5 overlaid onto an image of the undamaged aircraft wall. It should be noted that this is a maximum temperature for each location and may not necessarily have occurred at the same instant in time. The temperature distribution agreed with expectations of a high temperature about the center of the heater, with decreasing temperatures seen at longer distances away from the center. Thermocouples 1, 4, and 7 were significantly higher than 3, 6, and 9 as a result of the air movement around the heater.

Figure 21. Interior Thermocouple Maximum Temperature: Test 5

Tables 7 through 9 below provide the maximum temperatures for each thermocouple during each test.

Table 7. Maximum Quartz Heater Temperatures

Test Number	Quartz Heater 1 (°F)	Quartz Heater 2 (°F)	Quartz Heater 3 (°F)	Quartz Heater 4 (°F)	Average (°F)
1	1473	1462	1467	1064	1367
2	1284	1326	1350	1060	1255
3	1727	1718	1718	1536	1675
4	1590	1585	1563	1301	1510
5	1721	1725	1700	1506	1663
6	1750	1750	1706	1549	1689
7	1840	1893	1825	1722	1820

Table 8. Maximum Interior Temperatures

Test Number	Int.*1 (°F)	Int.*2 (°F)	Int.*3 (°F)	Int.*4 (°F)	Int.*5 (°F)	Int.*6 (°F)	Int.*7 (°F)	Int.*8 (°F)	Int.*9 (°F)
1	239	273	182	234	317	322	137	233	166
2	163	205	188	262	433	244	157	208	149
3	233	399	260	569	693	462	223	368	199
4	289	333	196	617	1021	332	258	325	186
5	349	362	283	500	571	274	319	312	229
6	321	355	257	364	213	341	347	316	123
7	267	376	161	395	418	214	202	205	106

* Int. = Interior

Table 9. Maximum Exterior Temperatures

Test Number	Pre-Test Average (°F)	Exterior 1 (°F)	Exterior 2 (°F)	Exterior 3 (°F)
1	64	82	84	78
2	73	74	74	74
3	64	72	91	73
4	65	66	66	66
5	66	68	68	67
6	52	59	56	62
7	57	57	57	58

Test 1 was characterized by low maximum temperatures because of the incrementation of heater temperature over a long period. The heat transferred to the aircraft wall was slowly transferred into the exterior, which was evident in the large change in exterior temperature shown in the test.

Test 3 represented a drastic change in temperature from previous tests as the heater set point was changed from incremental to maximum output from the test start. Exterior thermocouple 2 increased 27°F from the test start to maximum temperature. This was primarily because of the complete failure of the center test window and interior insulation, which is discussed in detail in section 3.1.6.

Test 4 showed a spike in interior temperature at thermocouples 4 and 5 as a result of an ignition of off-gassing. The test was aborted after a test stop order was issued by the interior response team. Test 4 showed a low maximum temperature recorded by the quartz heater assembly. There was no significant change in exterior temperature because of the short duration of the test.

Tests 6 and 7 exhibited relatively low interior temperatures caused by the aluminum panel that replicated a cargo container. This was accompanied by high maximum temperatures for the heater assembly, as the heat was reflected from the panel back into the heater assembly.

3.1.2 The IR Camera Performance—Earliest Detection.

This section discusses the performance of the IR cameras used during testing on the L-1011. Screen captures of the IR cameras used are provided in appendix A.

Test 1 provided a slow increase in interior temperature, as shown in figure 22.

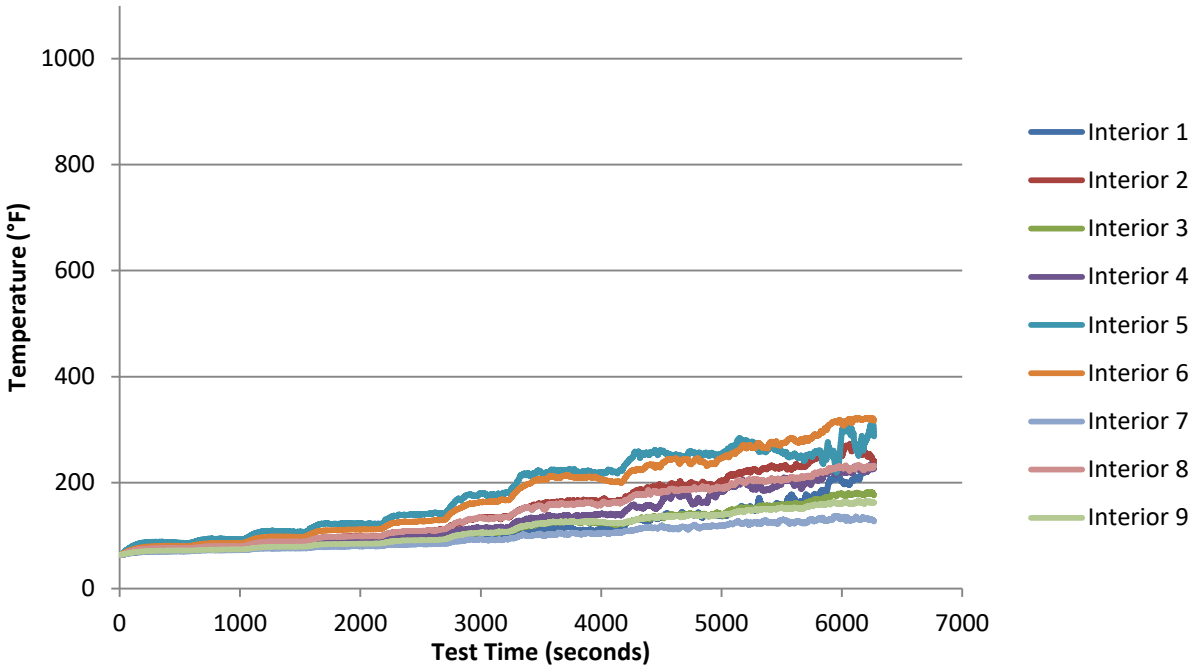

Figure 22. Interior Thermocouples: Test 1

In this test, interior heating was conducted slowly and at a low intensity so that the heat had ample time to transfer though to the exterior without serious damage to the aircraft. This allowed the identification of locations, which could become hot spots in situations that are given ample time to transfer heat. These hot spot locations were similar during tests with much higher heating rates. These locations include the window, frame members, and aircraft crown above the windows. A slow heating rate also eased the quantification of the lower limit of each camera's sensitivity by comparing the amount of time each camera required to identify a significant increase in temperature over the test area. Figure 23 displays each camera's earliest detection of a temperature increase in the test area. Detection was determined by identification of an increase in temperature over the test area by an IR camera operator who was aware of the heater location.

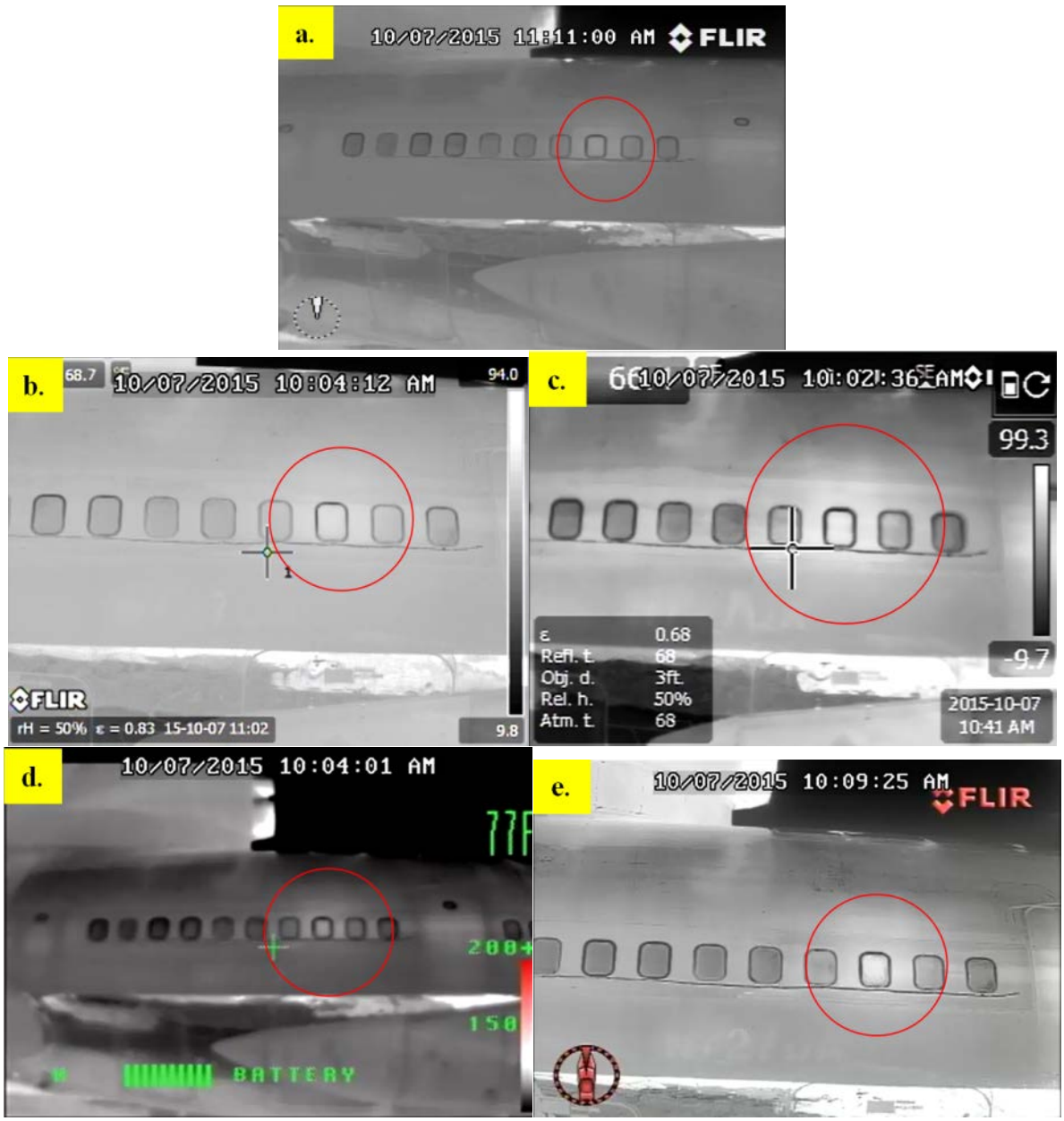

Figure 23. Earliest Detection of a Significant Increase in Temperature Over Test Area Using (a) Patrol IR, (b) P660, (c) T420, (d) XR, and (e) M625L

The data in table 10 shows the time to earliest detection and the highest interior temperature simultaneously, which correlates with the images in figure 23. It should be noted that camera A operated on a different DVR with a different internal time than the other cameras. The timestamp for camera A was normalized to the second DVR during analysis. All figures below display a different timestamp for camera A, although the figure displays the camera's view simultaneously.

Table 10. Earliest Detection of a Significant Increase in Temperature Over Test Area

Camera Label	Camera Model	Time to Earliest Significant Detection	Maximum Interior Temperature at Time of Detection (°F)
A	Patrol IR	25 minutes, 14 seconds	107.4
B	P660	27 minutes, 26 seconds	120.9
C	T420	25 minutes, 50 seconds	107.4
D	XR	27 minutes, 15 seconds	118.7
E	M625L	32 minutes, 39 seconds	122.1

The Patrol IR was the first to register the increase in exterior temperature, followed by the T420. Although detection was only 12 seconds behind the Patrol IR, the T420 showed a more pronounced temperature gradient on the aircraft exterior.

The XR was next to show the hot spot, followed shortly by the P660. The last to identify the hot spot was the M625L. This was most likely due to the wide view, which contained more of the aircraft's crown, overexposing the test section, as shown in figure 23(e).

3.1.3 Roll-up Camera Performance.

Roll-up position simulated an ARFF vehicle approaching the aircraft for the first time. The roll-up position is characterized by a greater distance between the aircraft and thermal cameras as compared to standoff distance. These positions are discussed in section 2. It should be noted that the views were taken while the vehicle was at a complete stop.

The identification of hot spots became difficult as more ancillary hot spots, or apparent hot spots not caused by a fire, became observable across the aircraft. Also, the presence of ambient areas, such as the sky, caused the cameras' scale to increase, which made smaller temperature changes less visible. An operator could incorrectly identify an ancillary hot spot as a fire-related hot spot.

Views through each camera are shown in figure 24. The heater is centered about the second to last window.

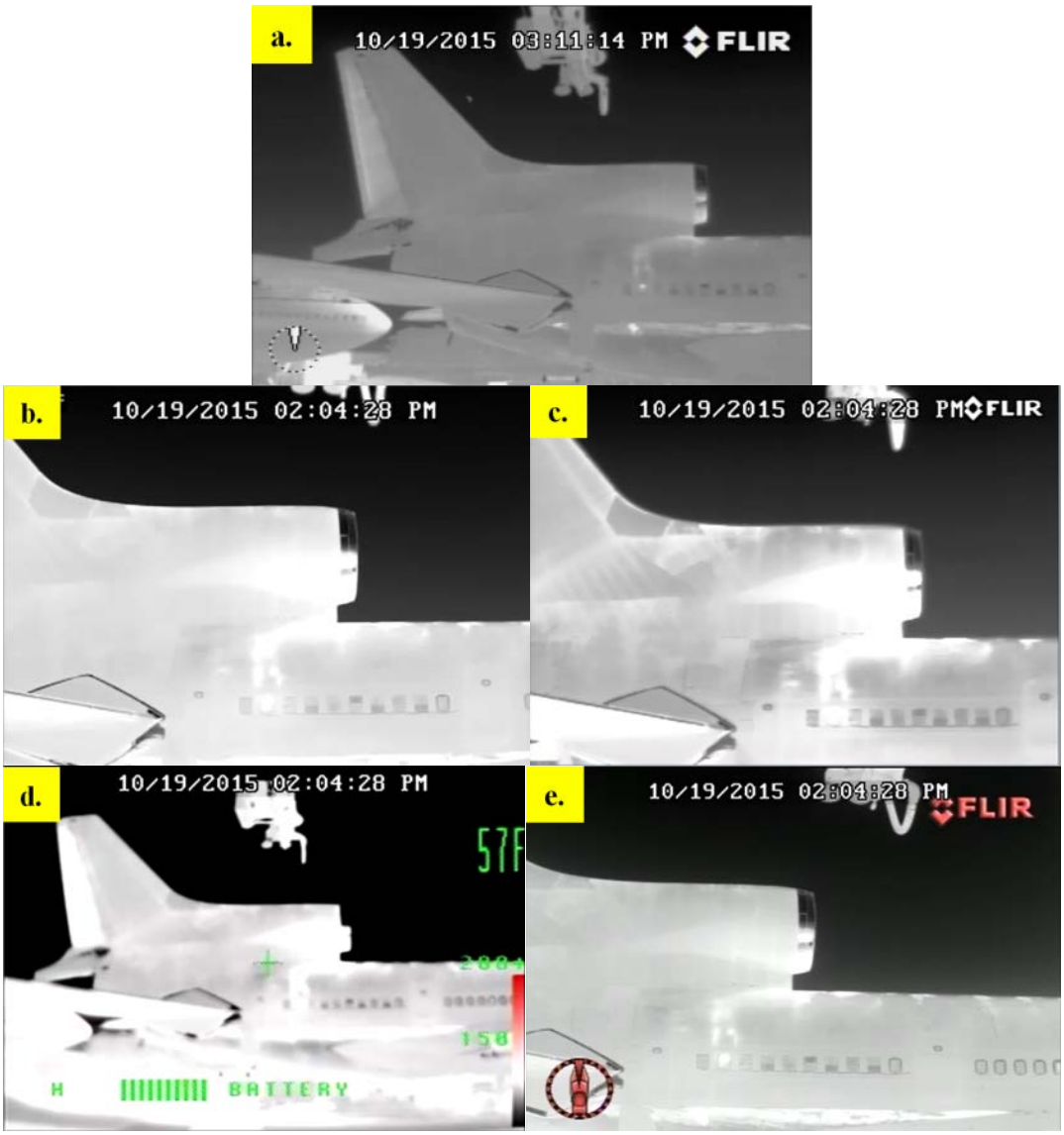

Figure 24. Roll-up Camera Performance Test 7 Using (a) Patrol IR, (b) P660, (c) T420, (d) XR, and (e) M625L

All cameras correctly identify the signature at the center of the heater. Camera performance was consistent across all tests in the roll-up position. The T420 displays the most severe hot spot but also the most ancillary signatures near the aircraft crown and top turbine housing. The M625L depicts the best combination of hot spot signature with minimal ancillary signatures.

3.1.4 Typical Hot Spots for Passenger and Cargo Configurations.

Areas of the aircraft consistently presented as hot spots during testing were the frame members above the aircraft windows and the windows in the test location. These two areas presented an increase in temperature prior to other parts of the exterior. It is suspected that the heat from the quartz panel heater ascended the interior wall and into the area above the overhead bins. These hot spots were visible prior to hot spots in damaged windows and frame members, and prior to

any major insulation damage, as observed in test 3. The typical hot spot locations are identified with a red box in figure 25, which shows images from test 3.

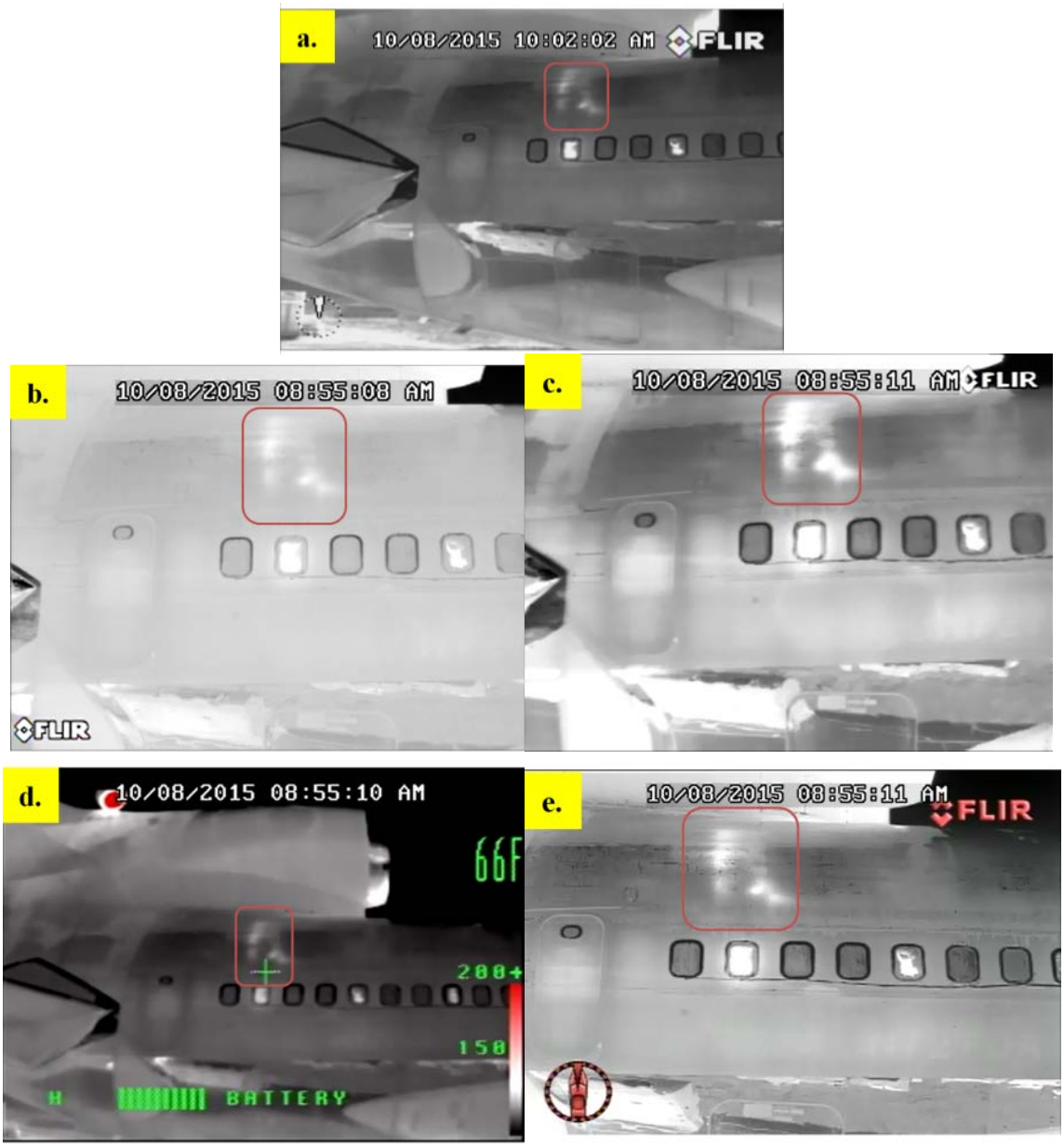

Figure 25. Typical Hot Spots Using (a) Patrol IR, (b) P660, (c) T420, (d) XR, and (e) M625L

3.1.5 Wet-Down Strategy Effectiveness.

A common strategy when attempting to identify hot spots onboard an aircraft is to use an HRET or bumper turret to wet the aircraft. The objective is to cool the areas around the hot spot to allow the heated area to become more easily identifiable. During tests 2, 3, and 5, this strategy was conducted. Figures 26 through 32 are a few samples of before and after images exhibiting the wet-down strategy. It should be noted that it is difficult to determine how long a hot spot will

be visible after a wet down since it depends on the heat source size and the materials the heat has to penetrate.

Figure 26. Before and After Wet-Down Strategy: Test 2 Using Patrol IR

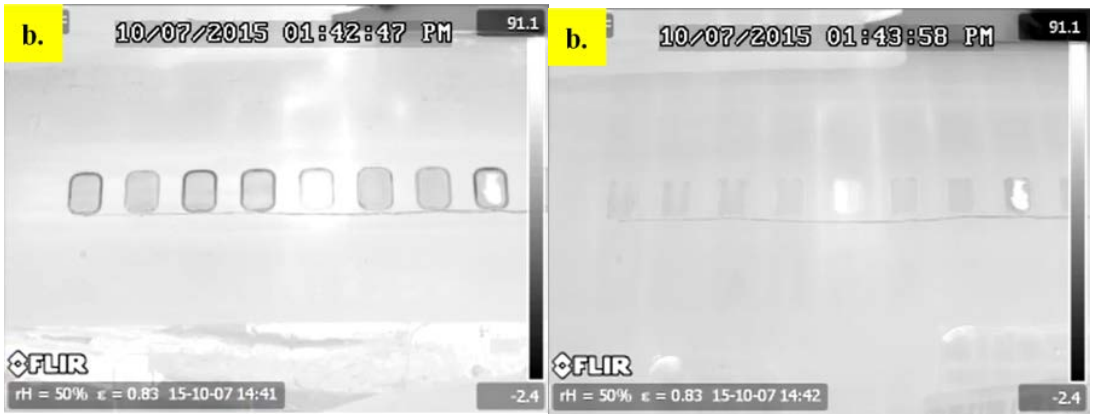

Figure 27. Before and After Wet-Down Strategy: Test 2 Using P660

Figure 28. Before and After Wet-Down Strategy: Test 2 Using T420

Figure 29. Before and After Wet-Down Strategy: Test 3 Using XR

Figure 30. Before and After Wet-Down Strategy: Test 3 Using M625L

Figure 31. Before and After Wet-Down Strategy: Test 5 Using T420

Figure 32. Before and After Wet-Down Strategy: Test 5 Using M625L

The wet-down strategy was an effective method for identifying hot spots in some instances. Frame members became more pronounced within the heated testing area. Areas of the aircraft that were not in the test area, but were shown to be similar to hot spots, were subdued after the strategy was used. An example of this occurrence is shown figure 33.

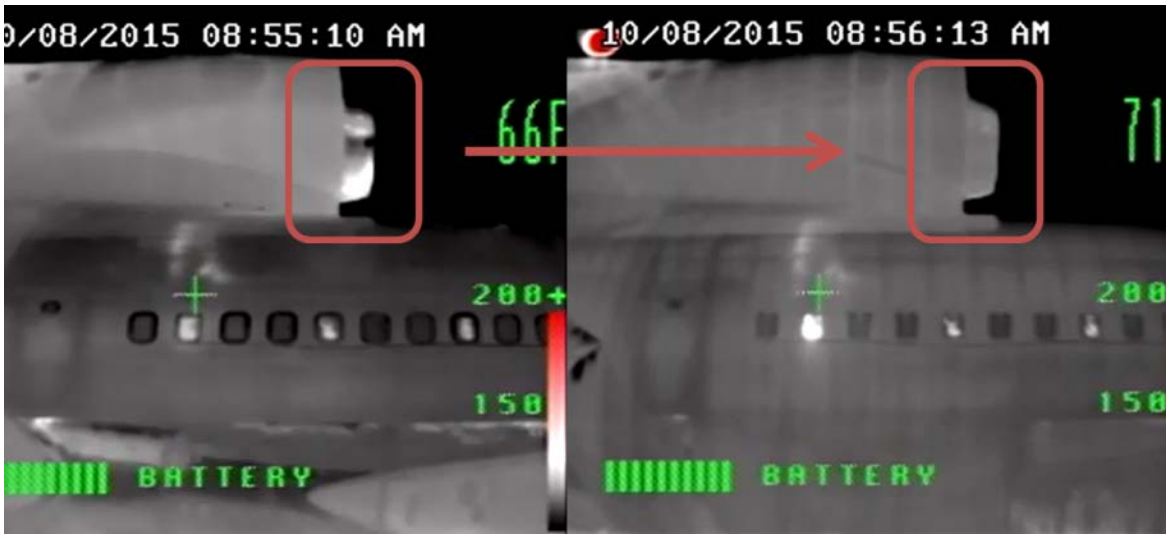

Figure 33. Reduction in Non-Test Area Hot Spots During Wet-Down Strategy: Test 3 Using XR

Wetting the aircraft temporarily decreased the temperature of the aircraft exterior. The exterior thermocouples are shown in figure 34. The decrease in exterior temperature lasts nearly 3 minutes until the exterior temperatures begin to climb again. The wet-down strategy may offer IR camera operators up to 6 minutes of reduced ancillary hot spots on the aircraft exterior.

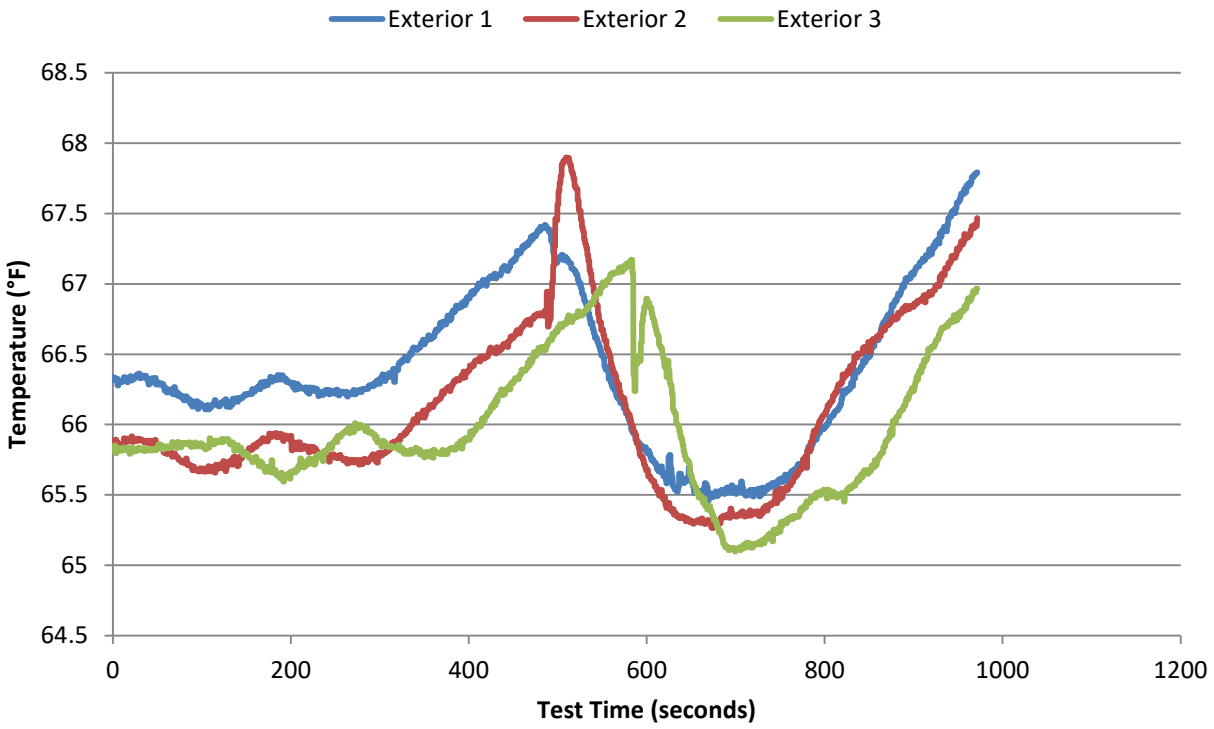

Figure 34. Exterior Temperature: Test 5

3.1.6 Passenger Configuration Damage and Fire Propagation.

Damage caused by the quartz heater assembly was a function of heater temperature and distance from the wall. Test 1 damage included discoloration of the interior panel, bubbling of the upper compartments, and failure of the interior and exterior windows. Damage to the insulation was also minimal. The insulation did not show evidence of charring and only minor heat-related damage. The damage to test section 1 is depicted in figure 35.

Figure 35. Damage to Aircraft Interior: Test 1

Test 2 damage was more rapid and severe than test 1 damage. Damage extended past the center window of the test area. Both interior and exterior windows failed as in test 1, and charring was noticeable on the insulation behind the interior panels, as shown in figure 36.

Figure 36. Damage to Aircraft Interior: Test 2

Test 3 presented the most severe damage to the aircraft interior. The entire center panel and the two flanking panels were charred. The left, right, and center windows failed during testing. The insulation behind test section 3 was severely charred and was replaced following the test. Figures 37 and 38 show the damage to test section 3.

Figure 37. Damage to Aircraft Interior: Test 3

Figure 38. Damage to Aircraft Insulation: Test 3

Fire was not propagated during any passenger configuration testing. Off-gassing was prevalent, but the interior did not present open flames, even with interior temperatures exceeding 690°F during testing. Figure 39 shows the before and after photos exemplifying passenger configuration testing. Figure 39(a) shows the aircraft interior during test 3 prior to test start. Figure 39(b) shows the test section just prior to test end at 15 minutes and 25 seconds of elapsed test time.

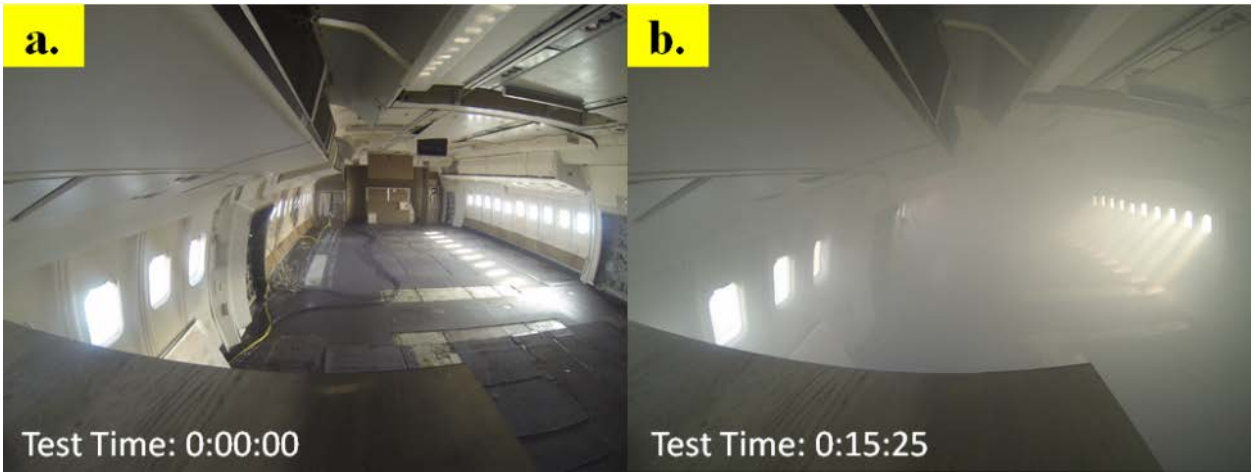

Figure 39. Off-Gassing During Passenger Configuration: Test 3 Interior Test Section Prior to (a) Start and (b) End

3.1.7 Cargo Configuration Damage and Fire Propagation.

Similar to passenger configuration testing, damage to the cargo aircraft interior configuration was proportional to heater temperature and distance to the wall. The quartz heater assembly was placed at the same distance and at the same set-point temperature as the passenger configuration, but results differed considerably. Ignition of off-gassing occurred at 6 minutes and 15 seconds into the test, causing a test stop condition. Interior temperatures were much higher during test 4 compared to the other tests, as shown in figure 40.

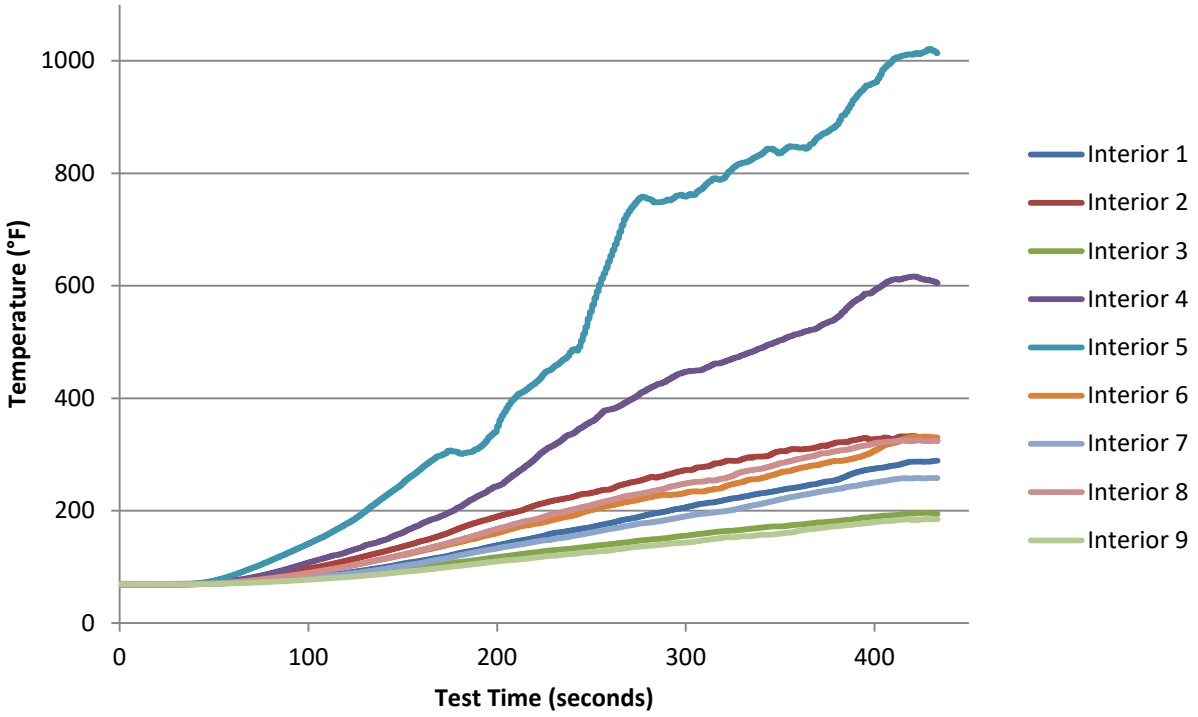

Figure 40. Interior Thermocouples Temperatures: Test 4

Damage to the cargo liner and insulation was severe, partly due to the fire that propagated between them. Figure 41 depicts the damages to the aircraft wall. It should be noted that the cargo liner was removed from the wall during the interior team's fire response efforts.

Figure 41. Damage to Aircraft Interior: Test 4

Ignition was most likely caused by an off-gas product contact with the heater assembly. The fire then spread back into the wall and between the cargo liner and insulation. The off-gassing

occurred through a tear in the wall, approximately 1/2 in. long, positioned in the center of the cargo-liner test section. An image of the ignition is shown in figure 42.

Figure 42. Autoignition: Test 4

Prior to test 5, the distance of the heater assembly to the aircraft wall was increased from 1 ft, 4in. to 2 ft, 1.5 in. This increase was to prevent autoignition and increase the likelihood of a full-length test. Damage to the aircraft interior during test 5 was similar but not quite as severe as test 4. There was significantly less off-gassing, and ignition did not occur. The damage caused by test 5 is shown in figure 43. It should be noted that the cargo liner was removed by the interior team to ensure that fire was not present after testing.

Figure 43. Damage to Interior: Test 5

Tests 6 and 7 simulated a ULD and cargo configuration test. An aluminum ULD was simulated by an aluminum panel fitted 1′ in front of the quartz heater assembly. During test 7, the aluminum panel distance was reduced to flush with the heater.

Test 6 exhibited much lower temperatures on the cargo liner wall as the heat was reflected by the aluminum panel. Damage to the cargo liner, insulation, and aluminum panel was negligible. A slight discoloration of the cargo liner around the aluminum panel was observed. Figure 44 shows damage to the interior during test 6.

Figure 44. Damage to Interior: Test 6

The third cargo configuration test section that was used for test 6 was reused during test 7 since there was minimal damage to the test section present after test 6. The aluminum panel simulating the ULD was moved flush with the heater to increase the aluminum panel's temperature. During test 7, the aluminum panel failed, causing a spike in interior temperature. A small fire occurred during test 7 when the failed aluminum panel came into contact with the cargo liner. The fire ignited the insulation behind the cargo liner and the test was aborted. Damage to the aircraft interior was similar to test 4 with damage to the insulation and cargo liner present. Off-gassing during tests 6 and 7 was not as severe as in test 5. Figures 45 and 46 show the fire caused by the failed aluminum panel, and the interior damage caused during test 7.

Figure 45. Fire Caused by Failed Aluminum Panel: Test 7

Figure 46. Damage to Interior: Test 7

The interior panels used during cargo configuration testing proved to be more flammable than the passenger configuration. Although both tests used the same heater parameters, cargo configuration test 4 experienced fire and ignition of off-gassing, whereas passenger configuration test 3 did not experience either.

3.1.8 Aircraft Damage Related to Thermal Signature.

Aircraft insulation was the primary barrier to thermal signature detection. This was shown through the relationship of aircraft damage to thermal signature. Figure 47 shows an image of interior damage taken post-test compared to a thermal image taken during test 3.

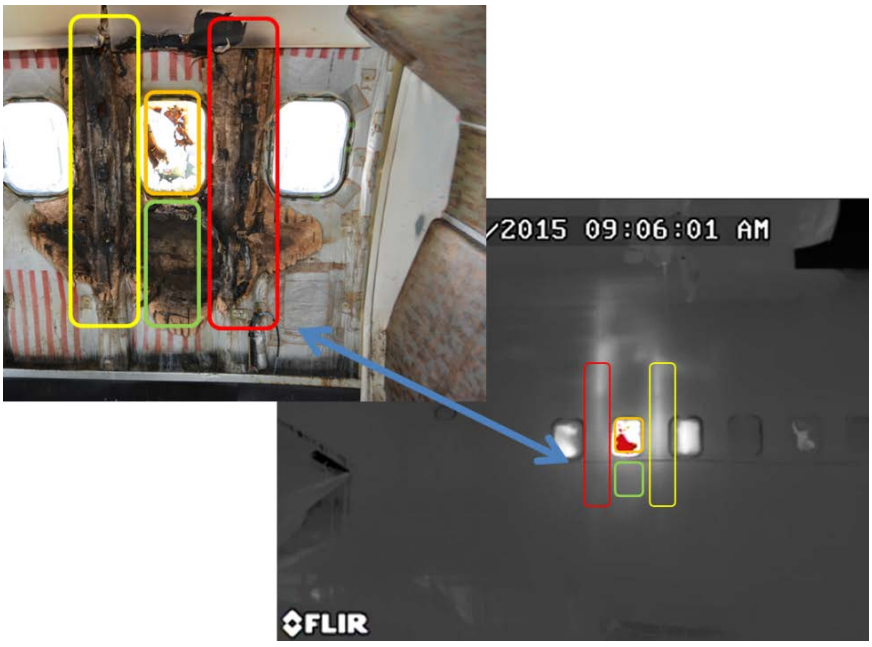

Figure 47. Aircraft Damage Related to Thermal Image: P660

If a fire is severe enough to damage insulation, it would display in the thermal image as a hot spot. Similarly, the failed aircraft window also displayed a thermal signature. These are the areas that are most likely to register as a hot spot during an aircraft fire.

3.2 SMALL-SCALE TESTING.

The test results from the experiments that used the quartz heater assembly in conjunction with aircraft fuselage material test panels are discussed in this section.

3.2.1 Characteristic Curves.

Characteristic curves were provided for the quartz heater assembly and the interior and exterior test panels. Since the same heater settings were used across all tests, these characteristics give insight into the typical temperatures achieved during testing for all panels.

3.2.1.1 Quartz Heater Assembly.

All heating curves are identical because the quartz heater assembly was given the same input of 1112°F. A single example of this curve is provided in figure 48.

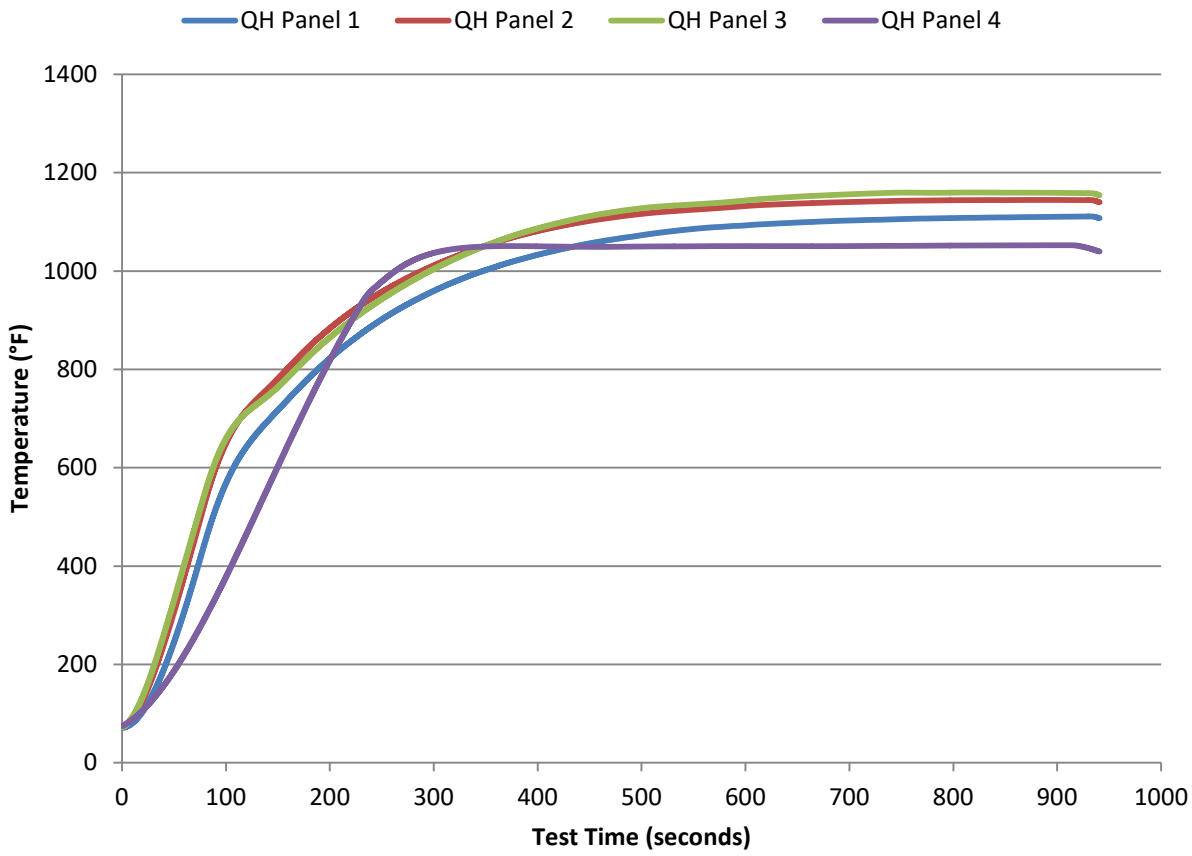

Figure 48. Quartz Heater Assembly Heating Curve

The heaters reached within ±5% of their set point of 1112°F within the first 6 minutes of the test. It should be noted that panel 4 had a lower maximum temperature of 1050°F because the heater operated on lower voltage. The lower maximum temperature was compensated by the higher maximum temperatures of panels 2 and 3, and as a result, the average maximum temperature equated to ±2% of the desired set point.

3.2.1.2 Test Panel Characteristic Curves.

With all of the variables except the camera and the panel material held constant, the test panels' surface temperature could be compared to gauge their relative heat transfer ability. The average of the five exterior panel thermocouples was taken for a test of each panel type and compared in figure 49. The temperatures were normalized about the average panel temperature at each test start.

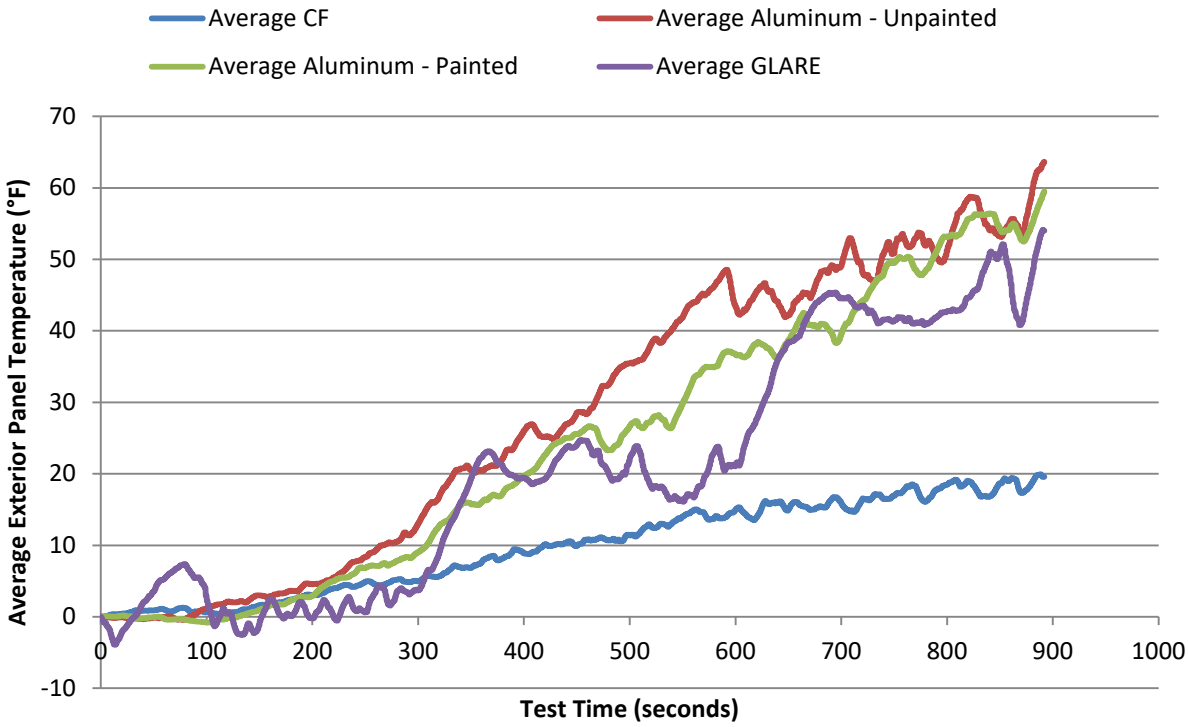

Figure 49. Comparative Heat Transfer Ability for Each Panel Type: Tests 1 Through 4

The aluminum panels transferred very similar amounts of heat to the exterior thermocouples. This was expected since the paint should not significantly affect conductivity to the thermocouples. GLARE was shown to transfer similar amounts of heat as the aluminum, while carbon fiber was shown to transfer much less than all other panels.

The average interior vs exterior temperature curves highlight the drastic difference in temperature between the interior and exterior panels, shown in figure 50. The primary cause was the insulation blanket. Similar to the testing within the L-1011, intact insulation played a pivotal role in preventing thermal signatures from being exposed to thermal cameras. In the case of

panel testing, a single layer of aircraft insulation provided a difference in temperature of up to 400°F.

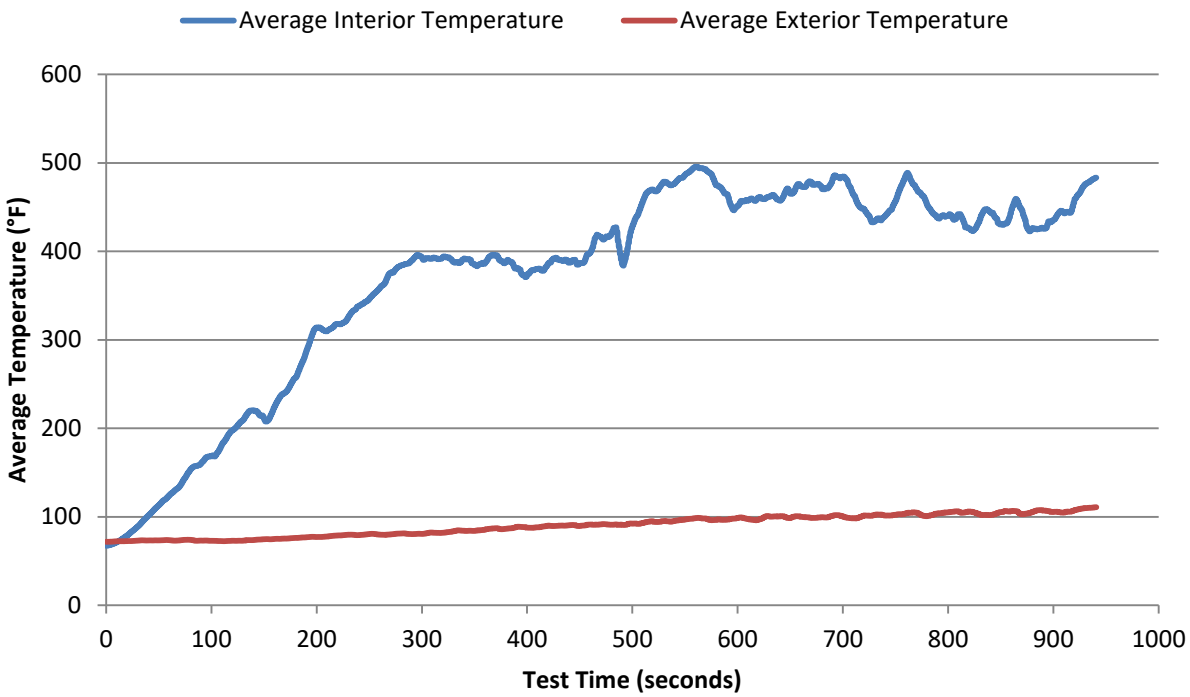

Figure 50. Average Interior vs Exterior Temperature: Test 1

3.2.2 Camera-Indicated Temperature vs Thermocouple Temperature.

Although the full set of test results is provided in appendix B, this section discusses differences between the camera-indicated temperature and the thermocouple temperature. Average measurement error for each panel, camera, and angle is displayed in tables 11 through 13.

Table 11 depicts the average camera measurement error for each panel. The difference between the true value (or thermocouple temperature) and measured value (or camera temperature) was averaged for each panel type.

Table 11. Average Camera Measurement Error by Panel Type

Panel Type	Average Camera Error (°F)
Carbon Fiber	-79.35
Aluminum—unpainted	0.242
Aluminum—painted	-41.47
GLARE	-60.29

Table 12 depicts average camera measurement error for each camera.

Table 12. Average Camera Measurement Error by Camera

Camera Type	Average Camera Error (°F)
T420	-56.27
P660	-43.228
XR	-39.56

Table 13 depicts average camera measurement error for each of the five angles tested.

Table 13. Average Camera Measurement Error by Camera Angle

Camera Angle	Average Camera Error (°F)
0°	-36.0
30°	-45.13
50°	-49.49
60°	-49.30
65°	-50.07

Nearly all camera measurements were at a higher apparent temperature than the thermocouples. This error may be attributed to several factors, the first being assumed emissivity. Each camera had its own default assumed emissivity for the surface that was measured. Since the test panels varied in their surface finish and material, their emissivity would also vary. The assumed emissivity may be closer for one panel than the other, reducing camera measurement error. An example of this assumed emissivity error is shown in figure 51.

The P660 screenshot shown in figure 51 defaults to an assumed emissivity of 0.95. The aluminum panel shown is smooth and painted with a paint that typically has an emissivity of 0.9 [6]. Assuming an incorrect emissivity would cause a measurement error.

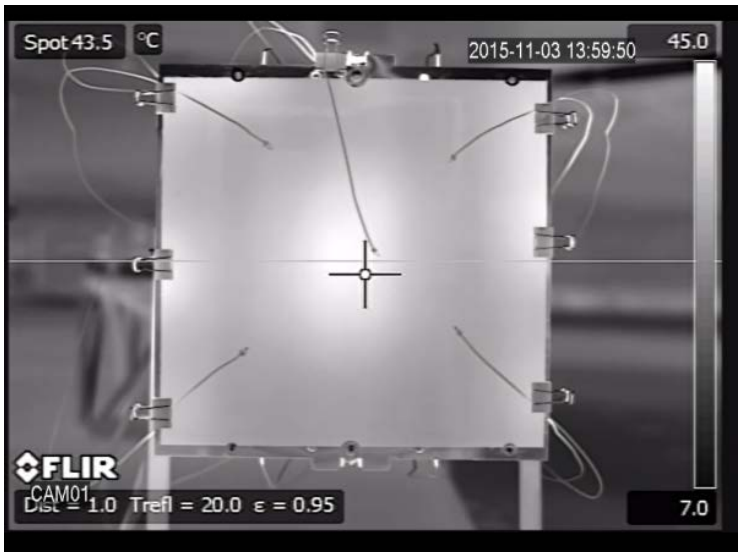

Figure 51. Sample of Assumed Emissivity Error

Unpainted aluminum had the smallest error compared to all other panels. This error was most likely due to its' low emissivity and high reflectiveness. Since the exterior panel was insulated from the heater, the indicated thermocouple temperature was not much higher than the ambient temperature. Instead of measuring the unpainted aluminum panel, the IR cameras instead read the scene behind the cameras, which decreased camera-indicated temperature. An example of this phenomenon is shown in figure 52, in which the reflection of the camera, camera stand, and background behind the camera were clear in the unpainted panel reflective surface. The camera did not correctly read the test panel temperature, but instead read the temperature of the scene behind the camera.

Figure 52. Sample of Panel Reflection Error

Average camera temperature was shown to increase as the cameras were positioned at a greater angle relative to the test panel. The primary cause of this error was likely due to the interference of the IR heaters. As the camera was positioned further away and at an increased angle from the

test panel, the camera's spot indicator area became larger, meaning the spot indicator took the average over a greater area. This, in combination with the heater panels accounting for a larger area in the camera's view, could account for the error increase in relation to increased camera angle. An example is shown in figure 53.

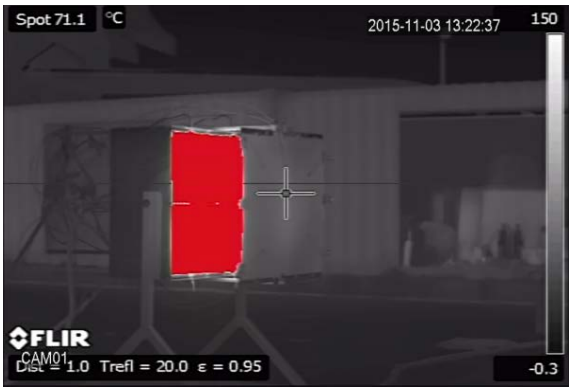

Figure 53. Sample of Camera Angle Error

Although the indicated temperature may contain error, thermal cameras offer the ability to view relative temperature across a surface. This capability provides identification of temperature gradients and hot spots. To determine accurate temperatures on various materials, the emissivity of each panel must first be determined.

3.2.3 Heat-Related Panel Damage.

Panel damage among the exterior test panels was little to none. The interior test panels exhibited charring and severe heat-related damages. An example of interior panel damage is shown in figure 54. The cargo liner or insulation blankets did not propagate an open flame at any point during the tests. The behavior and damage to the cargo liner panels was similar to the damage noticed in the L-1011 testing. During all tests, off-gassing was prevalent, and the insulation was also damaged. Both the insulation panel and the cargo liner panel were replaced after every test.

Figure 54. Sample of Insulation and Interior Cargo Liner Panel Damage

3.2.4 Identification of Hot Spots.

GLARE panels exhibited a tendency to spread heat across the panel compared to carbon fiber and aluminum panels. The heater assembly frame was far less identifiable in the heat signature

of the GLARE panel than the carbon fiber and aluminum panel. This is displayed in figures 55 and 56.

Pre-test (unheated) images are shown on the left sides of the figures , and the post-test warmed images are shown on the right. The GLARE panel has more consistent warming across the surface of the panel, as shown in its relatively consistent pink hue. This GLARE trait was consistent across all cameras tested, but was best illustrated with the XR due to its default high-contrast multicolor mode. The frame is identifiable in the heat signature of the carbon fiber panel as the absence of temperature, identifiable to the right and left of center, which is represented with the white shading.

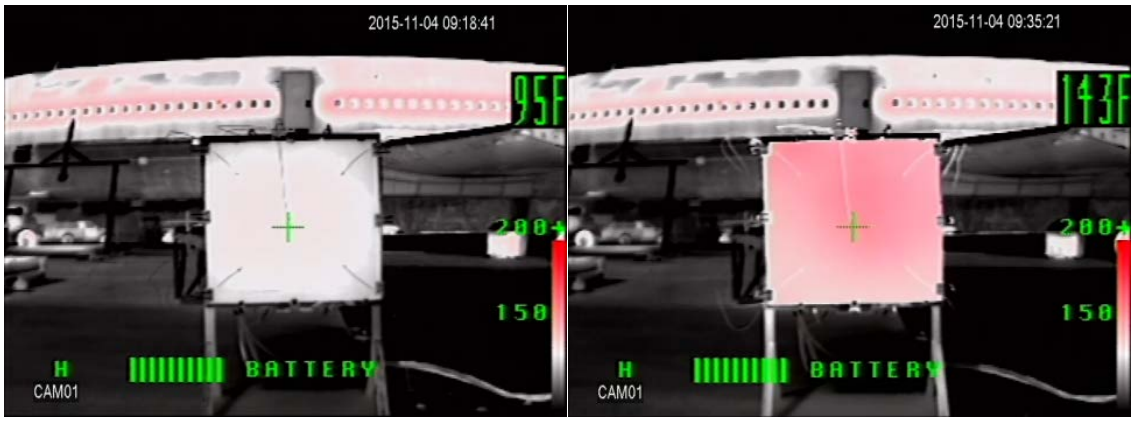

Figure 55. Hot Spot Identification for GLARE: XR

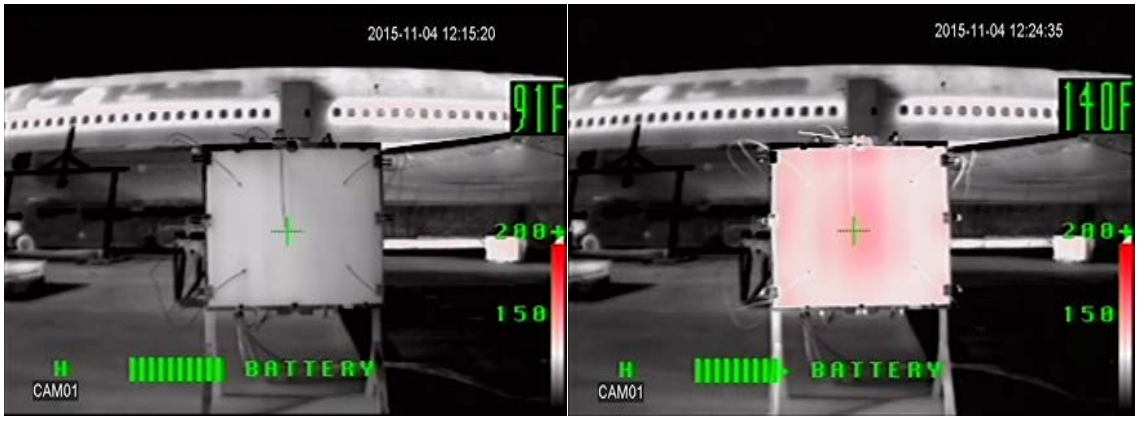

Figure 56. Hot Spot Identification for Carbon Fiber: XR

3.3 THE DEVS TESTS.

Acting as part of a DEVS, seven test scenarios were conducted to evaluate the performance of the different thermal cameras: a road test, a wooded area test, a rain test, a contrast filter evaluation, an auto-scaling test, 1500- to 2500-ft. aircraft detection tests, and a hot brakes test.

3.3.1 Road Test.

For this evaluation, some roads were partially wet from earlier rain; although at the time of the test, the sky was clear and sunny. Figures 57 and 58 show the different camera views when driving on an asphalt road. When comparing the cameras, it should be noted that the P660, the T420, and the XR provided a temperature range on the right side of their images, while the Patrol IR and the M625L did not provide any temperature range. In these two figures, although the Patrol IR and the IGG ELITE XR had similar images, the Patrol IR being more focused. The P660, T420, and M625L had similar images, with the M625L providing the most detail. The M625L provided clear distinction between trees along the road, and paint markings were clearly visible on the asphalt.

Figure 57. Asphalt Road Comparison I Using (a) Patrol IR, (b) P660, (c) T420, (d) XR, and (e) M625L

Figure 58. Asphalt Road Comparison II Using (a) Patrol IR, (b) P660, (c) T420, (d) XR, and (e) M625L

Figure 59 shows the view of the cameras when the FAA Striker was being driven on a dirt road. During testing, both the P660 and the T420 shifted slightly towards the right, showing more of the grass area than the dirt road. Although this occurred, the cameras showed a clear distinction between the grass area and the dirt road. The Patrol IR and XR had similar images, showing distinction between the grassy area and the dirt road; but the image from the XR was not well-focused. The M625L provided the most contrast between the grass area and the dirt road. Both the Patrol IR and the M625L had similar focus.

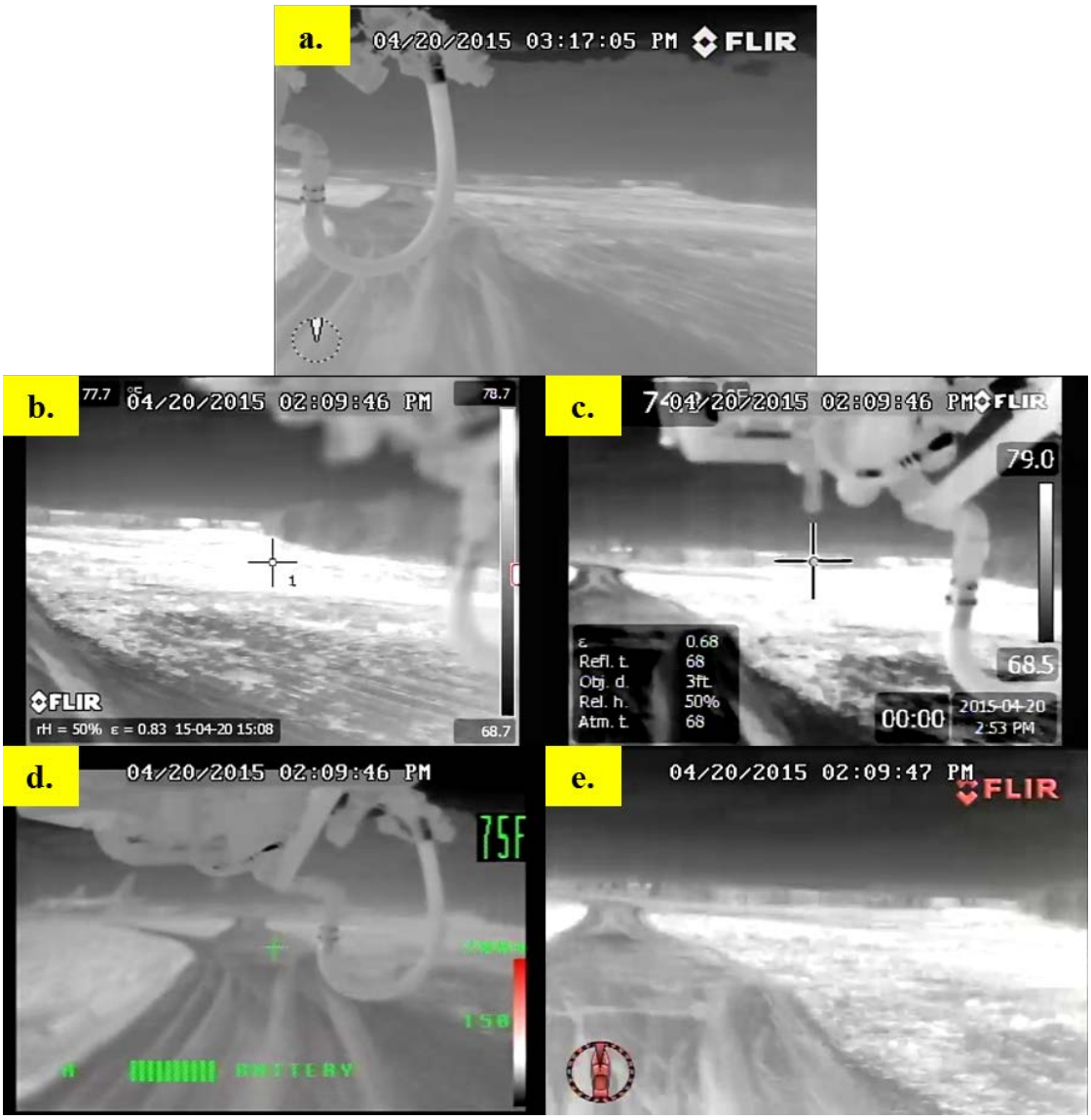

Figure 59. Dirt Road Comparison Using (a) Patrol IR, (b) P660, (c) T420, (d) XR, and (e) M625L

Figure 60 shows the view of the cameras when the FAA Striker was being driven on a gravel road. With the P660 and the XR, there was not a clear distinction between the grass area and the gravel road. The Patrol IR provided some contrast, but it was still difficult to differentiate the gravel road with the grass area. The T420 provided contrast between the gravel road and the grass area, but the image was not focused. The M625L provided both a clear contrast between the gravel road and the grass area and a clearly focused image.

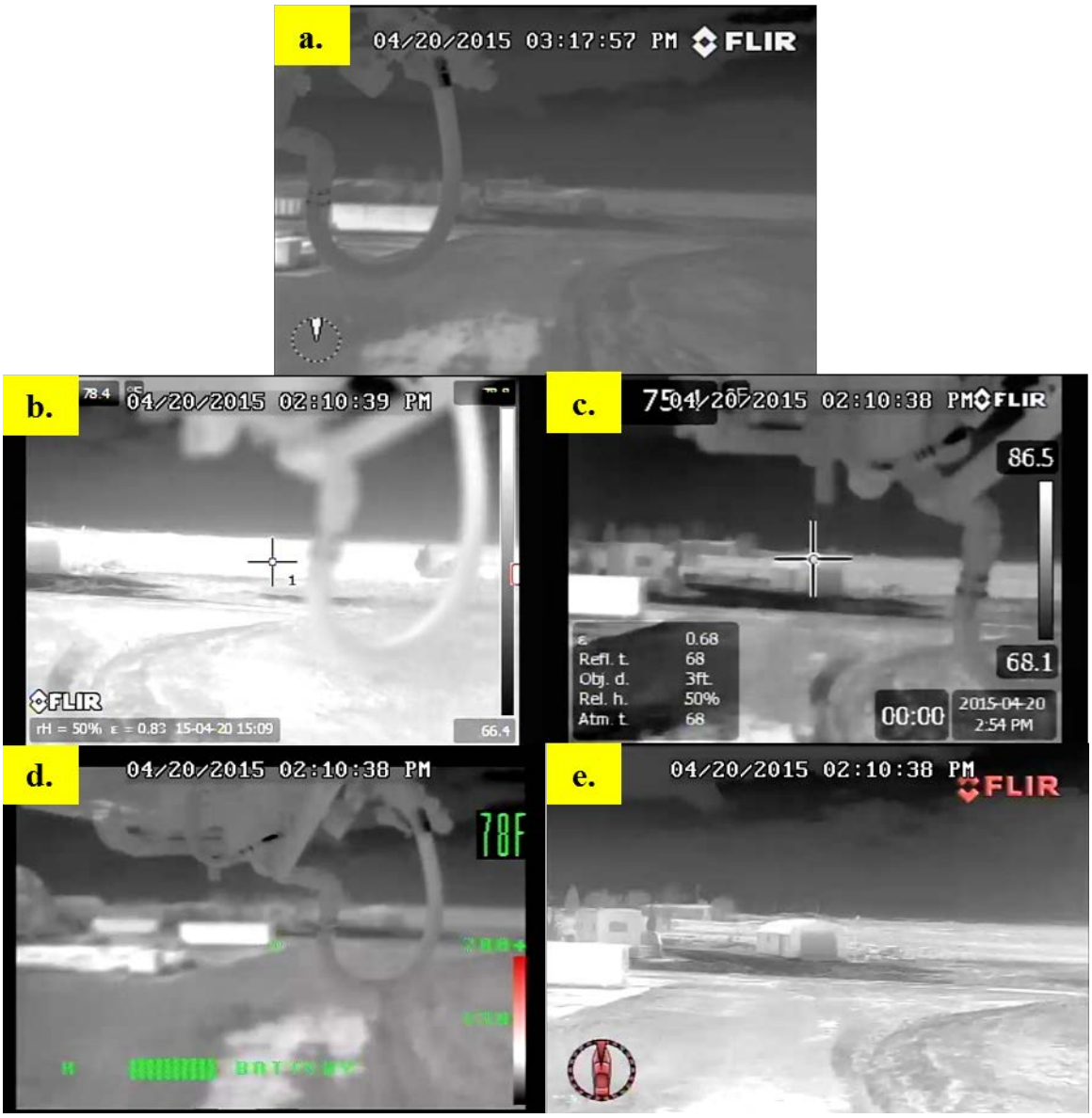

Figure 60. Gravel Road Comparison Using (a) Patrol IR, (b) P660, (c) T420, (d) XR, and (e) M625L

3.3.2 Wooded Area Test.

Many airports are located around wooded areas; and if an aircraft crashes in those wooded areas, the airport ARFF departments respond to the incident. Thermal cameras could be beneficial in not only locating the aircraft, but in locating passengers that may be wandering about the area. For this evaluation, the FAA Striker was positioned in front of a wooded area at the WJHTC, and the cameras were panned left and right to evaluate the visibility they offered when looking at the wooded area.

Different views from each camera are shown in figure 61. From the tests, the camera that provided the least amount of visibility was the XR. This camera did not provide a focused image

or a clear image of the trees. The Patrol IR provided a focused image but did not provide a clear image of the trees. The T420 camera provided a clear distinction between the trees, but did not provide a focused image because the camera was focused on the truck boom. Both the P660 and M625L provided a focused image and a clear distinction between the trees.

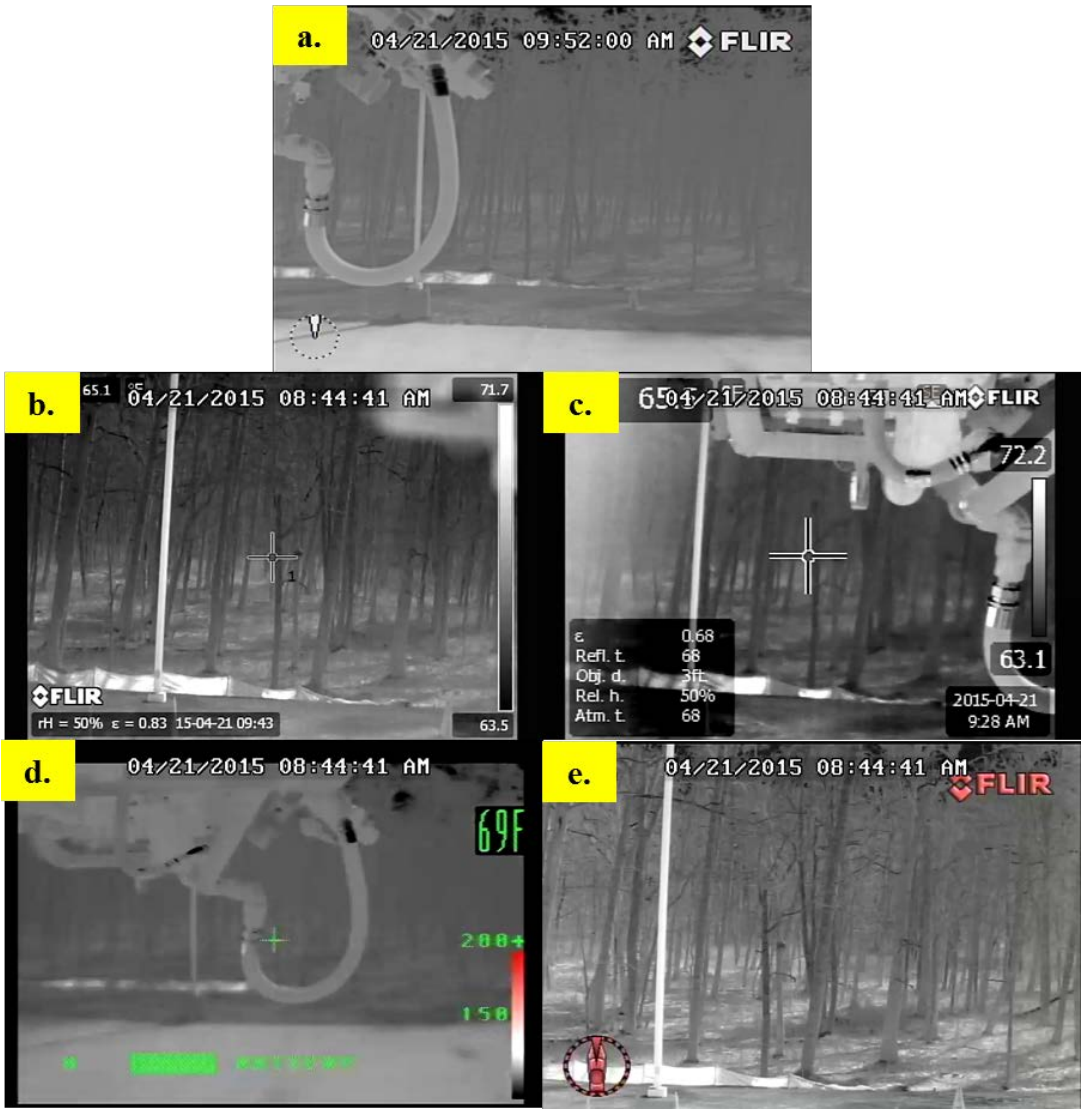

Figure 61. Wood Area Inspection Using (a) Patrol IR, (b) P660, (c) T420, (d) XR, and (e) M625L

3.3.3 Rain Test.

For the good weather conditions trial, the weather was clear with an ambient temperature of 70.0°F and a visibility of 10.0 miles. The clear weather trial is provided in figure 62. The non-paved road was distinguishable in all cameras tested; the clearest snapshot was taken with the M625L. If necessary, all five cameras tested could be used for navigation of the presented area.

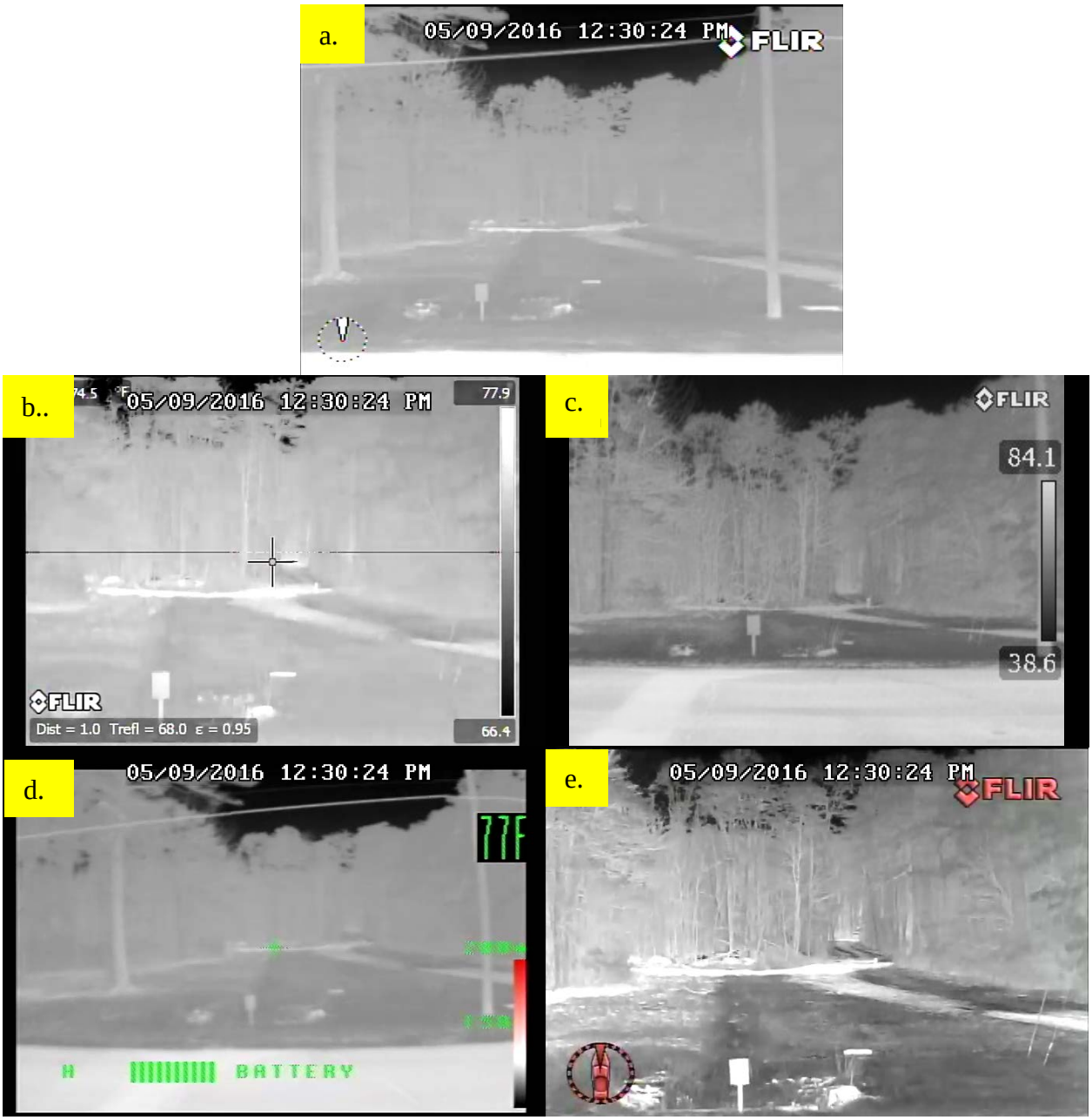

Figure 62. Baseline, Woods/Dirt Road View Using (a) Patrol IR, (b) P660, (c) T420, (d) XR, and (e) M625L

Moderate rain, defined as approximately 0.23 in./hour of perception, occurred during the test, as shown in figure 63. The weather conditions were 48.0°F with a visibility of 2.5 miles. Visibility through the thermal cameras was greatly reduced when compared to the clear weather conditions. The Patrol IR had the most drastic impact to visibility of the unpaved road and surrounding tree line. All cameras tested experienced a darkening of the image due to a reduction of IR light transmission through the rain. The M625L maintained the best image quality closely followed by the P660 and T420. If necessary, these three cameras could be used for navigation.

Figure 63. Moderate Rain, Woods/Dirt Road View Using (a) Patrol IR, (b) P660,(c) T420, (d) XR, and (e) M625L

Figure 64 is an image of the camera housing taken just after testing, which shows a clear view of the water accumulation on the camera lens. All cameras contained slight water accumulation during testing.

Figure 64. Rain Accumulation for Moderate Rain

The final test portrayed heavy rain conditions, defined as 0.53 in./hour of perception, which is shown in figure 65. The weather conditions were 48.0°F with a visibility of 1.0 miles and set in the same woods and road location as previous tests. All cameras tested produced images in which the road and wooded area were not easily detectable. The Patrol IR, T420, and XR produced images without recognizable landmarks. The P660 and M625L produced images with very little landmark detection with slight detection of the unpaved road. None of the cameras tested could be used for navigation in the heavy rain conditions experienced during testing.

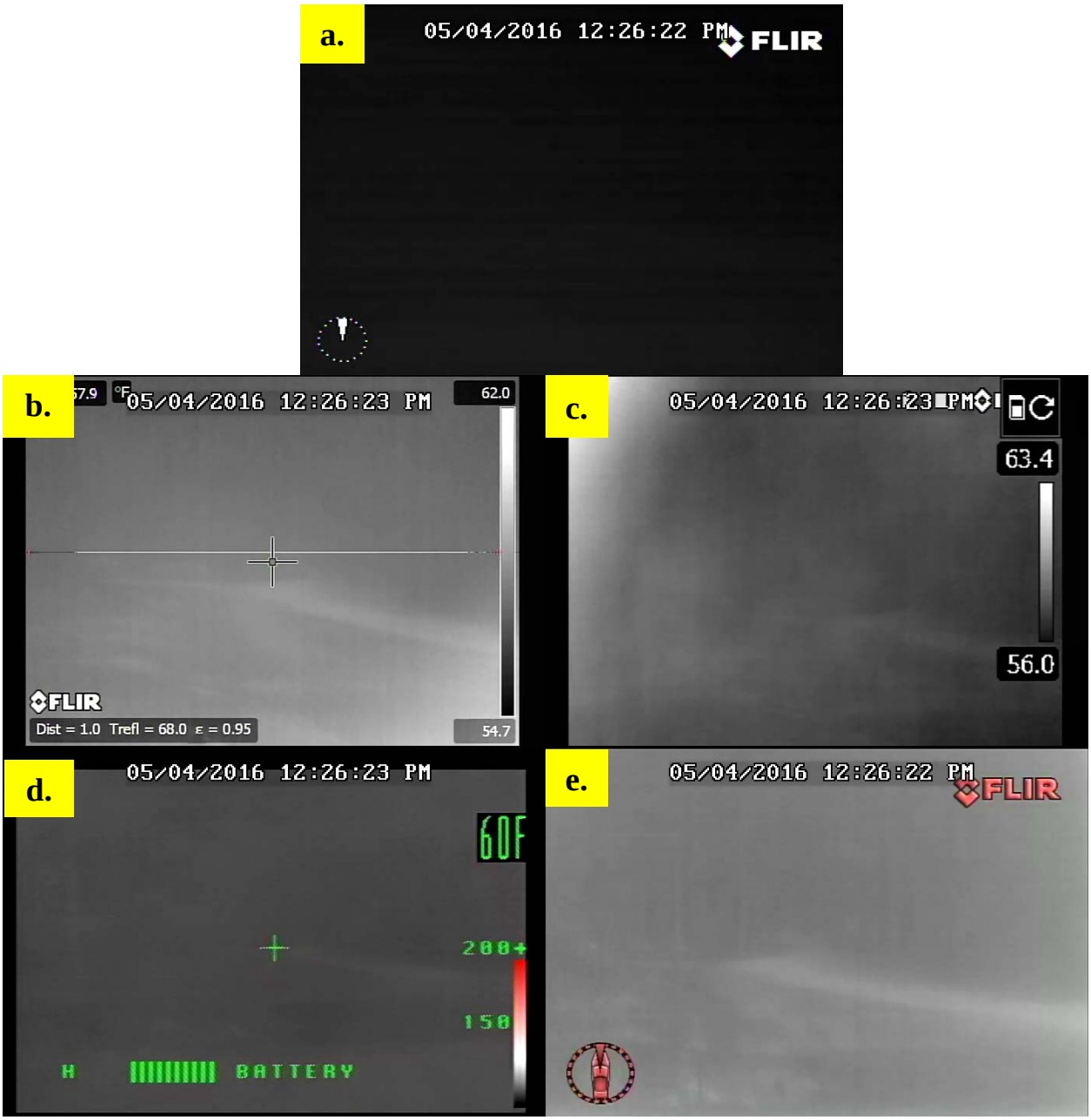

Figure 65. Heavy Rain, Woods/Dirt Road View Using (a) Patrol IR, (b) P660, (c) T420, (d) XR, and (e) M625L

Figure 66 shows the camera housing taken just after testing. Similar to figure 69, water accumulation on the lens is evident. Compared to moderate rain, the heavy rain trial resulted in larger water droplets on all lenses.

Figure 66. Rain Accumulation for Heavy Rain

3.3.4 Contrast Filter Test.

Figure 67 shows the five camera views before a fire was ignited. The XR provided the least distinguishable image out of the five cameras. It did not provide enough contrast between test setups and the surroundings and was not focused. The T420 provided contrast, but the image was still not focused. The Patrol IR provided a clear image and some contrast. The P660 and the M625L provided good contrast and a clear image.

Figure 67. The FAA Fire Test Facility Captured by (a) Patrol IR, (b) P660, (c) T420, (d) XR, and (e) M625L

Figure 68 illustrates the five camera views when there is a fire fully developed inside the 6-ft-square fire pan, and figure 69 shows when the extinguishing agent was applied into the fire. When evaluating the images from the P660 and the XR, the temperature range increases so high that the background was less visible. Furthermore, the high temperature from the fire was identified by the cameras by shading the areas red, which is known as overflow saturation color. They are "the areas that contain temperature outside the present level/span settings…" [7]. The background is almost completely black when looking at the P660. The Patrol IR and the T420 provided similar images of the fire. The background darkened but was still visible. For the M625L, although there were signs of image blooming about the fire, the contrast of the image was unaffected to a point that the firefighter is clearly visible. This was due to the M625L having a high-performance filter known as the digital detail enhancement (DDE). The DDE is "an advanced non linear image processing algorithm that preserves details in high dynamic range imagery. This detailed image is enhanced so that it matches the total dynamic range of the

original image, thus making the details visible to the operator even in scenes with extreme temperature dynamics" [8].

Figure 68. The 6-ft-Square Pan Fire Captured by (a) Patrol IR, (b) P660, (c) T420, (d) XR, and (e) M625L

Figure 69. The 6-ft-Square Pan Fire Being Extinguished Captured by (a) Patrol IR, (b) P660, (c) T420, (d) XR, and (e) M625L

Figure 70 displays a fully involved fire on the 3-D fire mockup. The ATRD team dispersed extinguishing agent into the 3-D mockup, as shown in figure 71 in screen captures from the five cameras. Like the previous test, the temperature range for both the P660 and XR was high enough to make the background less visible. Again, the fire was shaded red by both cameras. The T420 showed the fire, but nothing else was visible until the ATRD firefighter started applying agent into the fire. For the Patrol IR and M625L, the fire was so hot that gray shading appeared inside the fire. This is likely caused by the fire overwhelming parts of the camera. The M625L continued to provide the clearest image out of all the cameras.

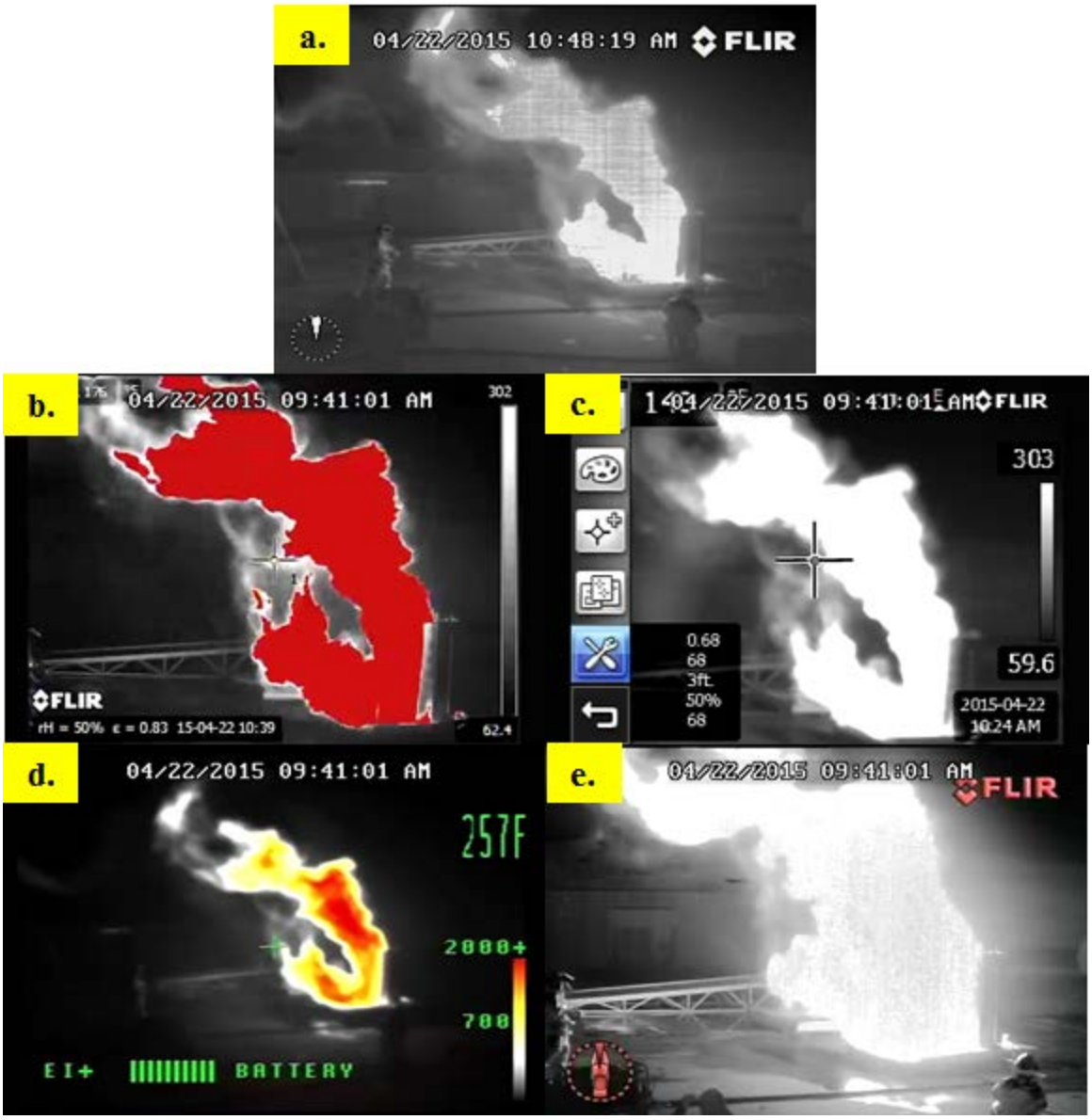

Figure 70. The 3-D Mockup Live Fire Captured by (a) Patrol IR, (b) P660, (c) T420, (d) XR, and (e) M625L

Figure 71. The 3-D Fire Being Extinguished Captured by (a) Patrol IR, (b) P660, (c) T420, (d) XR, and (e) M625L

3.3.5 Auto-Scaling Test.

The effect of auto-scaling was examined on cameras featuring the capability to change scaling ranges. The P660 and T420, which have the auto-scaling feature, were used to perform two tests using pan fires to analyze the effect of auto-scaling on the thermal cameras with this feature.

For the first test, the cameras were placed on their lowest scene scale. The cameras were directed towards the fire with the fire, surrounding area, and ATRD firefighters within the scene. The fire was then extinguished, and the test was repeated with the camera scene scale changed to the higher scene temperature range. Figure 72 shows the images provided from the two cameras with selectable scene scaling, where the lowest scene scale was selected. The fire was featured

in the center with an ATRD firefighter shown to the left of the test pan. The individual on the left and the surrounding area is clear on each camera.

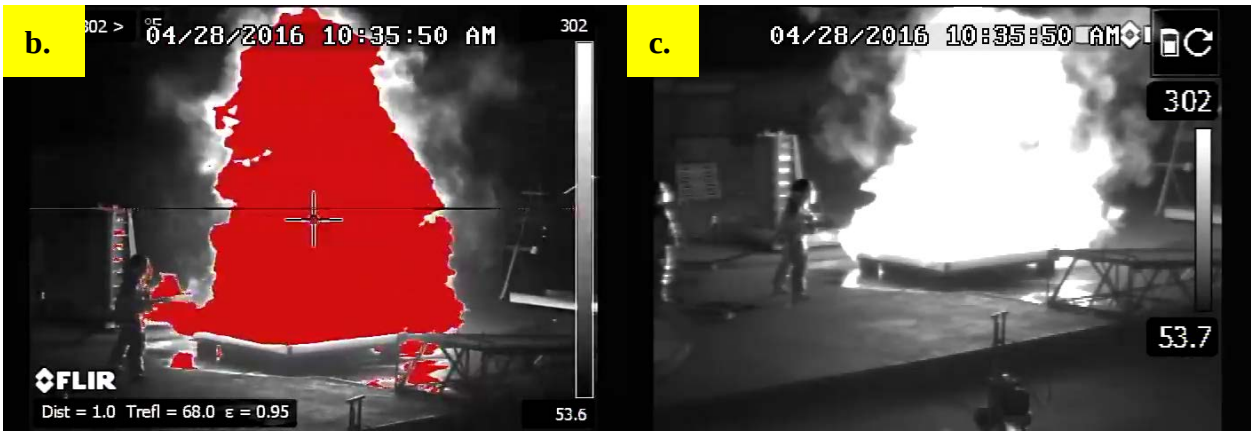

Figure 72. Pan Fire Test, Low-Temperature Scale Using (left) P660 and (right) T420

Figure 73 shows the images provided by two thermal cameras with selectable scene range with highest scene range selected. The fire is featured on the right with two ATRD firefighters shown on the left. When comparing the two selectable scene ranges, the lower selectable range provided the clearest images of the scene area with the fire, surrounding area, and individuals more visible than with the higher scene range. The higher selectable range darkens the area surrounding the test fire, leading to a more pronounced flame shape but reduced visibility of the ARTD firefighter and surrounding area.

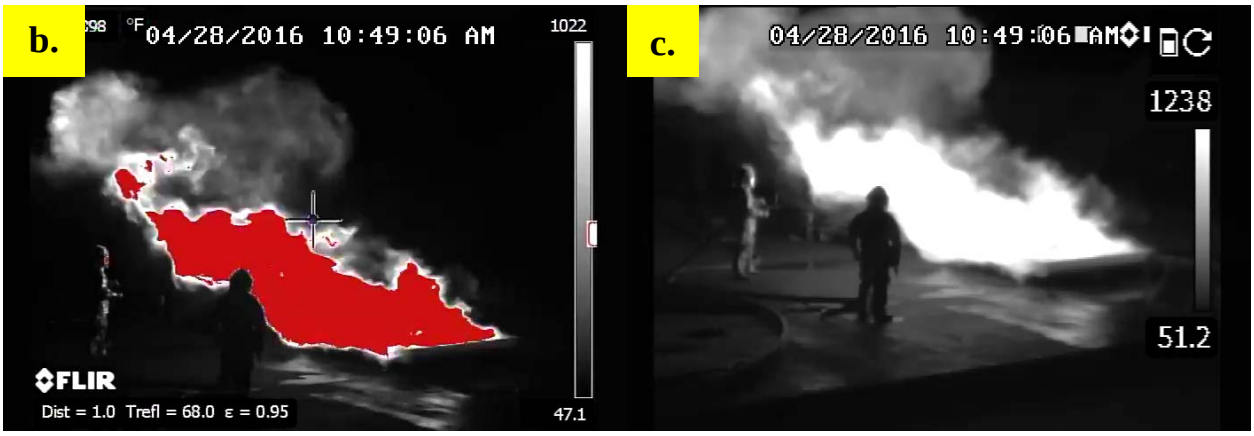

Figure 73. Pan Fire Test, High-Temperature Scale Using (left) P660 and (right) T420

3.3.6 Aircraft Detection Test.

DEVS distance evaluations were conducted at distances of both 1500 ft and over 2500 ft.

3.3.6.1 Evaluation at 1500 ft.

Evaluations for all cameras in the FLIR array began with an evaluation at 1500 ft. Displayed in figure 74 are images taken for each of the five cameras when the test vehicle was exactly 1500 ft away from the aircraft skin. The B-747SP aircraft is viewable in all six of the cameras, with the Patrol IR, P660 and M625L producing the clearest images. The aircraft is still detectable in the images produced by the T420 and XR, but the aircraft is more difficult to detect among the foliage. It should be noted that the focal points of the P660 and T420 cameras were adjusted by hand at the sighting position to the best of the operator's ability. The Patrol IR, the XR,and the M625L cameras did not have manual focal point adjustment.

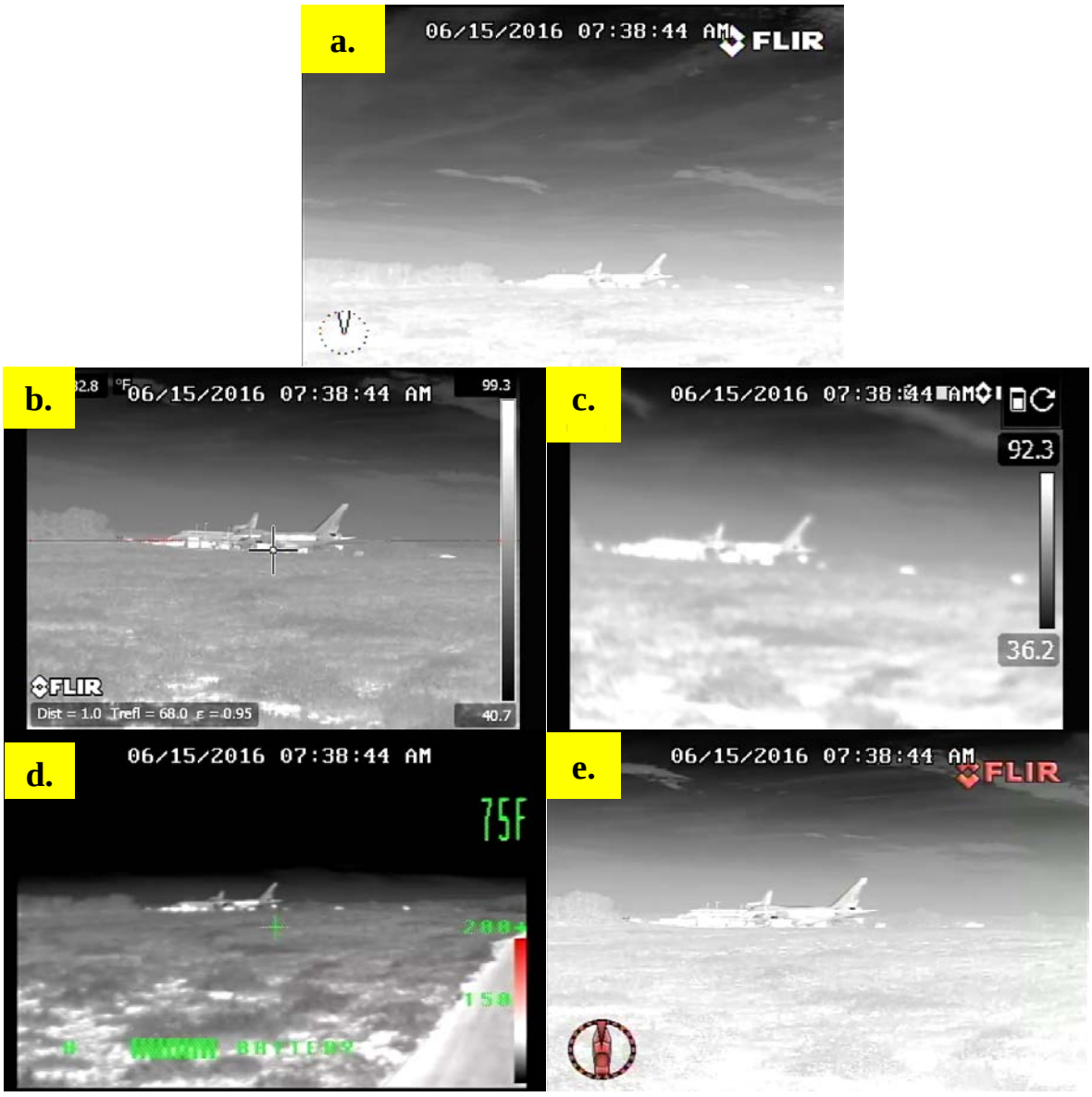

Figure 74. The 1500-ft DEVS Test Using (a) Patrol IR, (b) P660, (c) T420, (d) XR, and (e) M625L

Additional evaluations at a distance of 1500 ft were conducted using the L-1011. Screen captures of all cameras are provided in figure 75. The L-1011 is visible in all cameras at a distance of 1500 ft. The Patrol IR and M625L produced the best photos of the five tested. It should be noted that the Patrol IR has the zoom feature enabled in figure 75, whereas the feature was not enabled in figure 74. The P660 and T420 presented adequate aircraft images with some marginal contrast demarking the aircraft's fuselage and rear rudder. The XR produced the lowest quality image of the group. As in the prior test, the P660 and the T420 focal points were adjusted by the operator to exhibit their best possible performance.

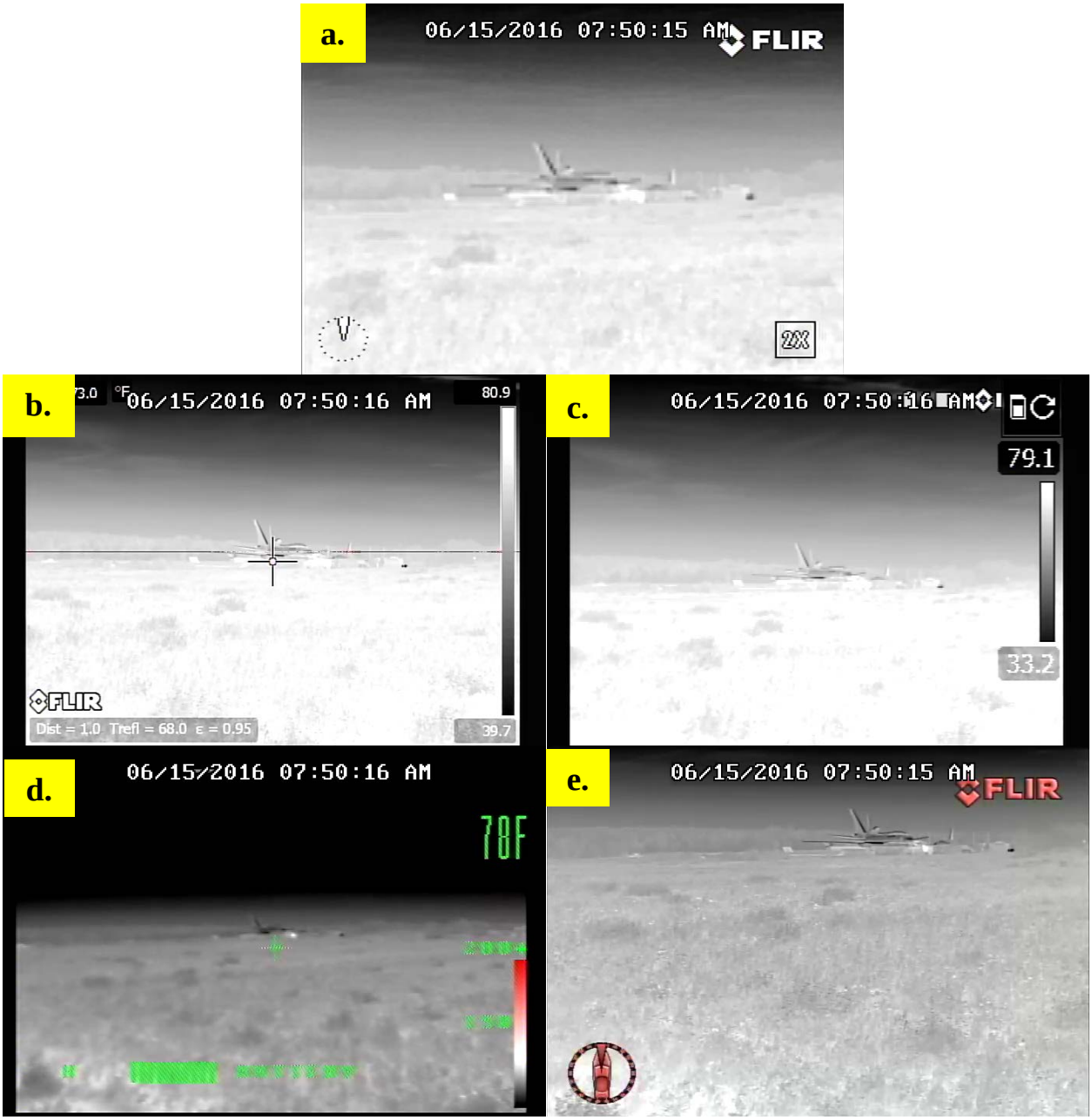

Figure 75. The 1500-ft DEVS Test Using (a) Patrol IR, (b) P660, (c) T420, (d) XR, and (e) M625L

3.3.6.2 Evaluation at Over 2500 ft.

Two tests of all thermal cameras were conducted at a distance of at least 2500 ft. One evaluation was conducted at nighttime, and the other was conducted during the daytime. The FAA Striker was positioned at the same location in the airport operations area of ACY, which provided sightlines to the runways, taxiways, and ramp areas. Aircraft undergoing normal operation around the airport were captured with the five cameras in the Striker's array on both occasions.

Figure 76 shows a turboprop passenger aircraft at approximately 3000 ft. The ambient conditions at the time were 75.0°F and 64% humidity. The aircraft can be viewed left of center in all of the thermal cameras. All cameras presented acceptable detection of aircraft in figure 75. Comparing the quality of the images provided, the Patrol IR, M625L, and P660 provided similar results. This was followed by the T420, which presents the aircraft but contains more IR noise from the environment, notably the grass in the bottom of the image. The XR provided an inferior image due to the field of range. The aircraft is difficult to detect as a result of the wide view provided by this camera.

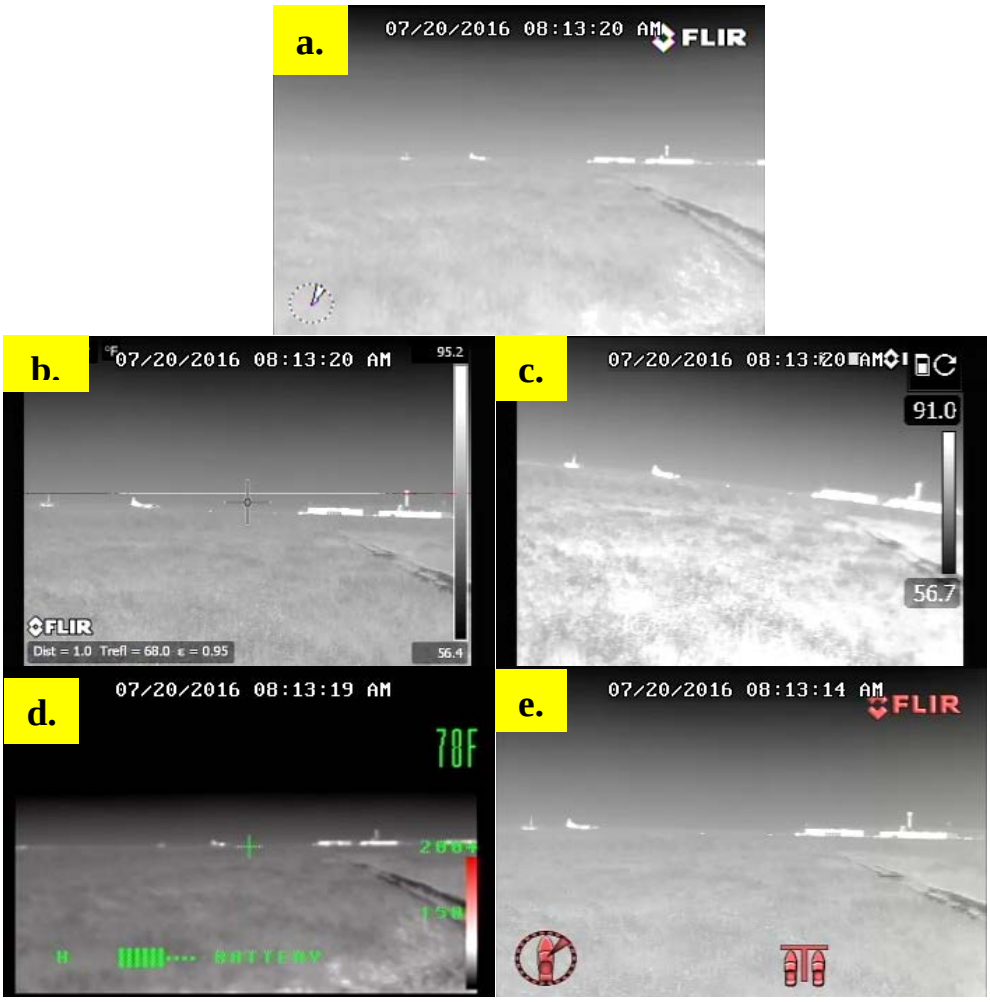

Figure 76. The 3000-ft DEVS Daytime Test Using (a) Patrol IR, (b) P660, (c) T420, (d) XR, and (e) M625L

Figure 77 contains images of a narrow-body commercial passenger aircraft during daytime operations. The aircraft was at approximately the same location as the aircraft shown in figure 76. The ambient conditions at the time were 75.0°F and 64% humidity. The aircraft is discernible in all images provided by the thermal camera array. The best image was developed by the M625L with the 2X digital zoom activated. The Patrol IR with 2X digital zoom activated, P660, and T420, produced very similar results. Although the aircraft can still be discerned in the XR's image, it presented the worst image quality of all cameras tested.

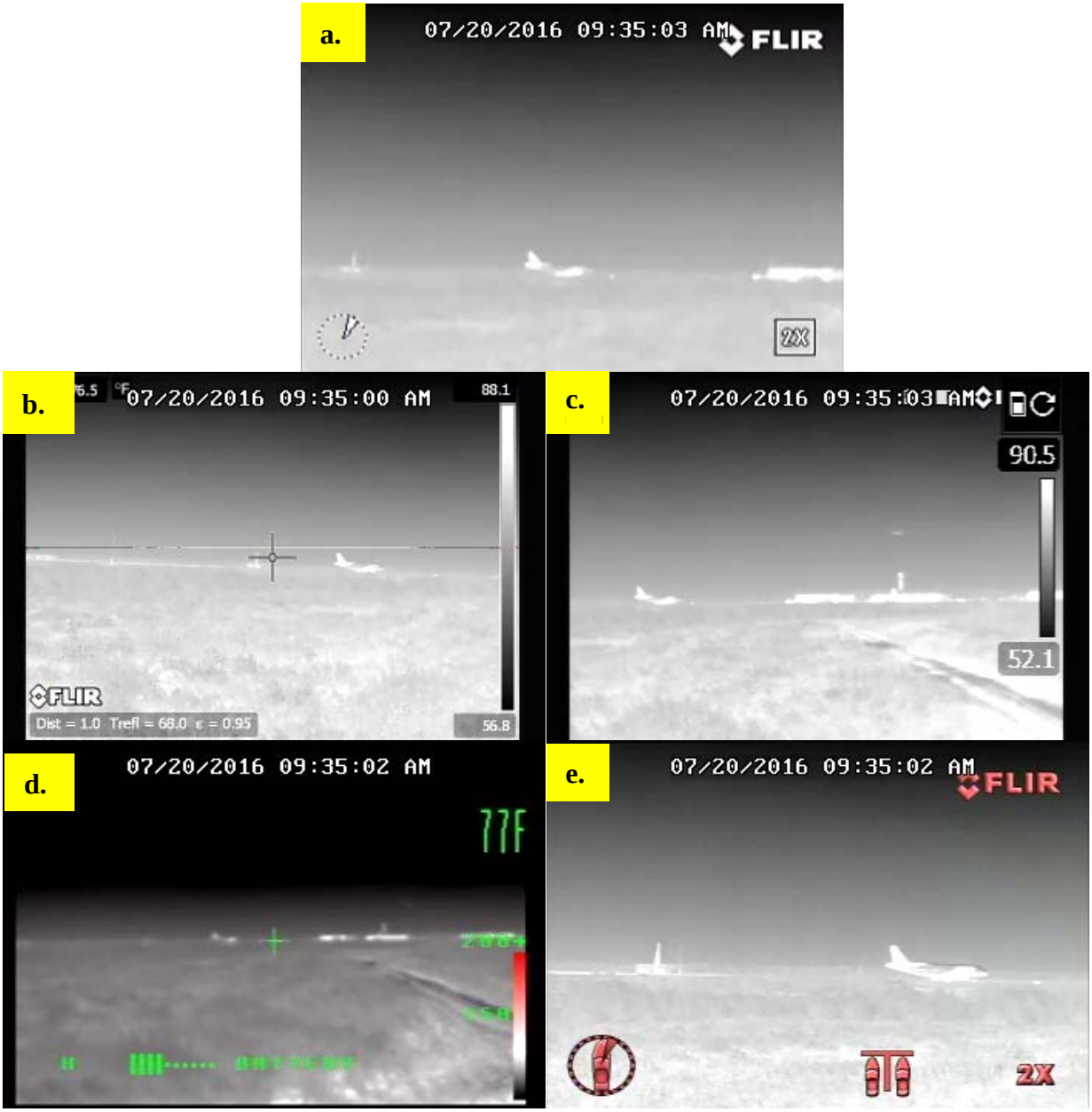

Figure 77. The 3000-ft DEVS Daytime Test 2 Using (a) Patrol IR, (b) P660, (c) T420, (d) XR, and (e) M625L

Figure 78 shows images produced by the thermal imaging array at nighttime. The aircraft was a medium-sized business jet taxing to a runway. The location of the aircraft is very similar to the aircraft in figures 76 and 77. The weather condition was 74.0°F with 68% humidity. Four of the five cameras tested provided an image of the aircraft that could be deemed as detectable by an operator. The M625L with the 4X digital zoom activated provided the clearest aircraft signature. The Patrol IR with 2X digital zoom activated, P660, and T420 provided similar results. The image created by the XR did not provide substantial evidence of the aircraft. Nighttime observation of the aircraft proved to be more difficult than daytime operation due to the thermal bloom created by the atmosphere just above the horizon. In this glow, the aircraft's thermal signature was difficult to detect without a digital zoom feature.

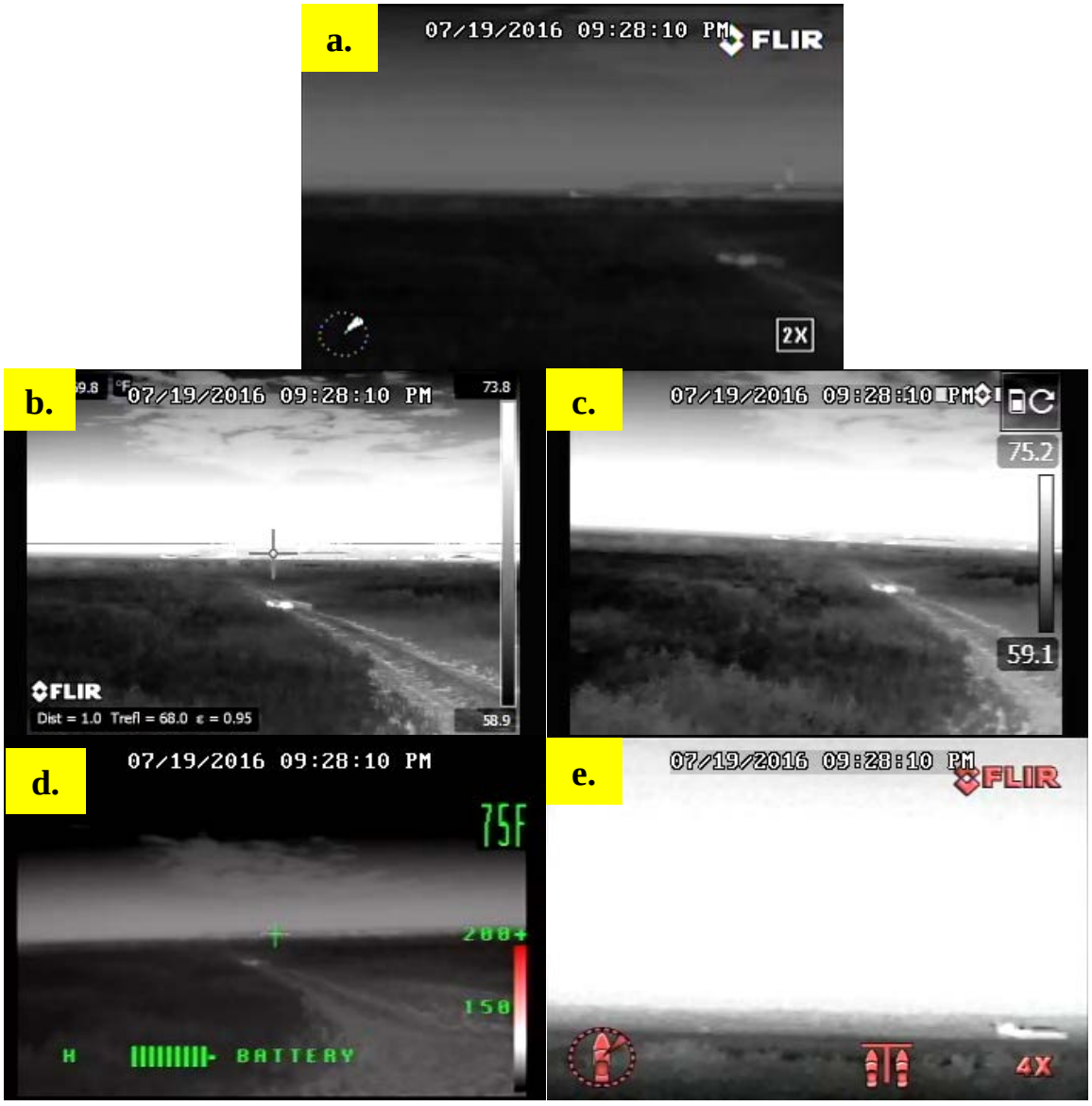

Figure 78. The 3000-ft DEVS Nighttime Test Using (a) Patrol IR, (b) P660, (c) T420, (d) XR, and (e) M625L

Another aircraft captured during nighttime operations was a narrow-body commercial passenger aircraft during landing and taxing. Images captured from all five cameras are provided in figure 79. The aircraft was approximately 2500 ft from the camera array with the same weather conditions as those described in the daytime test 2 shown in figure 78. All cameras presented a significant aircraft signature. The M625L with 2X digital zoom activated provided the clearest landing aircraft depiction, followed by the Patrol IR, the P660, and the T420, which all produced similar images. The Patrol IR may have produced a better image if the 2X digital zoom had been activated. The aircraft was barely visible in the XR camera, but a significant hot spot developed by the engine nacelle is evident in the image. Again, the aircraft signature can be difficult to ascertain because of the glow created by the atmosphere just above the horizon. This was especially prevalent in the P660 and T420 images.

Figure 79. The 2500-ft DEVS Nighttime Test Using (a) Patrol IR, (b) P660, (c) T420, (d) XR, and (e) M625L

3.3.7 Hot Brakes Test.

Different views of the B-727F test article's hot brakes are shown in figure 80. The Patrol IR and the XR provided the least amount of visibility were. The P660, T420, and M625L provided a focused image and clear brake thermal signatures. Because of the nature of the friction testing and the FAA Striker's role in the test being conducted, thermal aircraft brakes images from a closer proximity were not possible.

Figure 80. Hot Brakes Test Using (a) Patrol IR, (b) P660, (c) T420, (d) XR, and (e) M625L

The Patrol IR and M625L do not offer the ability to indicate a spot temperature, which may limit their usefulness in determining exact brake temperature. Further testing would be needed to

determine the correct emissivity setting for aircraft brakes to achieve accurate temperatures through the thermal cameras with spot temperature capability.

4. SUMMARY.

Thermal cameras are valuable tools ARFF personnel can use when assessing and responding to an incident. Currently, several different thermal camera tactics are taught to and used by ARFF personnel. The DFW FTRC showed students that TICs can be used to locate hot spots from the aircraft exterior and assist in finding the fire location.

During testing conducted within the L-1011 test article, all thermal cameras were shown to effectively locate the heat source within the aircraft and had similar performance with regard to detection time. It was determined that aircraft insulation is the greatest barrier to thermal camera identification of aircraft hot spots. Damage to insulation was proportional to the severity of the thermal signature from the aircraft exterior. The typical early hot spots included aircraft windows, or window blanks, and the frame members above the windows along the aircraft crown. There was not a significant difference between passenger and cargo configuration thermal signatures when the window blanks were properly insulated.

The wet-down strategy was shown to be effective in reducing false hot spots on the aircraft when using thermal cameras, especially when used in conjunction with a roll-up position, where more of the plane is in view, compared to a stand-off position.

During panel testing, all cameras were shown to contain error in indicated temperature vs actual temperature across all panel types. The Patrol IR and M625L were excluded from panel testing because of their lack of portability, permanence of mounting on the FAA Striker, and lack of spot temperature indicator. Error increased when the camera angle increased relative to the target. The cameras were, however, effective at displaying temperature gradients and at showing hot spots, even if reported temperatures were not accurate. GLARE panels were shown to exhibit less hot spots compared to aluminum and carbon fiber panels. Carbon fiber panels were shown to transmit the least amount of heat compared to aluminum and GLARE panels.

This research effort also examined how different thermal cameras affected the performance of a DEVS. Four different thermal cameras were evaluated and compared to a thermal camera that is used for current DEVS. The XR had the worst performance, and the M625L had the best performance. This result was consistent for moderate rain, but all cameras were not usable in heavy rain. For long distance (2500+ ft) aircraft detection, the M625L and Patrol IR exhibited the best performance, which can be attributed to their digital zoom features. The optimal maximum auto-scaling setting for the thermal cameras with the zoom feature was below 400°F. For hot brake performance, the P660, T420, and M625L provided a focused image and clear thermal signatures of the brakes when compared to the other cameras. The M625L does not offer the ability to indicate a spot temperature, which may limit its usefulness in determining exact brake temperature. Even if a camera offers this capability, more testing is required to determine the correct emissivity for finding brake temperatures.

When considering all potential uses of a thermal camera in an aircraft emergency scenario, the M625L camera performed the best. Cameras with a spot temperature feature offer the widest

array of functionality to an ARFF responder provided the emissivity is set properly for the surface that is being measured.

5. REFERENCES.

1. Vollmer, M. and Möllmann, K.-P., *Infrared Thermal Imaging: Fundamentals, Research and Applications*, Wiley-VCH, Germany, 2010.

2. Wright, J., Hampton, L., Grant, T., and Lewis, R., "Driver's Enhanced Vision System (DEVS)," FAA report DOT/FAA/CT-94/99, January 1995.

3. Federal Aviation Administration, "Driver's Enhanced Vision System (DEVS)," Advisory Circular (AC) 150/5210-19A, June 12, 2009.

4. Doig, W., "Aircraft Skin-Penetrating Nozzle Testing of a Freighter Aircraft Cargo Liner," FAA report DOT/FAA/TC-12/48, December 2012.

5. Torres, J. and Kreckie, J., "Full-Scale Evaluation of ARFF Tactics for Cargo Fires on Freighter Aircraft," FAA report DOT/FAA/TC-13/30, August 2013.

6. Brewster, M. Quinn, *Thermal Radiative Transfer and Properties*, John Wiley & Sons, Inc., Hoboken, New Jersey, 1992.

7. FLIR Systems, Inc., "User's Manual, FLIR B6xx series, FLIR P6xx series, FLIR SC6xx series," October 7, 2011.

8. FLIR Commercial Vision Systems B.V., "Digital Detail Enhancement (DDE)," FLIR technical note TN_0109_0003_EN, Breda, Netherlands, 2009.

APPENDIX A—LOCKHEED L-1011 THERMAL IMAGING CAMERA TEST RESULTS

Figures A-1 through A-35 show photographs of infrared (IR) camera screen captures of test evolutions for tests 1 through 7 using the following cameras: FLIR® Patrol IR (Patrol IR), FLIR® P660 (P660), FLIR® T420 (T420), ISG® ELITE XR, and FLIR® M625L (M625L).

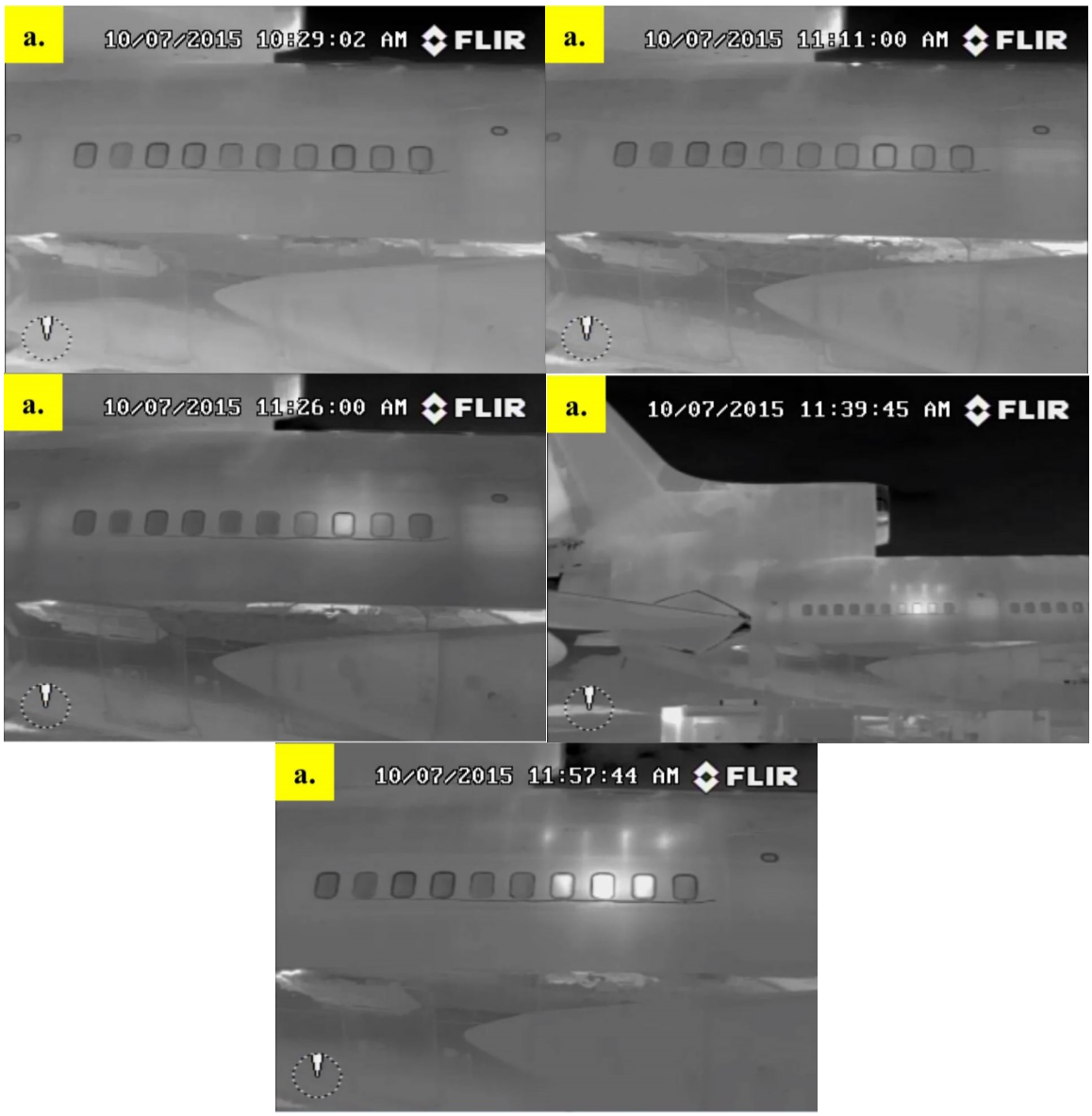

Figure A-1. Test 1 IR Camera Screen Captures: Patrol IR

Figure A-2. Test 1 IR Camera Screen Captures: P660

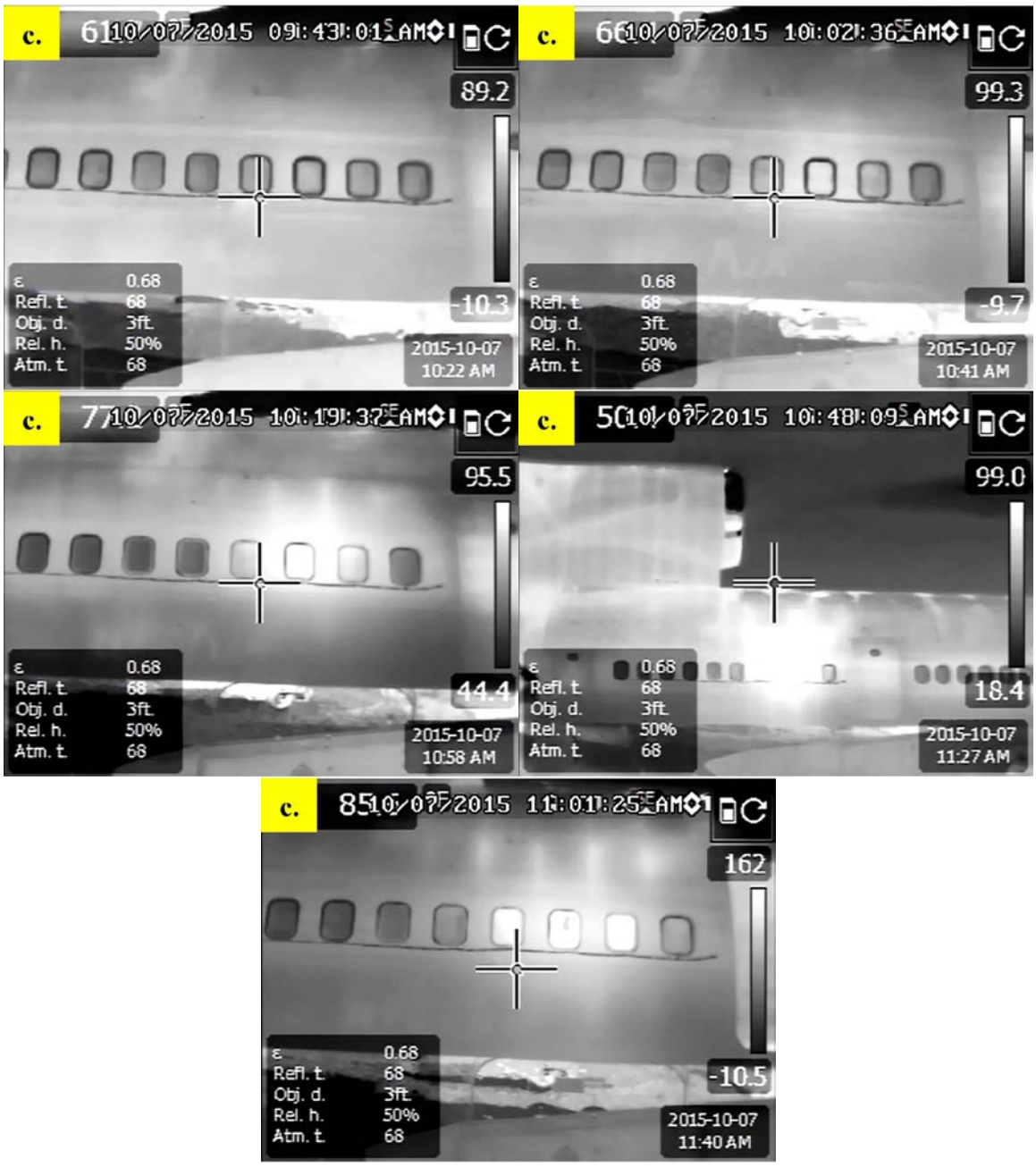

Figure A-3. Test 1 IR Camera Screen Captures: T420

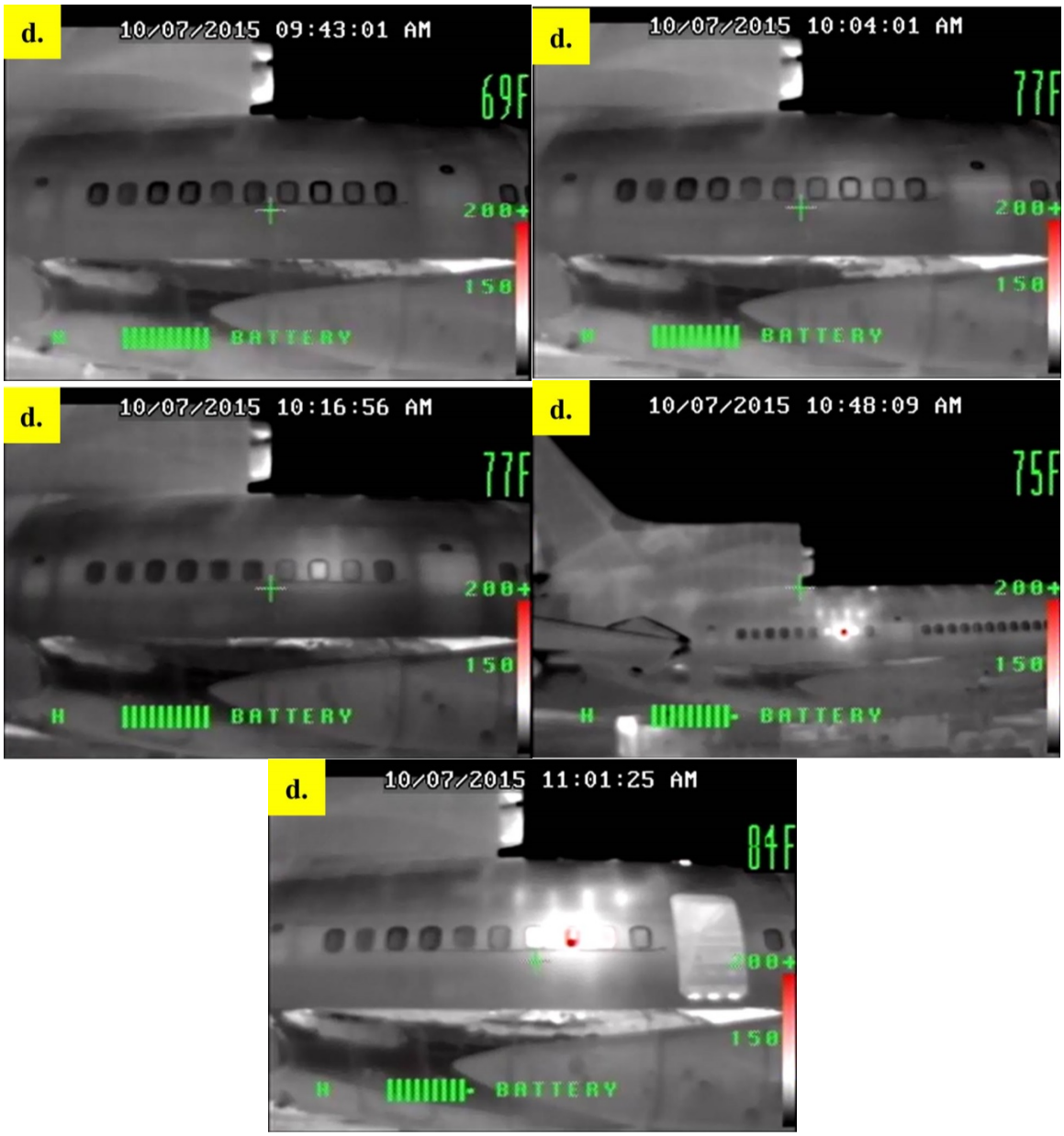

Figure A-4. Test 1 IR Camera Screen Captures: XR

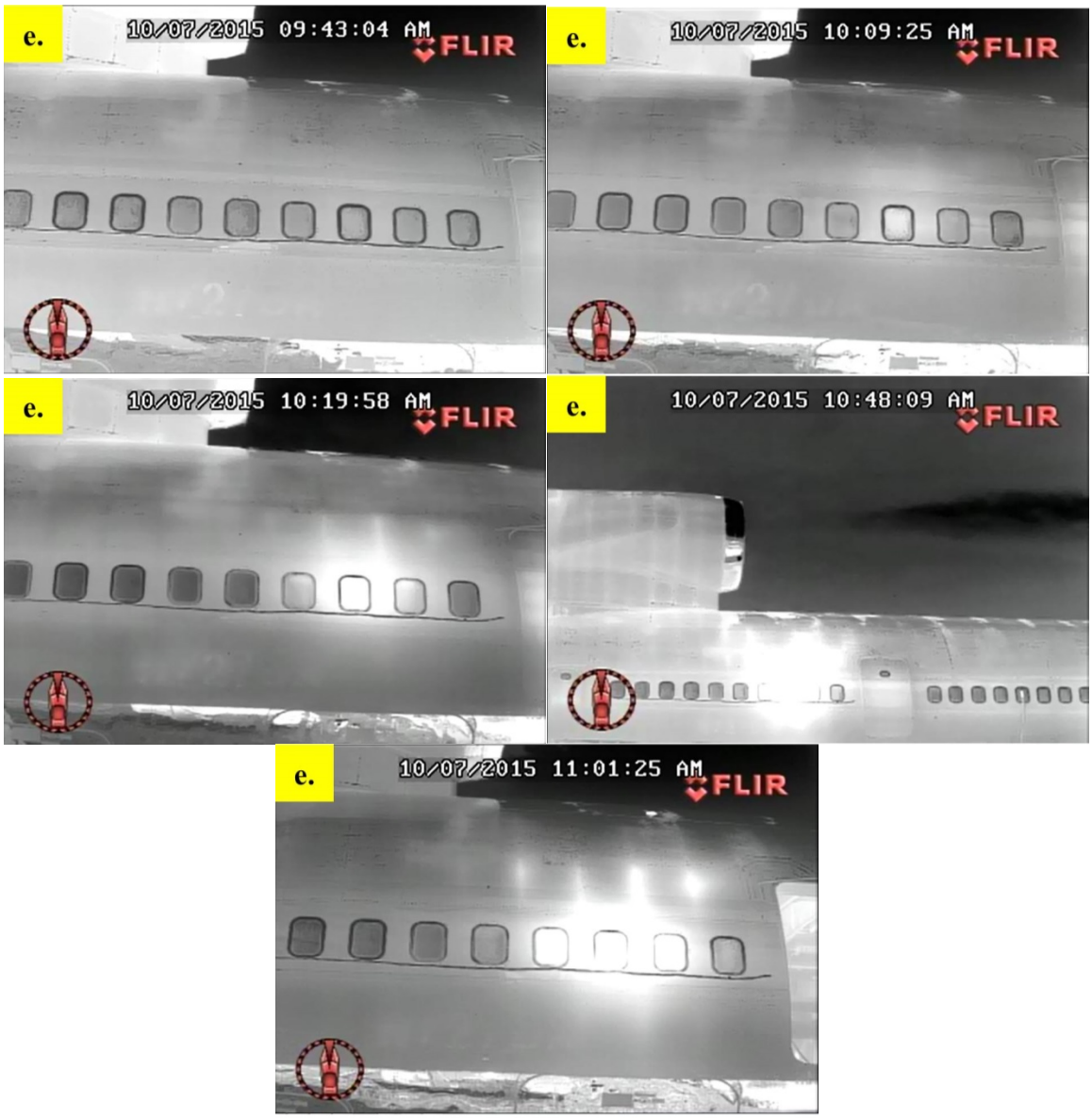

Figure A-5. Test 1 IR Camera Screen Captures: M625L

Figure A-6. Test 2 IR Camera Screen Captures: Patrol IR

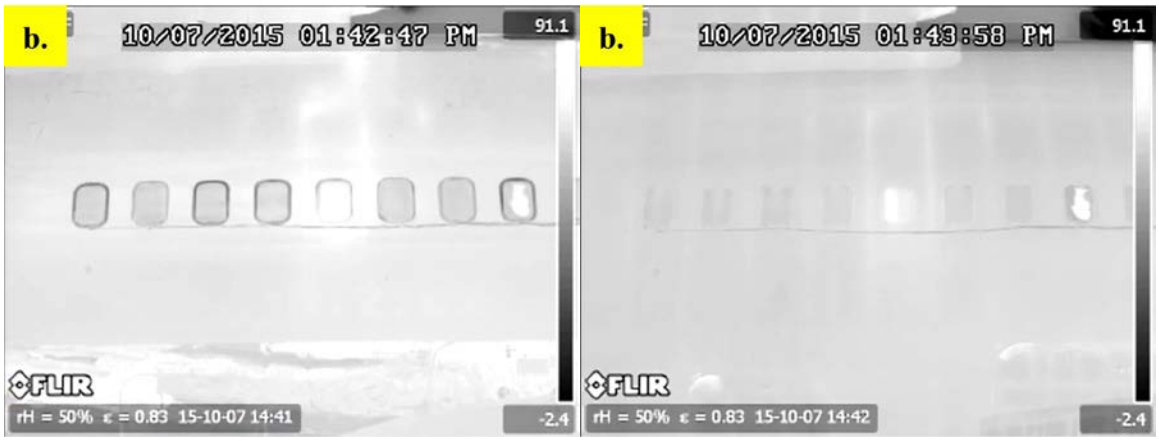

Figure A-7. Test 2 IR Camera Screen Captures: P660

Figure A-8. Test 2 IR Camera Screen Captures: T420

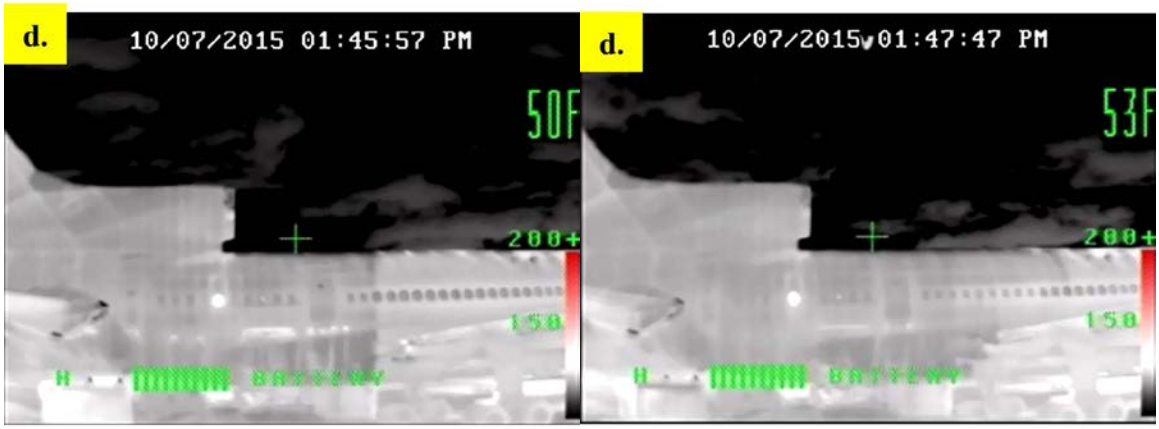

Figure A-9. Test 2 IR Camera Screen Captures: XR

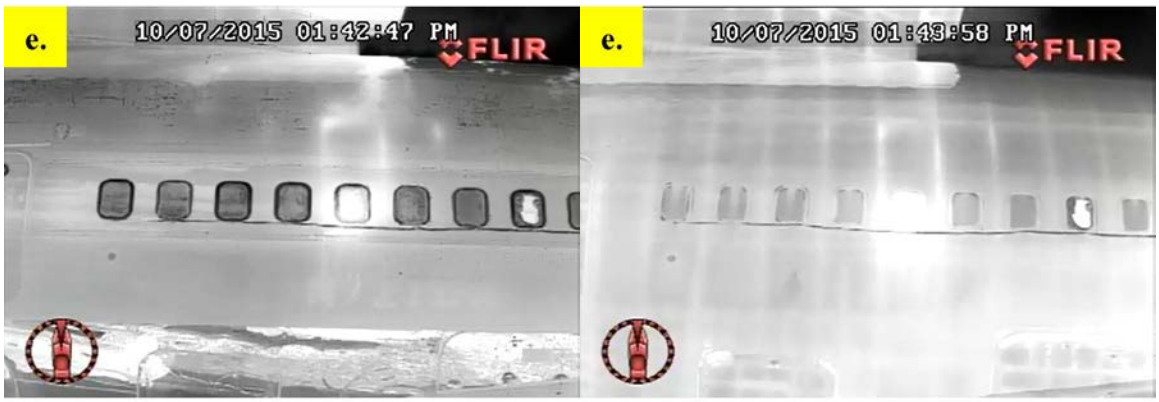

Figure A-10. Test 2 IR Camera Screen Captures: M625L

Figure A-11. Test 3 IR Camera Screen Captures: Patrol IR

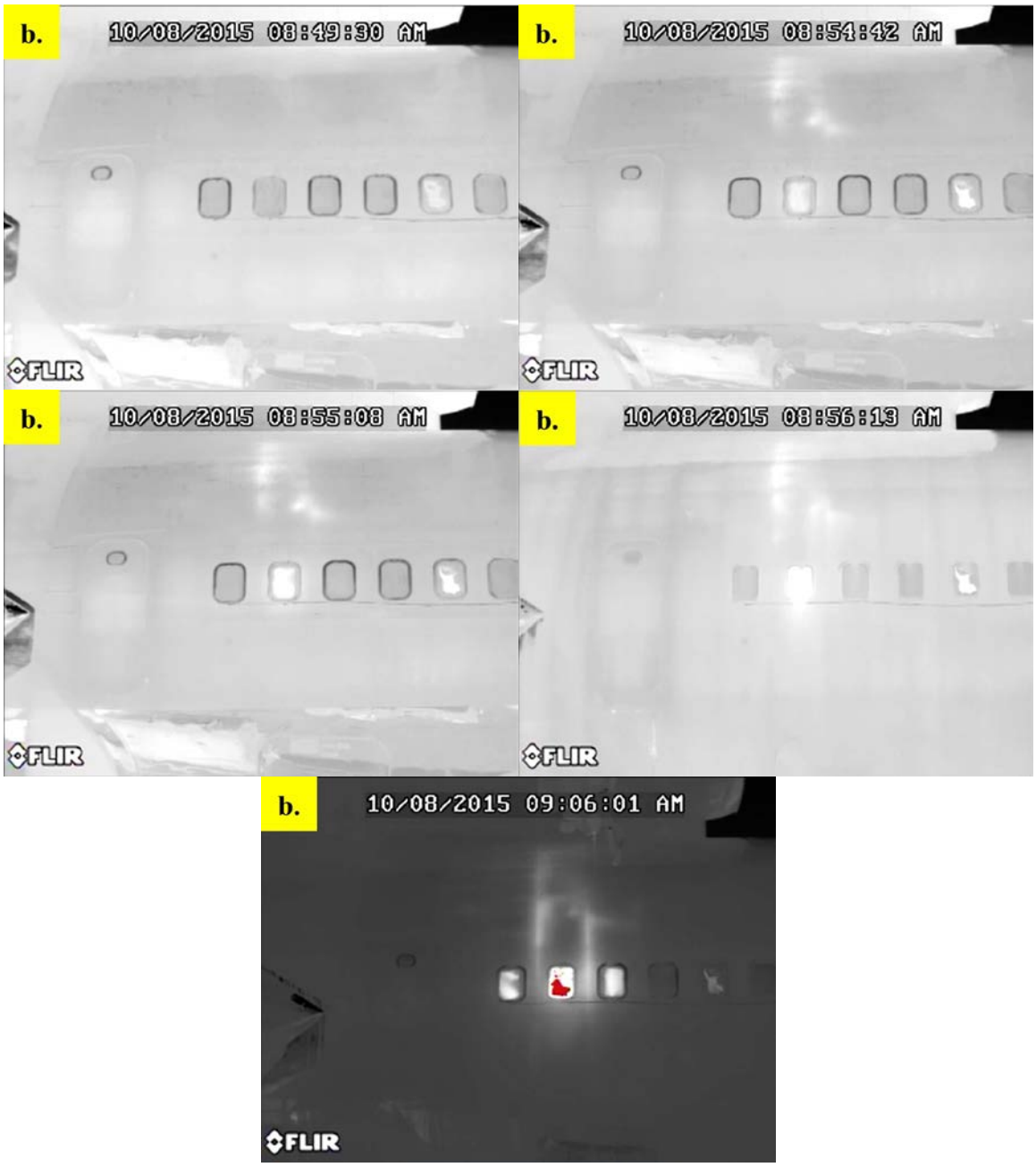

Figure A-12. Test 3 IR Camera Screen Captures: P660

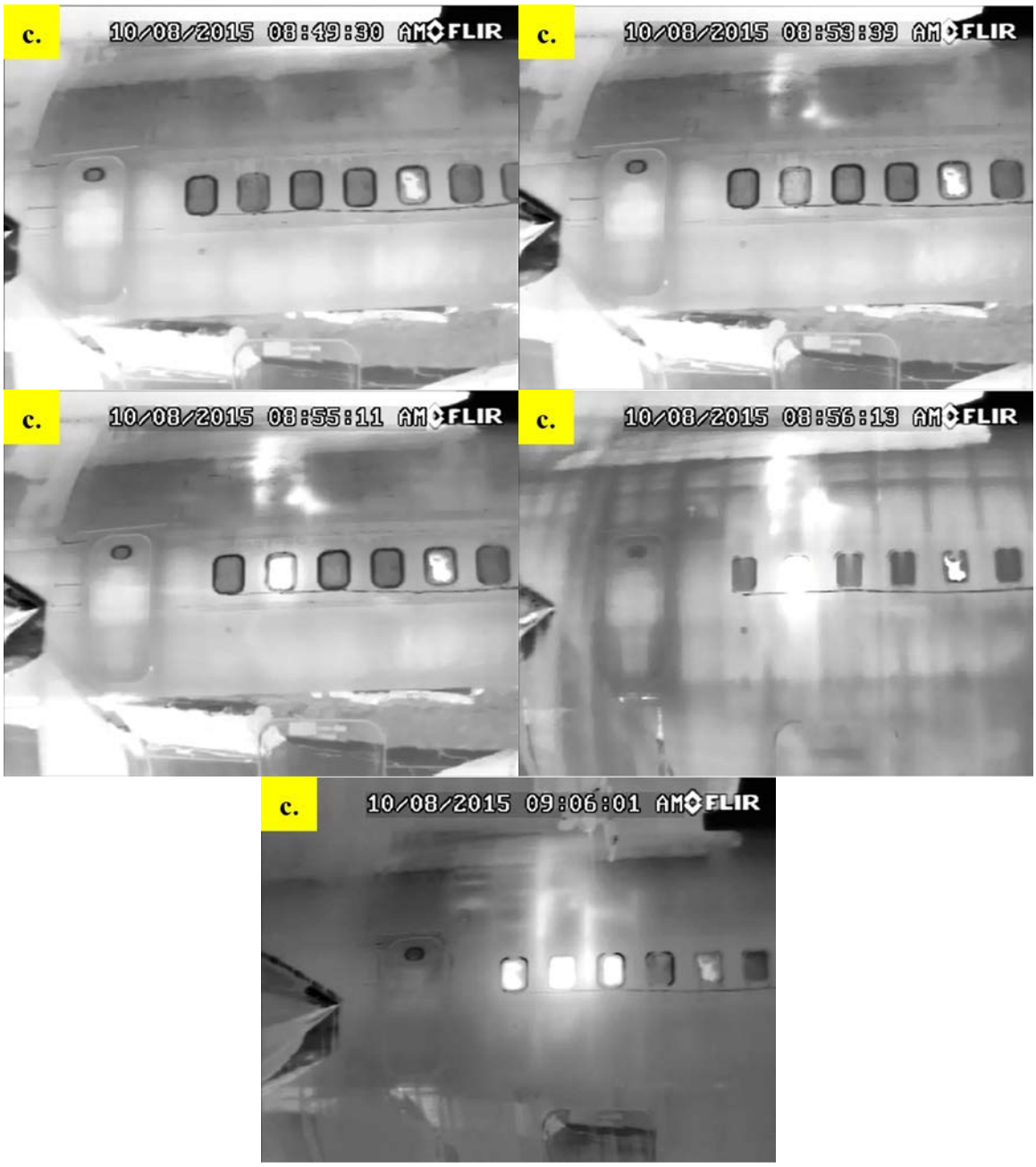

Figure A-13. Test 3 IR Camera Screen Captures: T420

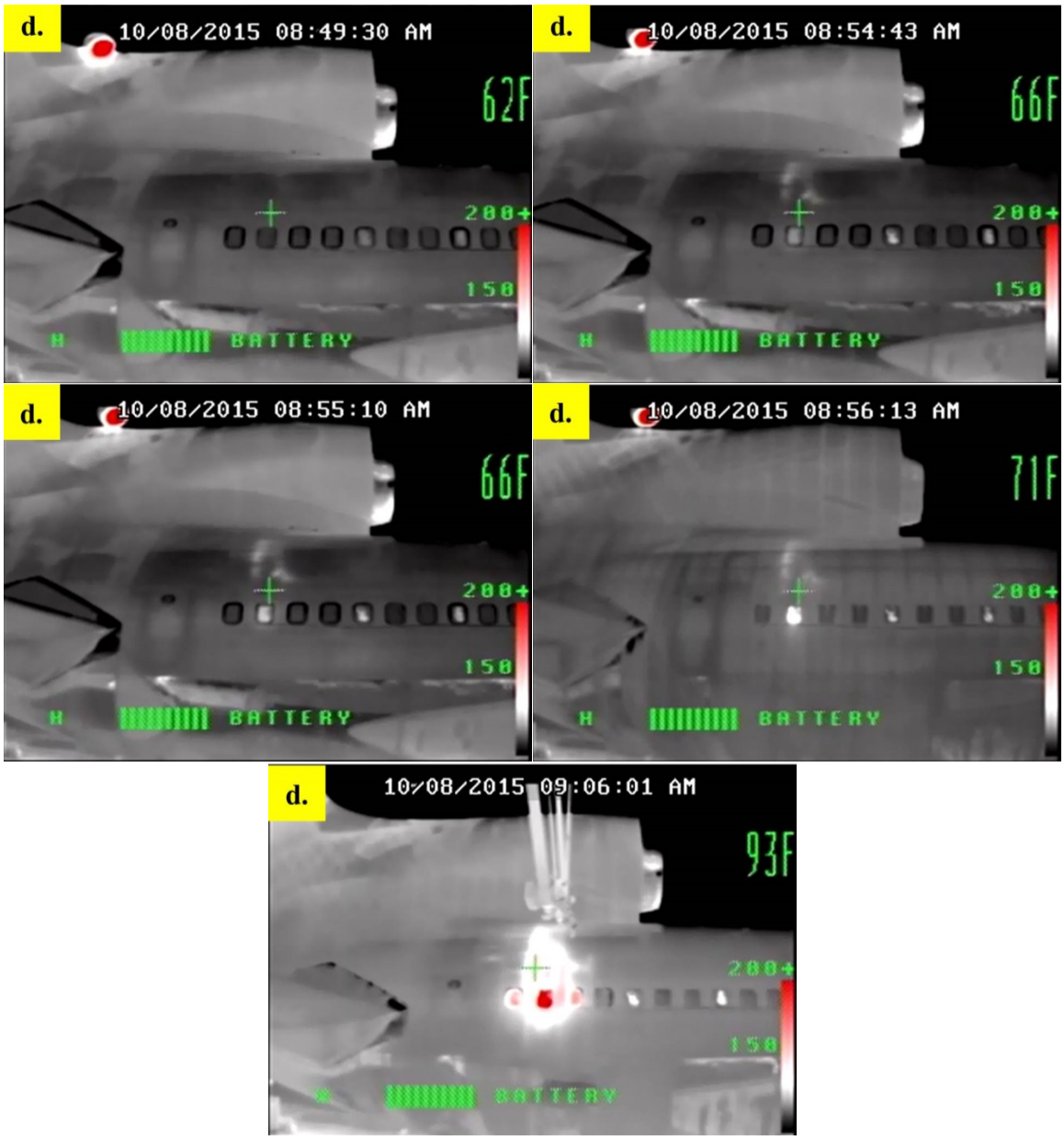

Figure A-14. Test 3 IR Camera Screen Captures: XR

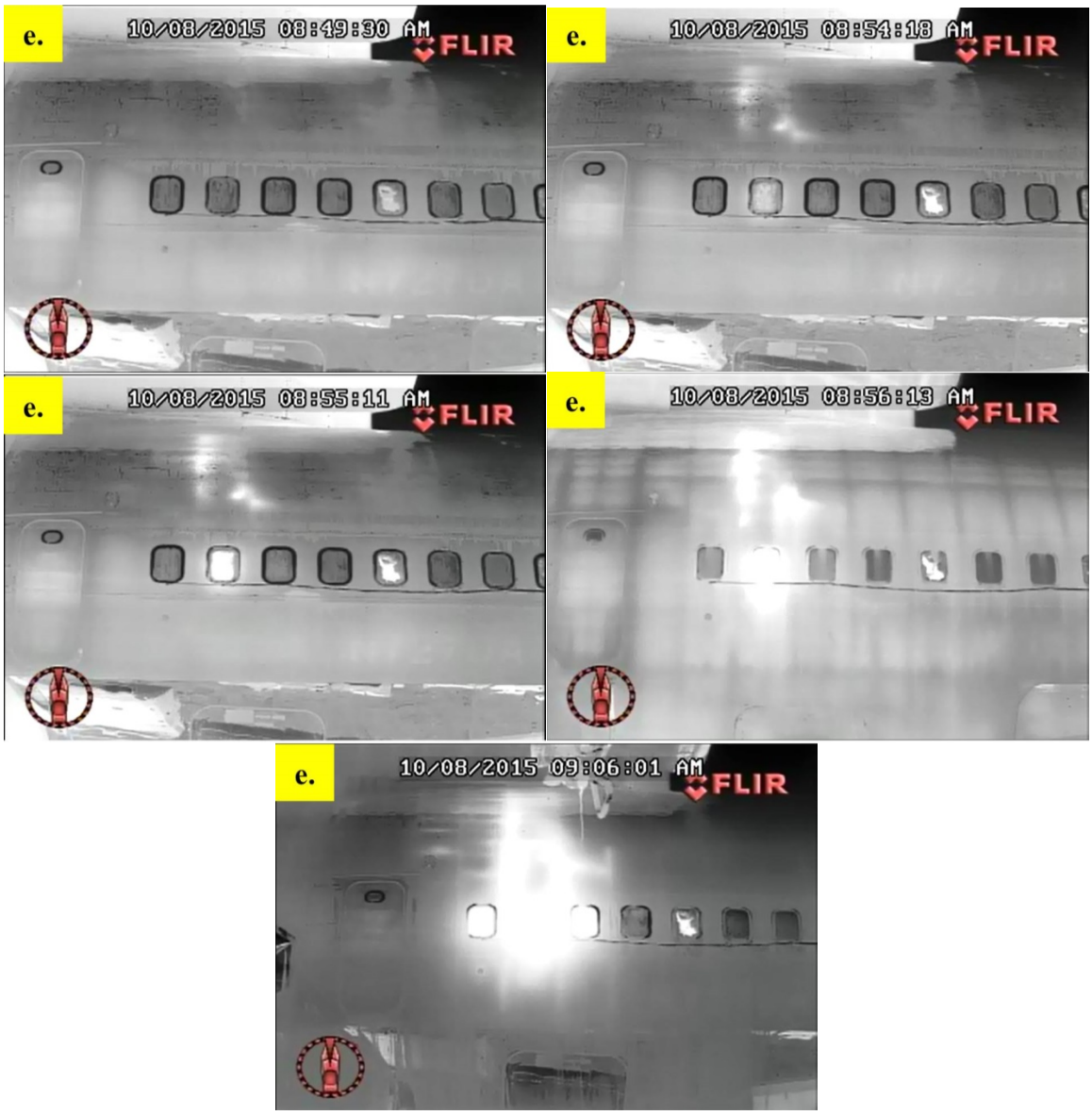

Figure A-15. Test 3 IR Camera Screen Captures: M625L

Figure A-16. Test 4 IR Camera Screen Captures: Patrol IR

Figure A-17. Test 4 IR Camera Screen Captures: P660

Figure A-18. Test 4 IR Camera Screen Captures: T420

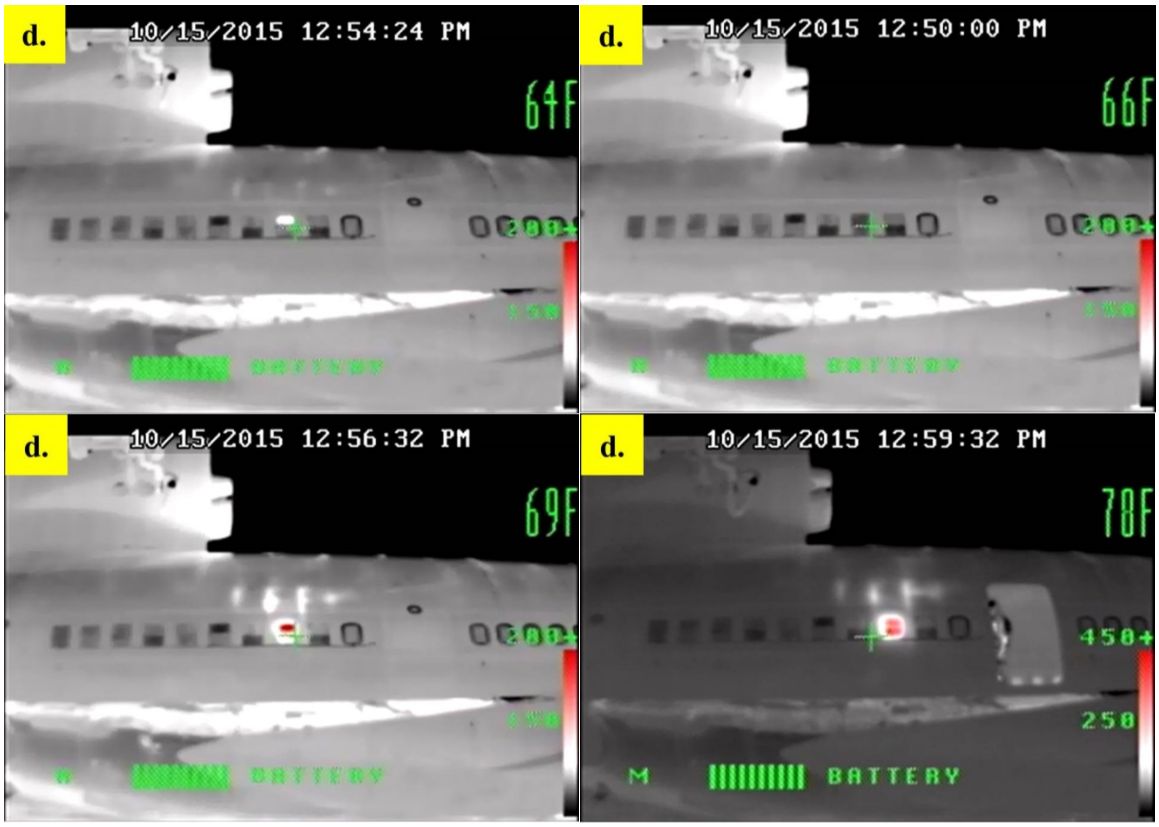

Figure A-19. Test 4 IR Camera Screen Captures: XR

Figure A-20. Test 4 IR Camera Screen Captures: M625L

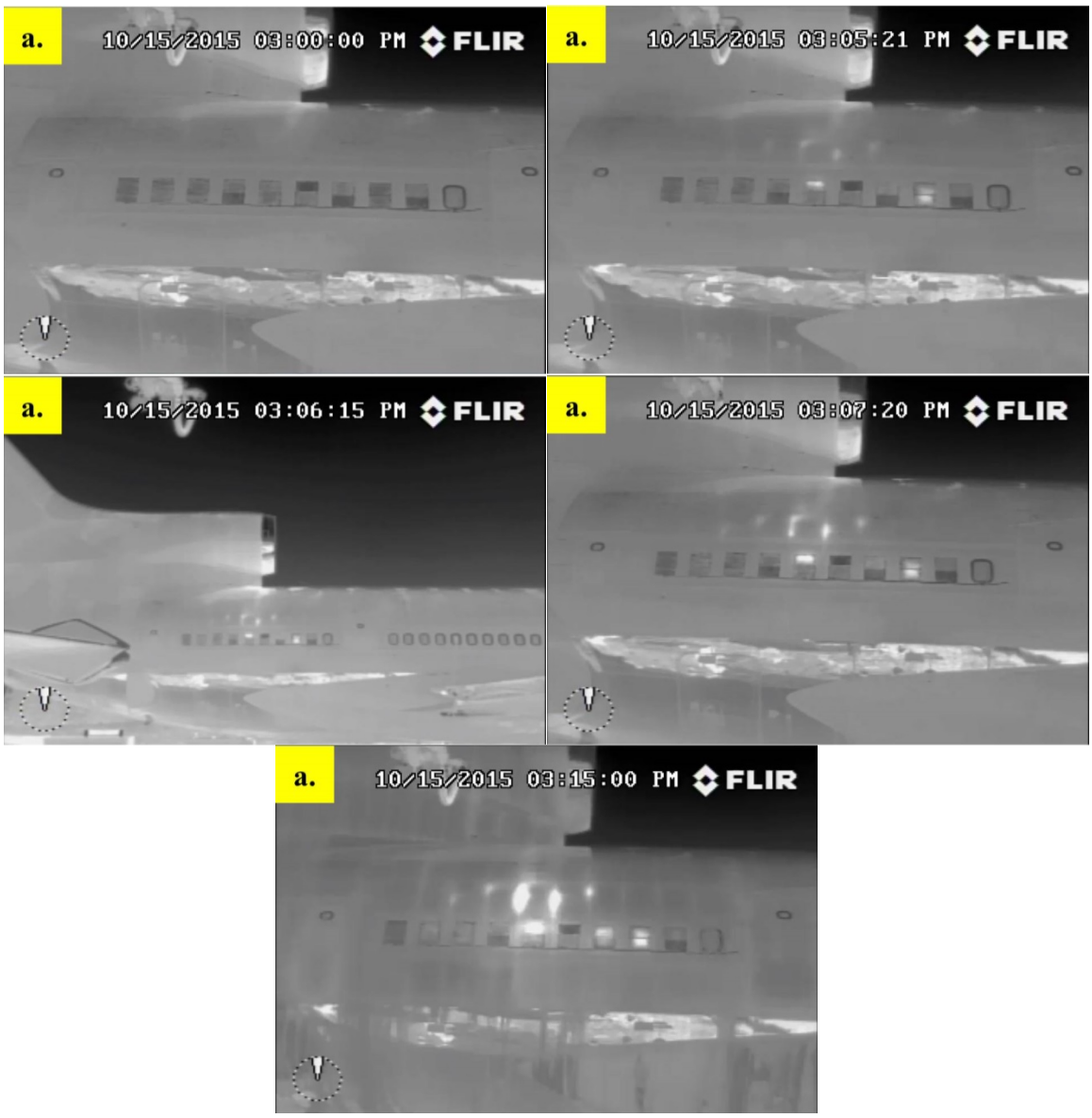

Figure A-21. Test 5 IR Camera Screen Captures: Patrol IR

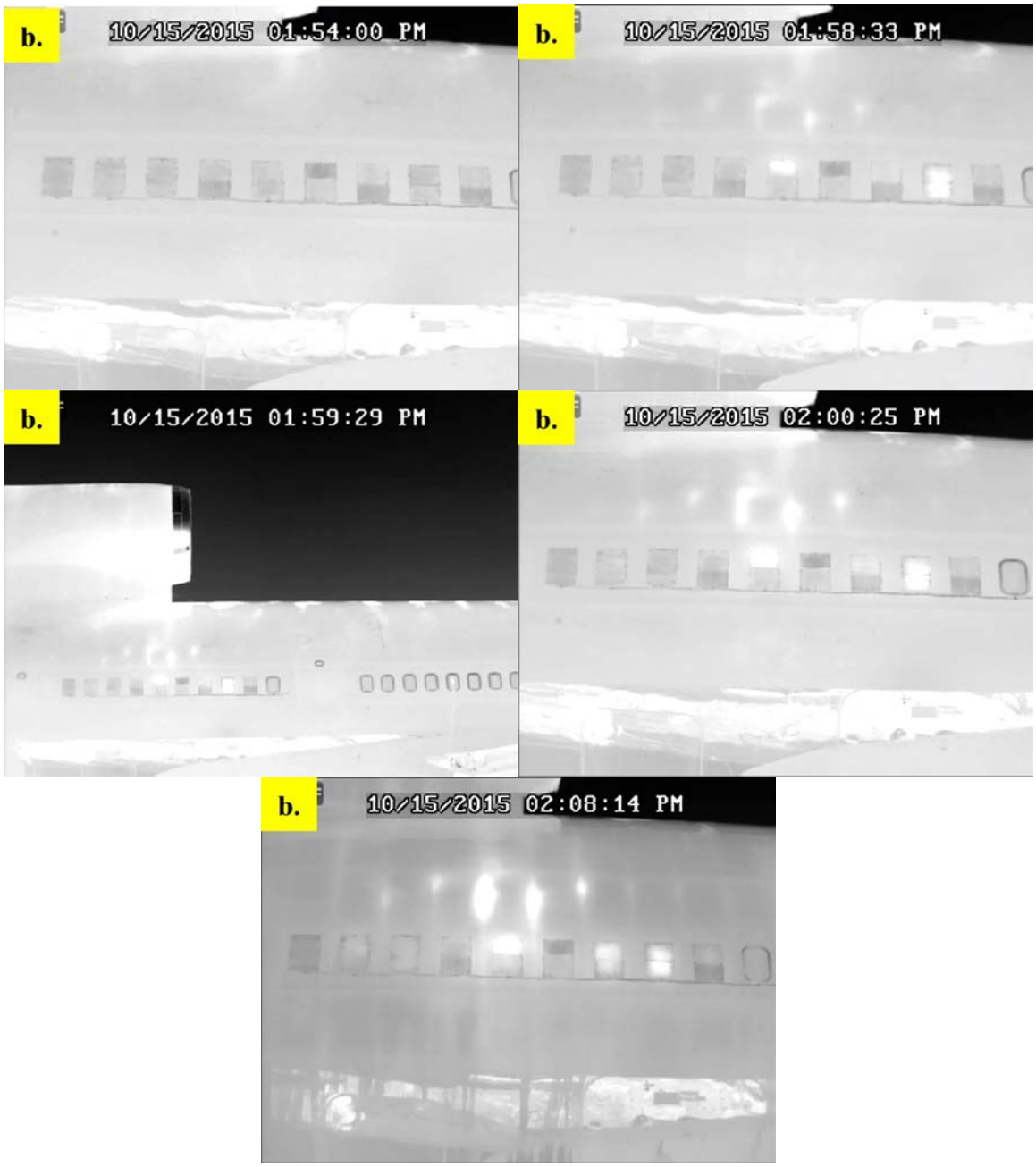

Figure A-22. Test 5 IR Camera Screen Captures: P660

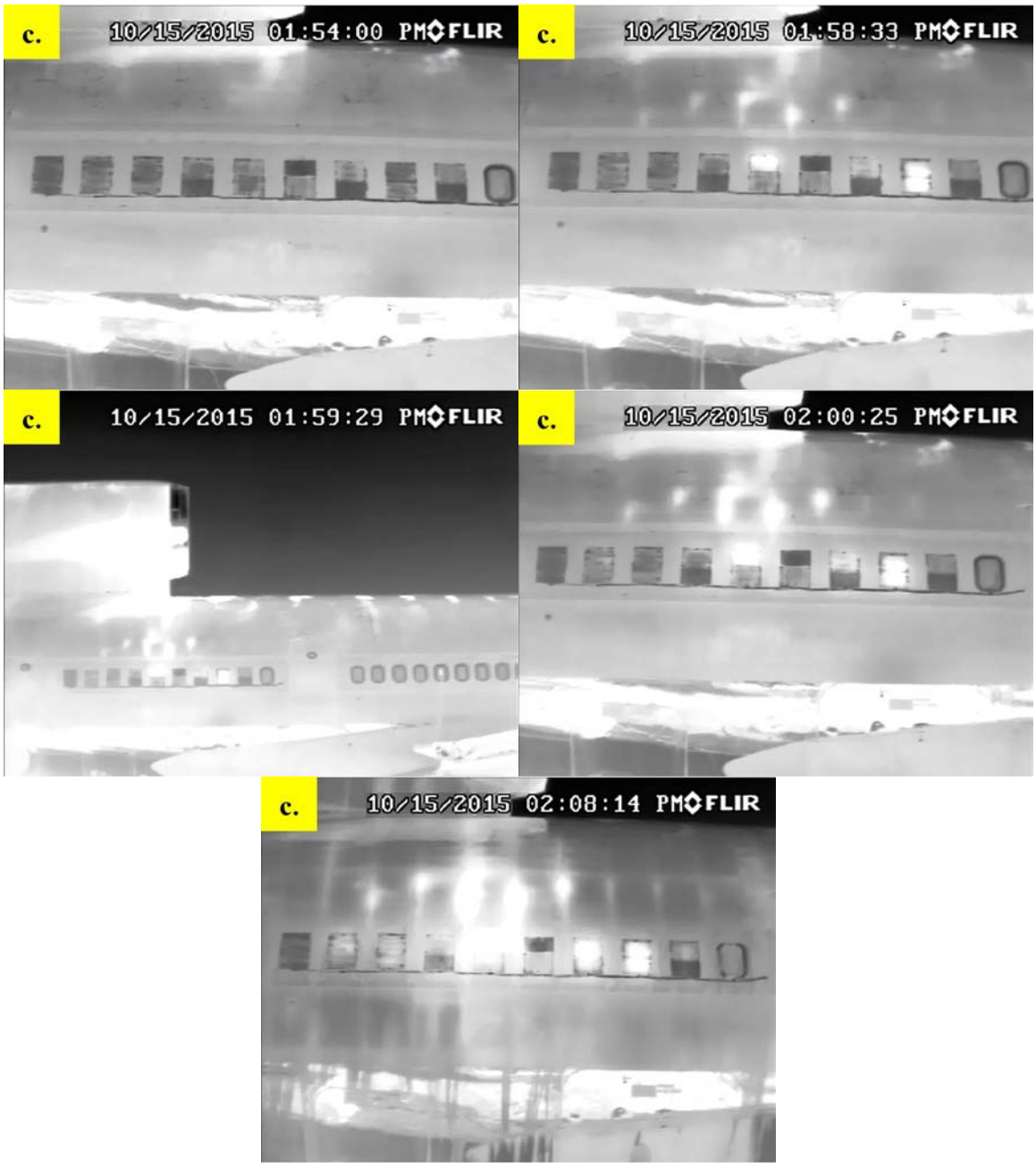

Figure A-23. Test 5 IR Camera Screen Captures: T420

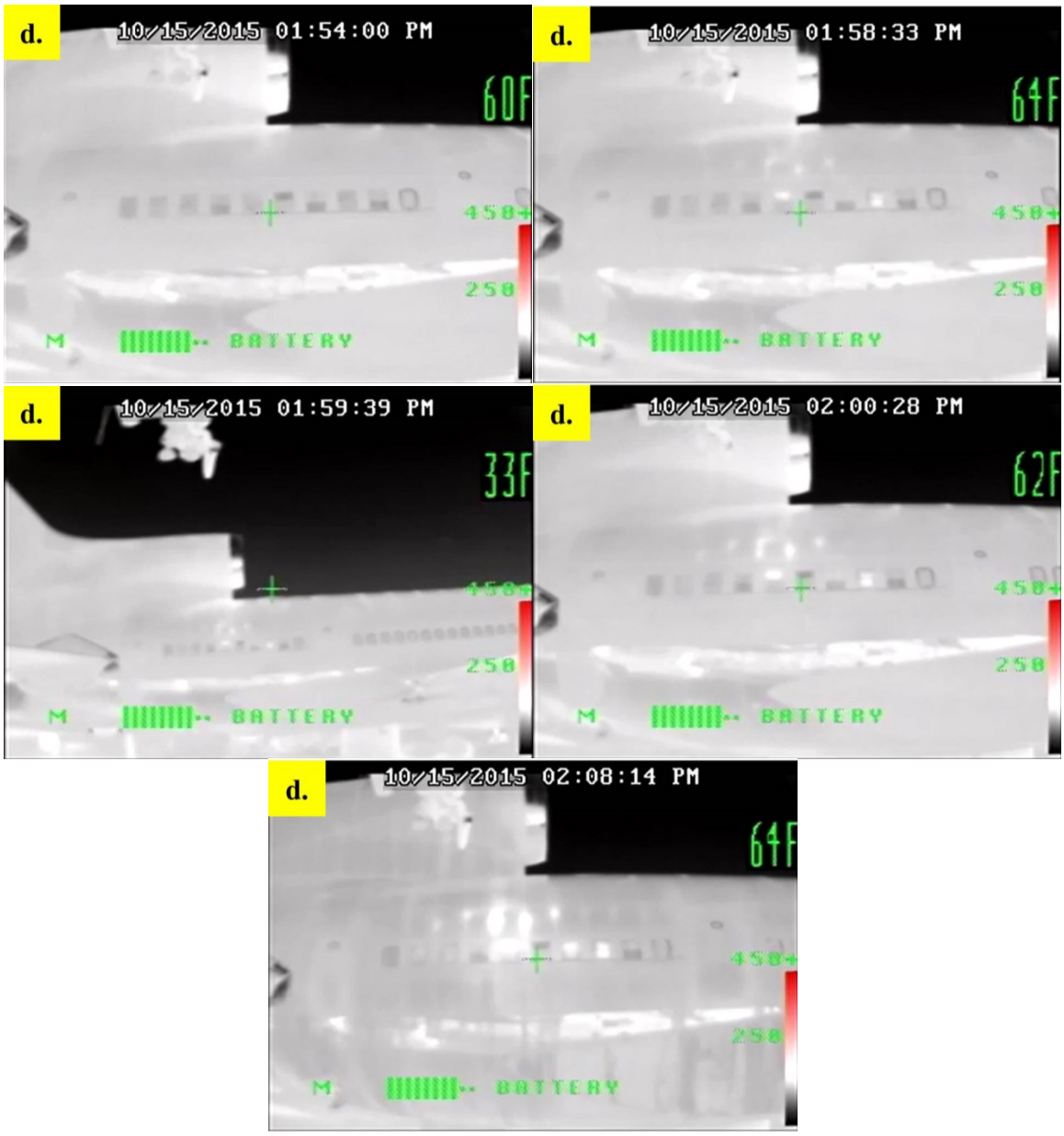

Figure A-24. Test 5 IR Camera Screen Captures: XR

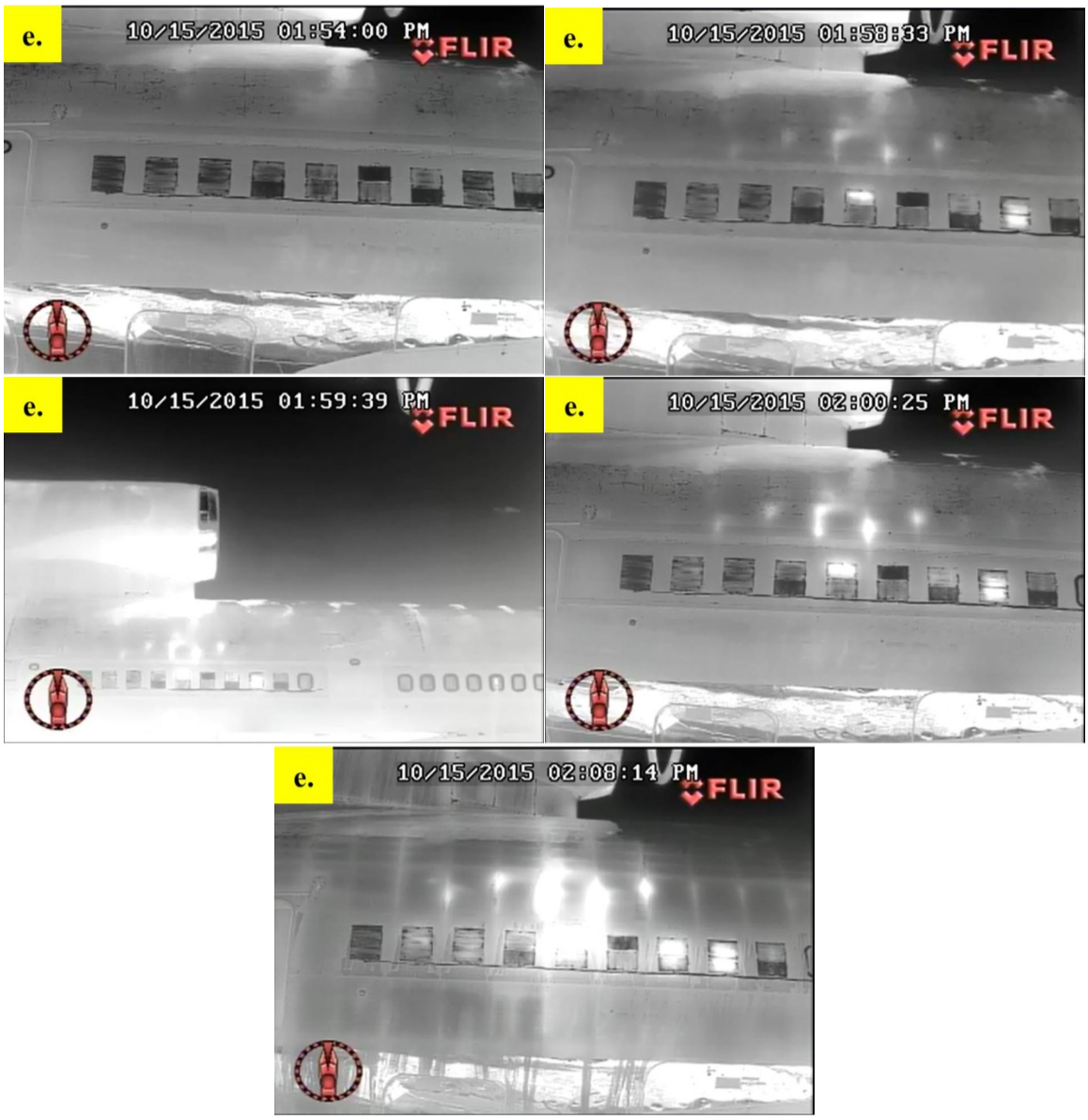

Figure A-25. Test 5 IR Camera Screen Captures: M625L

Figure A-26. Test 6 IR Camera Screen Captures: Patrol IR

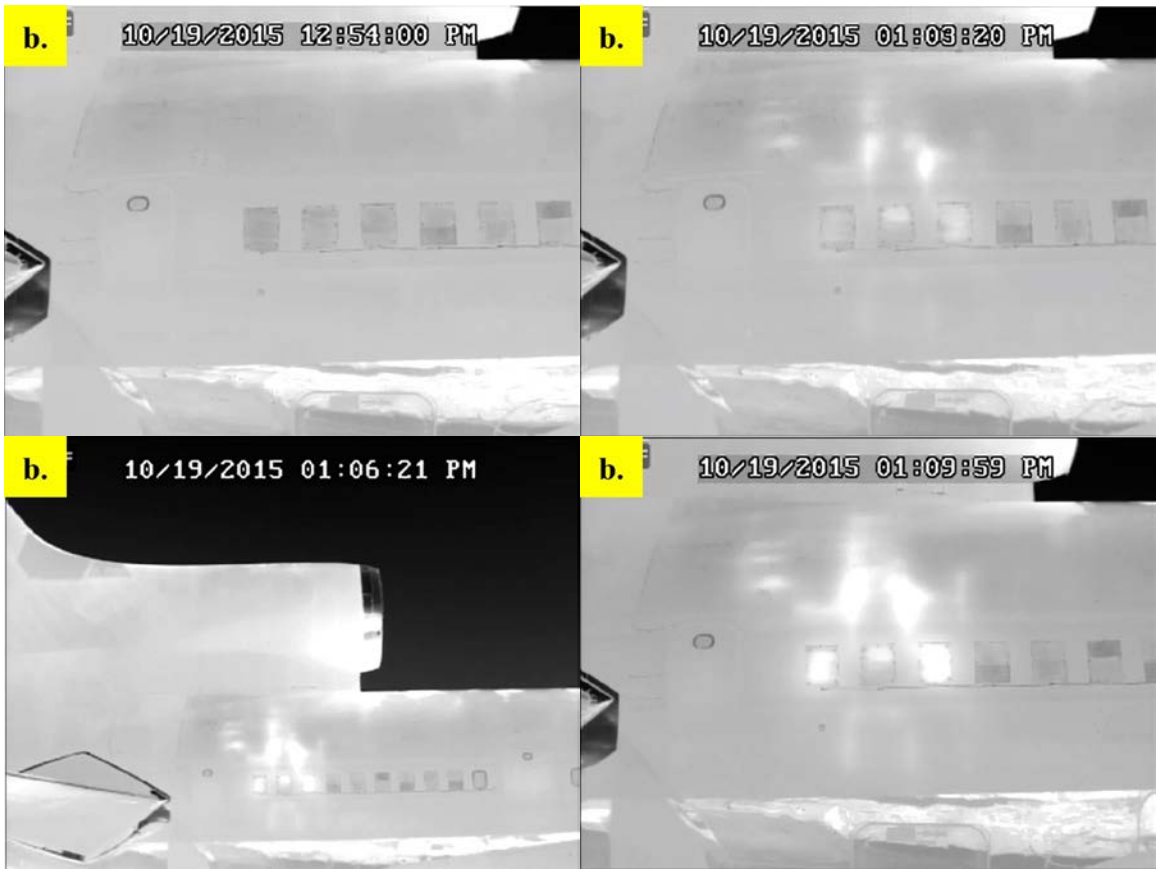

Figure A-27. Test 6 IR Camera Screen Captures: P660

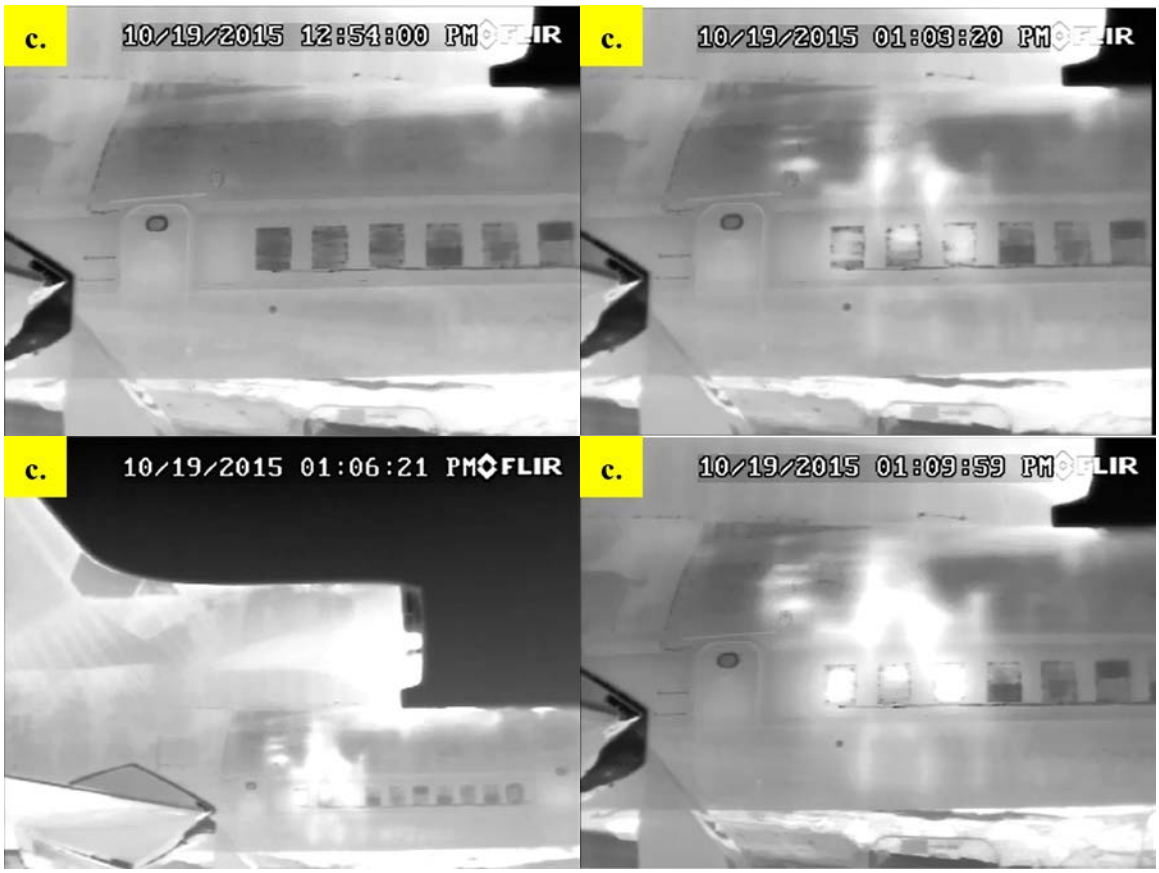

Figure A-28. Test 6 IR Camera Screen Captures: T420

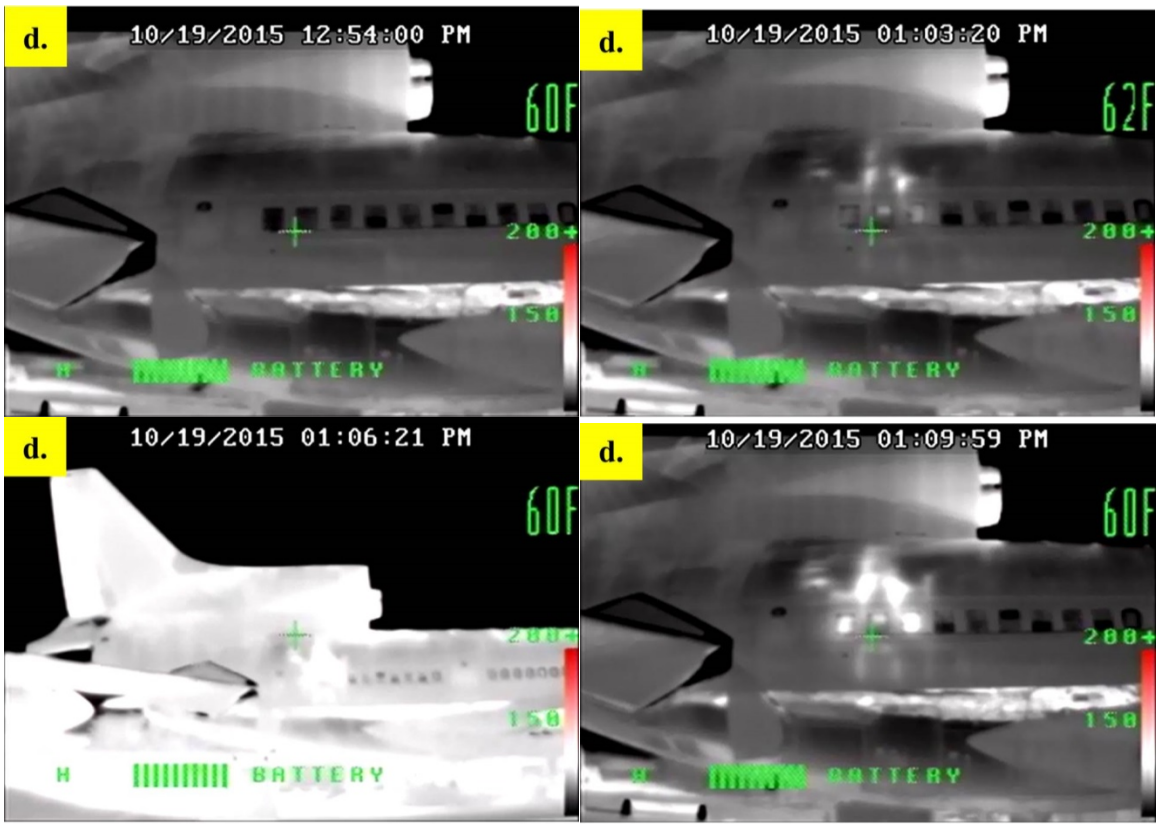

Figure A-29. Test 6 IR Camera Screen Captures: XR

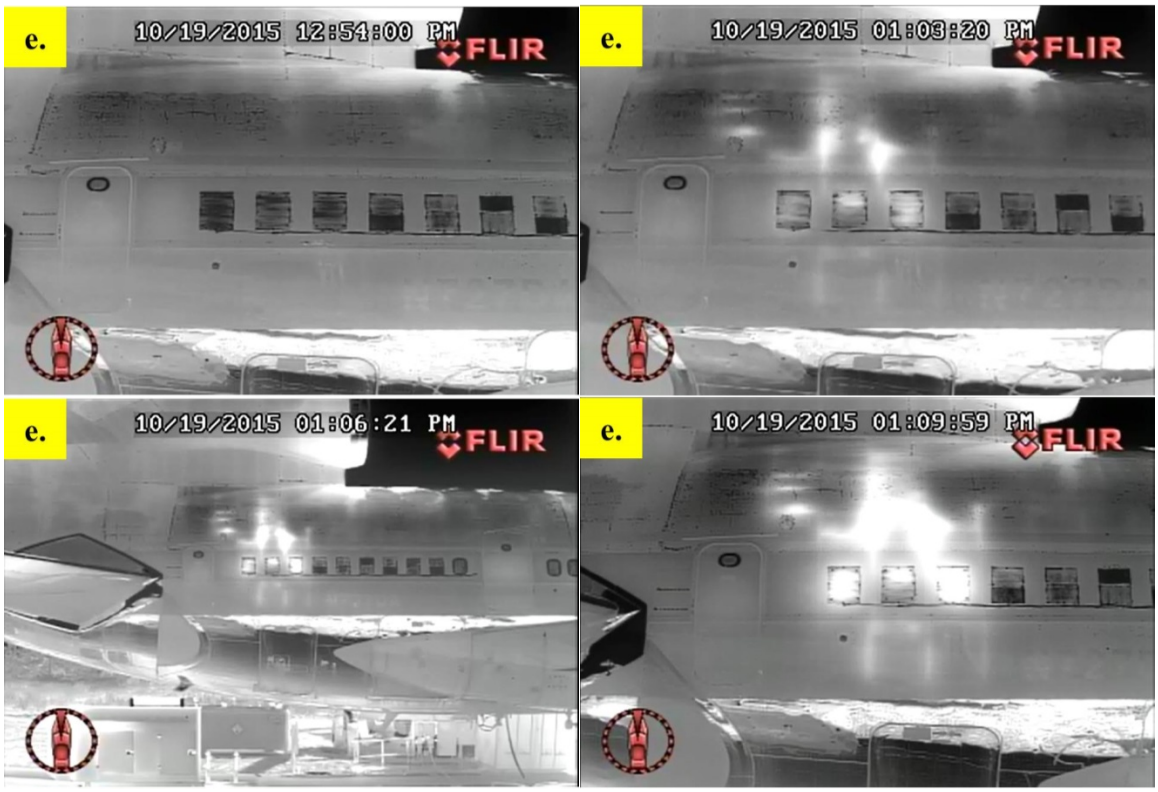

Figure A-30. Test 6 IR Camera Screen Captures: M625L

Figure A-31. Test 7 IR Camera Screen Captures: Patrol IR

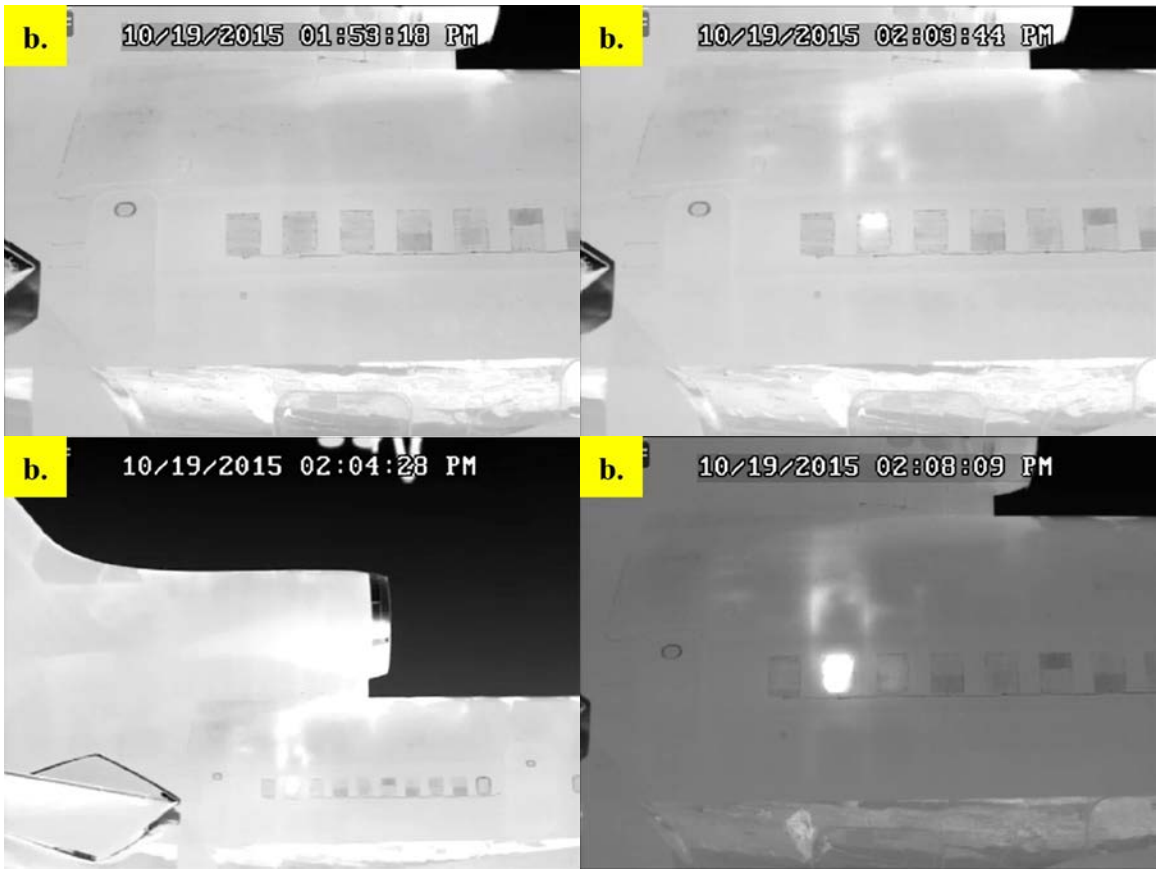

Figure A-32. Test 7 IR Camera Screen Captures: P660

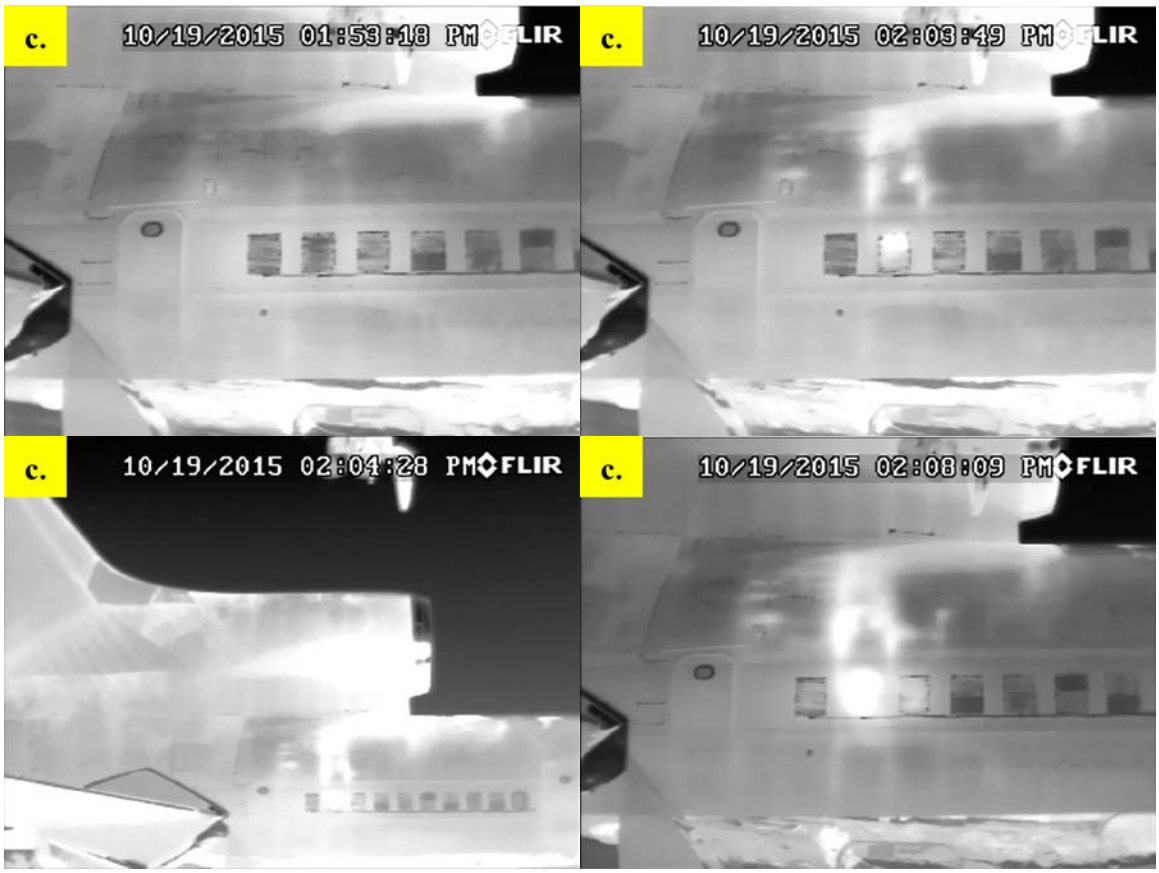

Figure A-33. Test 7 IR Camera Screen Captures: T420

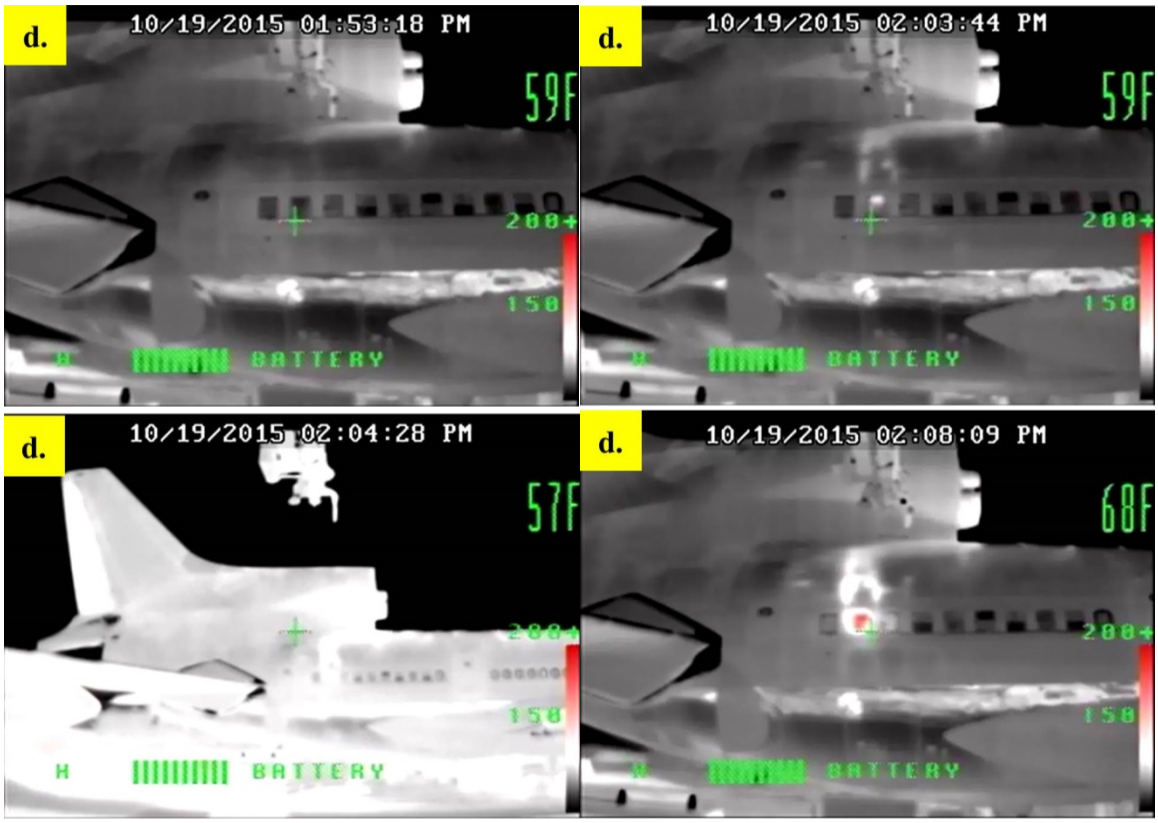

Figure A-34. Test 7 IR Camera Screen Captures: XR

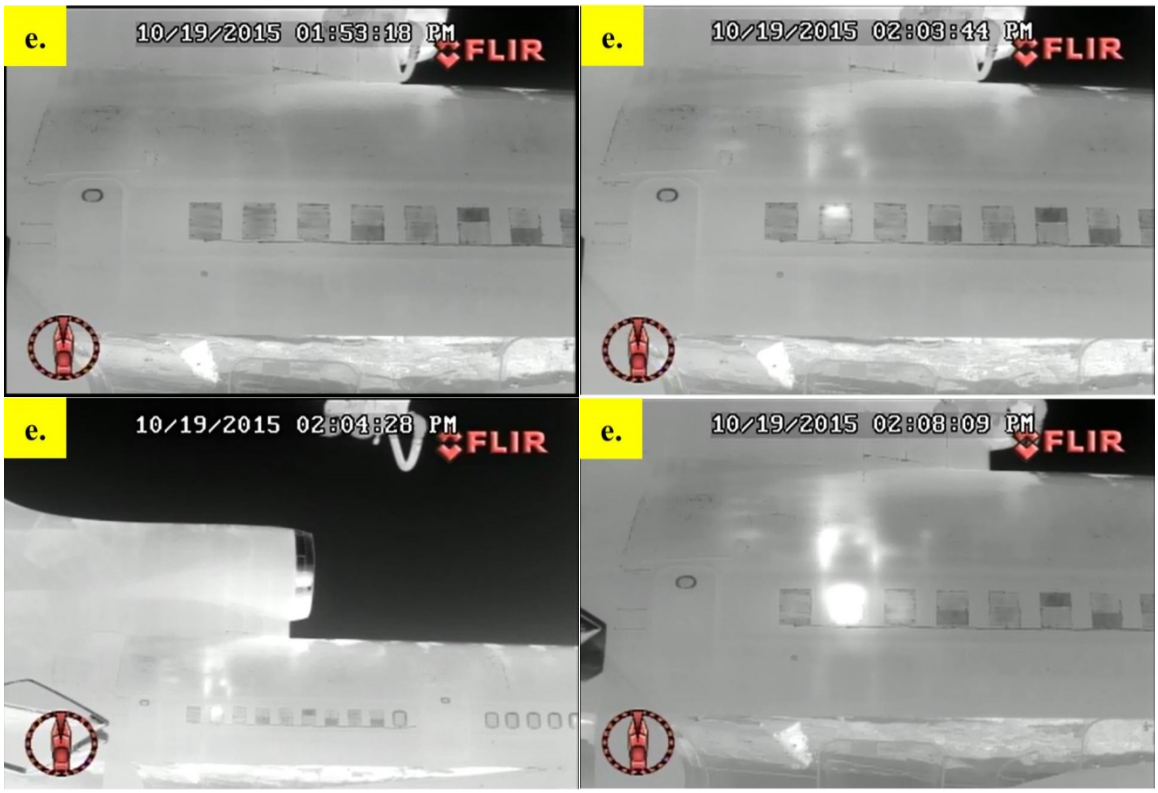

Figure A-35. Test 7 IR Camera Screen Captures: M625L

APPENDIX B—PANEL TEST RESULTS

Table B-1 shows the thermal camera temperature readings for each heated panel tests when using the cameras at different angles, which were the temperature readings of thermocouples that were attached to the panels. Cameras used included FLIR® Patrol IR (Patrol IR), FLIR® P660 (P660), FLIR® T420 (T420), ISG® ELITE XR, and FLIR® M625L (M625L). Panel materials included carbon fiber, aluminum and Glass Laminate Aluminum-Reinforced Epoxy (GLARE).

Table B-1. Panel Test Results

Test Number	Camera Model	Panel Type	Angle (°)	Camera Indicated Temperature (°F)	Thermocouple Indicated Temperature (°F)	Error (°F)
1	T420	Carbon fiber	0	188	95.2	-92.8
1	T420	Carbon fiber	30	191	94.79	-96.21
1	T420	Carbon fiber	50	196	97.09	-98.91
1	T420	Carbon fiber	60	196	101.5	-94.5
1	T420	Carbon fiber	65	209	105.9	-103.1
2	T420	Aluminum - unpainted	0	67.8	93.5	25.7
2	T420	Aluminum - unpainted	30	77.9	92.5	14.6
2	T420	Aluminum - unpainted	50	89.9	96.92	7.02
2	T420	Aluminum - unpainted	60	88.3	103	14.7
2	T420	Aluminum - unpainted	65	87.8	104	16.2
3	T420	Aluminum - painted	0	154	98.6	-55.4
3	T420	Aluminum - painted	30	161	93.5	-67.5
3	T420	Aluminum - painted	50	160	96.2	-63.8
3	T420	Aluminum - Painted	60	169	99	-70
3	T420	Aluminum - Painted	65	169	98.8	-70.2
4	P660	GLARE	0	n/a	n/a	n/a
4	P660	GLARE	30	229	142.1	-86.9

Table B-1. Panel Test Results (Continued)

Test Number	Camera Model	Panel Type	Angle (°)	Camera Indicated Temperature (°F)	Thermocouple Indicated Temperature (°F)	Error (°F)
4	P660	GLARE	50	240	141.8	-98.2
4	P660	GLARE	60	224	148.1	-75.9
4	P660	GLARE	65	234	147.3	-86.7
5	P660	Carbon fiber	0	197.3	122.3	-75
5	P660	Carbon fiber	30	204.8	115.4	-89.4
5	P660	Carbon fiber	50	205.3	124.1	-81.2
5	P660	Carbon fiber	60	219.2	122.5	-96.7
5	P660	Carbon fiber	65	203.9	132.2	-71.7
6	P660	Aluminum - unpainted	0	84.74	112.7	27.96
6	P660	Aluminum - unpainted	30	94.5	109.3	14.8
6	P660	Aluminum - unpainted	50	87.3	113	25.7
6	P660	Aluminum - unpainted	60	108.5	114.8	6.3
6	P660	Aluminum - unpainted	65	134.4	110.75	-23.65
7	P660	Aluminum - painted	0	138	110.8	-27.2
7	P660	Aluminum - painted	30	138.6	110.7	-27.9
7	P660	Aluminum - painted	50	151.2	113.5	-37.7
7	P660	Aluminum - painted	60	157.1	118.9	-38.2
7	P660	Aluminum - painted	65	143.96	122.5	-21.46
8	P660	GLARE	0	114.62	86.5	-28.12
8	P660	GLARE	30	102.2	89.8	-12.4
8	P660	GLARE	50	130.28	87.6	-42.68
8	P660	GLARE	60	132.8	85.7	-47.1
8	P660	GLARE	65	133	88.86	-44.14

Table B-1. Panel Test Results (Continued)

Test Number	Camera Model	Panel Type	Angle (°)	Camera Indicated Temperature (°F)	Thermocouple Indicated Temperature (°F)	Error (°F)
9	T420	GLARE	0	177	102.3	-74.7
9	T420	GLARE	30	177	98.2	-78.8
9	T420	GLARE	50	177	97.5	-79.5
9	T420	GLARE	60	176	99.9	-76.1
9	T420	GLARE	65	181	98.9	-82.1
10	XR	GLARE	0	138	93.66	-44.34
10	XR	GLARE	30	141	96.9	-44.1
10	XR	GLARE	50	145	94.7	-50.3
10	XR	GLARE	60	143	94	-49
10	XR	GLARE	65	140	95.6	-44.4
11	XR	Carbon fiber	0	143	89.6	-53.4
11	XR	Carbon fiber	30	149	92.46	-56.54
11	XR	Carbon fiber	50	154	92.1	-61.9
11	XR	Carbon fiber	60	150	89.6	-60.4
11	XR	Carbon fiber	65	149	90.5	-58.5
12	XR	Aluminum - unpainted	0	107	92.3	-14.7
12	XR	Aluminum - unpainted	30	116	92.5	-23.5
12	XR	Aluminum - unpainted	50	122	92.1	-29.9
12	XR	Aluminum - unpainted	60	118	89.9	-28.1
12	XR	Aluminum - unpainted	65	120	90.5	-29.5
13	XR	Aluminum - painted	0	113	92.8	-20.2
13	XR	Aluminum - painted	30	123	90.1	-32.9
13	XR	Aluminum - painted	50	122	90	-32

Table B-1. Panel Test Results (Continued)

Test Number	Camera Model	Panel Type	Angle (°)	Camera Indicated Temperature (°F)	Thermocouple Indicated Temperature (°F)	Error (°F)
13	XR	Aluminum - painted	60	116	90.1	-25.9
13	XR	Aluminum - painted	65	122	90.3	-31.7